Alessandra Cavalcanti Duarte Lupi

Regulação luminosa e hormonal do gene de biogênese e manutenção plastidial *GOLDEN 2-LIKE 2* de tomateiro e seu efeito na qualidade nutricional dos frutos

Light and hormonal regulation of the tomato plastidial development and maintenance gene *GOLDEN 2-LIKE 2* and its effect on fruit nutritional quality

São Paulo

2017

Alessandra Cavalcanti Duarte Lupi

Regulação luminosa e hormonal do gene de biogênese e manutenção plastidial *GOLDEN 2-LIKE 2* de tomateiro e seu efeito na qualidade nutricional dos frutos

Light and hormonal regulation of the tomato plastidial development and maintenance gene *GOLDEN 2-LIKE 2* and its effect on fruit nutritional quality

Dissertação apresentada ao Instituto de Biociências da Universidade de São Paulo, para a obtenção de Título de Mestre em Ciências, na Área de Botânica.

Orientadora: Maria Magdalena Rossi

São Paulo

2017

Ficha Catalográfica

Lupi, Alessandra

Light and hormonal regulation of the tomato plastidial development and maintenance gene GOLDEN 2-LIKE 2 and its effect on fruit nutritional quality

84 páginas

Dissertação (Mestrado) - Instituto de Biociências da Universidade de São Paulo. Departamento de Botânica.

1. Chloroplast 2. Tomato 3. Golden 2-Like 4. Light 5. Phytohormones

I. Universidade de São Paulo. Instituto de Biociências. Departamento de Botânica.

Comissão Julgadora:

Prof(a). Dr(a).

Prof(a). Dr(a).

Profa. Dra. Maria Magdalena Rossi

Orientadora

Dedicatória

Dedico este trabalho a todos que lutam pela sobrevivência
da ciência brasileira. Que venham tempos melhores.
Não desistiremos.

Epígrafe

"A scientist in his laboratory is not a mere technician:
he is also a child confronting natural phenomena
that impress him as though they were fairy tales."

- Marie Curie

Agradecimentos

Agradeço ao Departamento de Botânica do Instituto de Biociências – USP pela estrutura acadêmica, e ao apoio financeiro da CAPES.

A realização deste trabalho só foi possível graças à dedicada orientação da Profª. Maria Magdalena Rossi e a co-orientação do Prof. Luciano Freschi, que sempre estiveram presentes e disponíveis quando precisei. Aprendi muito com vocês. Obrigada por todo o projeto, vocês são responsáveis por um grande crescimento pessoal e profissional durante esses quase 3 anos de laboratório.

Agradeço também as colaborações do Prof. Eduardo Purgatto com as análises de açúcares e ao Prof. Diego Demarco por todo o auxílio com o microscópio eletrônico.

Este trabalho só foi possível graças a todos do Laboratório de Genética Molecular de Plantas: As queridas GGDR (Giovanna Gramegna e Daniele Rosado), Bruninha Trench, Silvia Blanco e Bruno Lira. Muito obrigada por todo o apoio sempre, tanto no profissional quanto nas milhares de fotos de gatos compartilhadas. Agradeço também a todos os colegas do Laboratório de Fisiologia Vegetal, em especial ao Ricardo Bianchetti, Frederico Rocha e Aline Bertinatto; do Laboratório de Biologia Celular de plantas; e do Lignin Lab, em especial ao Prof. Dr. Igor Cesarino.

A todos que acompanharam essa jornada e foram de grande importância no suporte emocional: vocês são os melhores (e piores) amigos que eu poderia ter. Bios, nuzofers e gixers, valeu por tudo! Verena, Carlinha e Brunno, vocês são simplesmente essenciais. Não teria conseguido sem ter todos vocês comigo.

À família incrível que eu tenho, muito obrigada. Aurea, minha mãe que teve a honra de ter seu nome por toda a dissertação, obrigada por todo o apoio desde sempre. Vô, gostaria muito que pudesse ter visto esse capítulo da minha vida se concluindo. Obrigada por plantar a semente da ideia de trabalhar com genética de plantas muito antes de eu saber que me apaixonaria por esse tema.

Pela linda ilustração que decora minha capa e minha pele, muito obrigada Tiê Zerbeto!

Kami e Ivy, obrigada por deixarem as madrugadas de trabalho em casa bem melhores.

Aos compositores clássicos que me ajudaram durante a parte escrita, ao café que me permitiu trabalhar durante as manhãs e à terapia que me manteve relativamente sã.

Muito obrigada a todos que participaram da minha vida nesses quase 3 anos!

Index

Contents

Resumo

Os plastídios são organelas responsáveis por diversos aspectos essenciais do desenvolvimento das plantas como a fotossíntese, assimilação de nitrogênio e síntese de diversos compostos do metabolismo secundário. A diferenciação e atividade dos cloroplastos são altamente reguladas pela luz, e diversas proteínas e mecanismos envolvidos nestes processos têm sido caracterizados. Os fatores de transcrição GOLDEN 2-LIKE (GLKs) controlam a expressão de diversos genes relacionados à fotossíntese, biogênese e manutenção plastidial. *Solanum lycopersicum* possui duas cópias desses genes, *SlGLK1* e *SlGLK2* e, embora sejam funcionalmente redundantes, seu padrão de expressão é diferente, uma vez que *SlGLK1* predomina nas folhas ao passo que *SlGLK2* é expresso apenas nos frutos, mais precisamente na região pedicelar. Durante o processo de domesticação do tomateiro, a seleção de variedades de amadurecimento uniforme resultou na fixação da mutação *uniform ripening* (*Slglk2*) na maioria das variedades cultivadas, resultando em mudanças na composição metabólica dos frutos. Neste contexto, este trabalho teve como objetivo geral caracterizar funcionalmente o gene *SlGLK2* visando compreender de que forma a luz (mediada por fitocromos) e os fitormônios (particularmente citocininas e auxinas), regulam a expressão deste gene e como a presença de SlGLK2 afeta a qualidade nutricional dos frutos. Para isso, foi realizado um detalhado perfil transcricional de *SlGLK2* em frutos de plantas selvagens, *Slglk2* mutantes e deficientes para a percepção luminosa e para a sinalização hormonal. O efeito de *SlGLK2* sobre a qualidade nutricional foi avaliado caracterizando o metabolismo de carbono e de vitamina E. Adicionalmente, foi quantificada a atividade da proteína repórter GUS em plantas transgênicas que expressam o gene *uidA* sob controle de promotores responsivos a citocininas ou auxinas em plantas com genótipo *SlGLK2* ou *Slglk2* para analisar se a atividade hormonal é afetada pela presença de SlGLK2. Finalmente, com o intuito de verificar se a presença de *SlGLK2* é suficiente para reverter o fenótipo clorótico do mutante *aurea*, promovendo a diferenciação e maturação plastidial mesmo na ausência de fitocromos funcionais, foram geradas linhagens transgênicas sobreexpressando o gene *SlGLK2* em fundo genético *aurea-Slglk2*. A Análise dos resultados permitiu concluir que o conteúdo de açúcares solúveis e vitamina E correlacionam com a expressão de *SlGLK2*, que a expressão de *SlGLK2* é reprimida por auxinas, que SlGLK2 participa positivamente da sinalização de citocininas, e que a sua sobreexpressão reverte, parcialmente, o fenótipo dos frutos da mutante *aurea-Slglk2*. Os resultados obtidos nos levam a uma melhor compreensão da rede regulatória que interconecta o gene *SlGLK2*, os fitormônios e a luz promovendo a atividade plastidial e, por consequência, determinando a qualidade nutricional dos frutos de tomateiro, importante componente da dieta humana.

Abstract

Plastids are organelles responsible for several essential aspects for plant development, like photosynthesis, nitrogen assimilation and synthesis of several compounds of secondary metabolism. Chloroplasts differentiation and activity are highly regulated by light, and several proteins and mechanisms involved in these processes have been characterized. The GOLDEN 2-LIKE (GLK) transcription factors controls the expression of several genes related to photosynthesis, plastid biogenesis and maintenance. *Solanum lycopersicum* genome harbors two copies of this gene, *SlGLK1* and *SlGLK2* and, although they are functionally redundant, their expression pattern is different, once *SlGLK1* predominates in leaves, while only *SlGLK2* is expressed in fruit, precisely at the pedicel region. During tomato domestication, selection for varieties that ripened evenly resulted in the fixation of *uniform ripening* mutation (*Slglk2*) in most cultivated varieties, resulting in alterations in fruit metabolic composition. In this context, the objective of this work was to functionally characterize *SlGLK2* gene aiming to understand in which way phytochrome mediated light and phytohormones, particularly auxins and cytokinins, regulates this gene expression, and how SlGLK2 presence affects fruit nutritional quality. To achieve this, a detailed transcriptional profile of *SlGLK2* was performed in fruits of wild plants, *Slglk2* mutant and plants deficient for light perception or hormonal signaling. The effect of *SlGLK2* over nutritional quality was evaluated by characterizing carbon and vitamin E metabolism. Additionally, reporter protein GUS activity was quantified in transgenic plants that express *uidA* gene under control of promoters responsive to cytokinins or auxins in *SlGLK2* or *Slglk2* genotypes, to analyze if hormonal activity is affected by SlGLK2 presence. Finally, in order to verify if the presence of SlGLK2 is sufficient to reverse the chlorotic phenotype of the mutant *aurea*, promoting the differentiation and plastidial maturation even in the absence of functional phytochromes, transgenic lines were generated by overexpressing the *SlGLK2* gene on *aurea-Slglk2* genetic background. The integrated data analysis allowed us to conclude that the content of soluble sugars and vitamin E correlate with the expression of *SlGLK2*, that the expression of *SlGLK2* is repressed by auxins, that SlGLK2 positively participates in the signaling of cytokinins, and that its overexpression partially reverts the phenotype of the *aurea-Slglk2* mutant fruits. The results obtained in this work contributes to a better understanding of the regulatory network that interconnects *SlGLK2* gene, phytohormones and light, promoting the plastidial activity and consequently, determining the nutritional quality of the tomato fruit, an important component of the human diet.

I. Introduction

1.1. Plastid biogenesis, differentiation and maintenance

Plastids are organelles with a great diversity of shapes and functions, and they are found in all photosynthetic eukaryotes. Besides being responsible for photosynthesis, depending on the plant development stage, these organelles are also responsible for other functions, such as synthesis of amino acids, fatty acids, nitrogenous bases, pigments and hormones. Additionally, they also participate on the assimilation of sulfur and nitrogen (Jarvis & López-Juez 2013).

Land plants have many plastids that play different functions (Figure 1). Proplastids are found mainly in meristematic tissues, and are the precursors of other plastids. Amyloplasts accumulates starch and are found mainly in storage organs, such as roots, seeds and tubercles, having a key role in energy storage and gravitropism. Gerontoplasts, which are mostly found in senescent tissues, originate from the disassembly of photosynthetic machinery and macromolecule degradation, playing a main role in nutrient recycling and remobilization towards sink organs. Chloroplasts synthetize and accumulate chlorophyll and maintain all the machinery responsible for light capture and photosynthetic activity, allowing atmospheric carbon fixation, on which most forms of life depend. Chromoplasts are found in flowers of different species and also in fleshy fruits, in which they perform various functions, including synthesis and accumulation of a wide spectrum of metabolites, many of them with nutraceutical relevance, *i.e.* antioxidants. In this regard, great effort has been made to understand minutely the mechanisms responsible for differentiation and maintenance of plastid structure and metabolism, aiming the improvement of nutritional quality of edible fruits (Jarvis & López-Juez 2013).

Among the exogenous factors that influence the differentiation of proplastids into chloroplasts, the light signal has a prominent role ensuring this transition only in appropriate conditions for photosynthetic activity. The main photoreceptors involved in the light perception that regulates this conversion are the PHYTOCHROMES (PHYs). Structurally, PHYs are homodimeric proteins whose unit is composed of an apoprotein bound to a tetrapyrrole chromophore, *i.e.* phytochromobilin (Gyula *et al.* 2003). In the darkness PHYs are found inactive in the cytoplasm while, in the presence of light, phytochromobilin undergoes an isomeric alteration that changes the structure of the apoprotein, directing the active PHYs to the cellular nucleus (Bae & Choi 2008). Within the nucleus, they promote degradation of PHYTOCHROME INTERACTING FACTORS (PIFs), negative regulators of light signal transduction. In turn, PIFs repress the expression of *ELONGATED HYPOCOTYL 5* (*HY5*), a positive regulator of photomorphogenesis, and GOLDEN

2-LIKE (GLKs) transcription factors (Song *et al*. 2014) involved in plastidial biogenesis and activity maintenance (Fitter *et al*. 2002). Additionally, HY5 positively regulates *Arabidopsis thaliana GLK2* (Lee et al. 2007). Together, HY5 and GLKs activate transcription of several proteins related to the photosynthetic machinery and, consequently, chloroplast differentiation (Jarvis & López-Juez 2013).

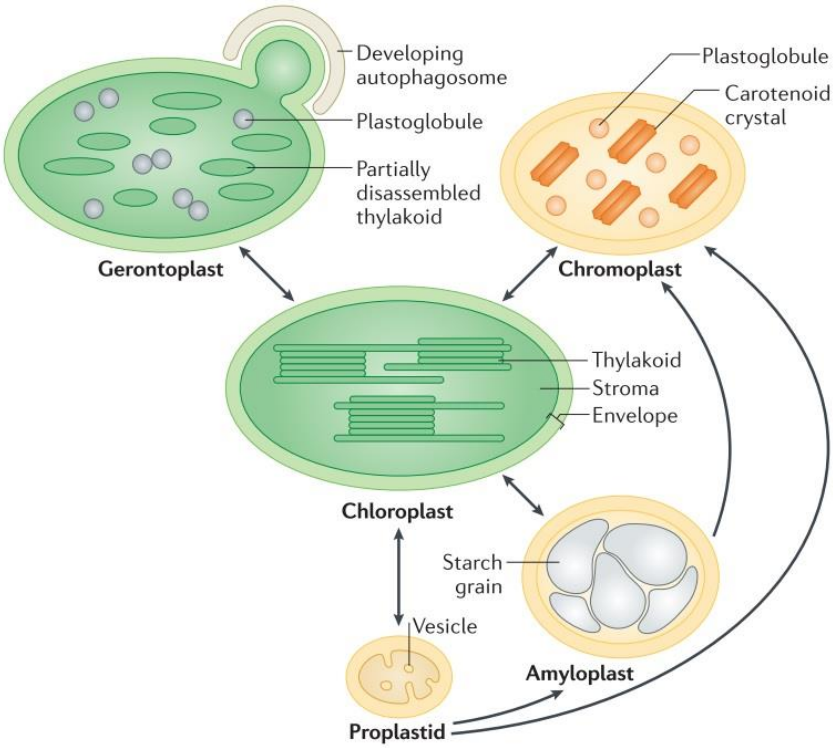

Figure 1: Plastid diversity and interconnections. Proplastids are able to differentiate into other plastids, according to physiological stimuli of the cell; amyloplasts accumulates starch; chloroplasts are photosynthetic plastids; gerontoplasts are formed during senescence by disassemble of photosynthetic machinery and autophagy; and chromoplasts accumulates other pigments such as carotenoids. Adapted from Jarvis & López-Juez (2013).

In relation to endogenous factors, plastidial biogenesis and differentiation is also influenced by different phytohormones. Auxins and cytokinins, for example, regulates plastidial differentiation in different plant organs. At the seedling stage, cytokinins play a key role in chloroplast differentiation and division during de-etiolation, whereas auxin has an inhibitory effect, preventing, for example, the development of chloroplasts in the roots (Cortleven & Schmulling 2015; Kobayashi *et al*. 2017).

1.2. Importance of plastid metabolism for nutritional quality of Solanum lycopersicum fruits

Because of its nutritional importance, widespread consumption in the western population and economic importance, the tomato (*Solanum lycopersicum*) has been configured as the model species for the study of fleshy fruits development and ripening (Giovannoni 2004).

The development of the tomato fruit begins after pollination with a phase of intense cell division comprising the immature green stages (IG), followed by a period of cell expansion until the fruit reaches its final size at mature green stage (MG). During these green stages, the fruits have

active photosynthetic machineries (Carrara *et al*. 2001). Although fruits in general are sink organs, requiring more photoassimilates than they produce, local photosynthesis in tomatoes seems to be responsible for up to 20% of the total carbon in ripe fruits (Cocaliadis *et al.* 2014).

From MG stage onwards, the fruits become responsive to ethylene, which triggers ripening, turning fruits from MG to breaker stage (Br), when the fruit starts to change color from green to yellow. During this process, a progressive conversion of chloroplasts into chromoplasts is observed involving several biochemical alterations that will contribute to the definition of the color, flavor, aroma and texture of the ripe fruit (five days after Br onwards, Br+5). Gradual chlorophyll degradation leads to loss of green coloration, and the released phytol is recycled and used, at least in part, for tocopherol (vitamin E, VTE) production (Almeida *et al.* 2016). Carotenoid biosynthetic route is intensely stimulated during ripening, resulting in accumulation of lycopene, responsible for the intense red color of ripe tomato fruits (Giovannoni 2004). The induction of several aromatic amino acid decarboxylases leads to increased production of volatile compounds, such as phenylethanol and phenylacetaldehyde, which confer the characteristic aroma of tomatoes (Tieman *et al*. 2006; Tieman *et al*. 2007). Fruit softening is induced by cell wall hydrolases, changing fruit texture (Fischer & Bennet 1991). Finally, the degradation of starch and cell wall increases the content of soluble sugars and organic acids, determining the texture and density of tomato puree, *i.e.* the °Brix, a feature of great industrial importance considering that two-thirds of the world's production is consumed as processed tomato (Carrari & Fernie 2006; Sila *et al*. 2009). All the described changes determine the nutritional and industrial quality of the fruit (Giovannoni 2004; Fraser *et al.* 1994; Egea *et at*. 2011).

The most valuable nutraceutical compounds in fleshy fruits, *e.g.* carotenoids and tocopherols, are synthetized in chloroplast/chromoplast. Therefore, chloroplast abundance and activity in the green stages of the fruits collaborate not only for the synthesis of part of the photoassimilates necessary to the organ development, but also determine future capacity of these fruits to produce nutraceutical compounds in the chromoplasts. In this way, the increment in the number of active chloroplasts, as well as the enhancement of plastidial metabolism, appears as a key target for of fleshy fruit yield and quality improvement (Isaacson *et al.* 2002; Nashilevitz *et al.* 2010).

In this work, we focused on tocopherol nutraceutical compound, since it is a subject of special interest in our research group. Moreover, tomato fruit carotenogenesis has been extensively characterized (Liu *et al.* 2015). Since 2011, our group have published several papers characterizing the biosynthesis of tocopherols in *S. lycopersicum*, including all the enzyme-encoding genes and the limiting steps for its production (Almeida *et al*. 2011; Quadrana *et al*. 2013). Moreover, we have

revealed the mechanisms by which some of these limiting steps are regulated (Almeida *et al*. 2015; Almeida *et al*. 2016; Quadrana *et al*. 2013; Lira *et al*. 2016).

Tocopherols are lipophilic antioxidants that, together with tocotrienols, are collectively called VTE. They are synthetized in the chloroplasts and accumulate in plastoglobuli (Vidi *et al.* 2006). These two families of metabolites are composed by a polar head and a hydrophobic side chain, and exist in four different forms each (α, β, γ and δ) (Figure 2) (Mène-Saffrané & Dellapenna 2010).

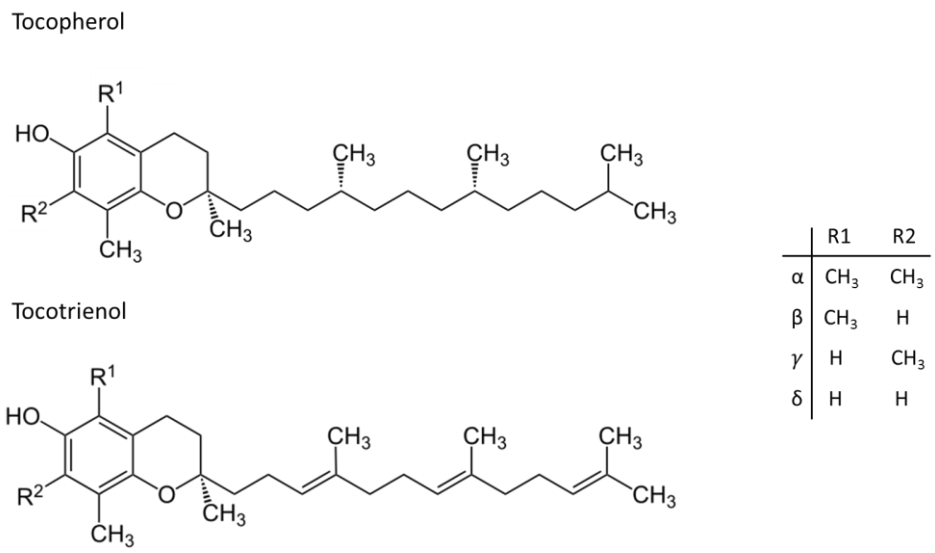

Figure 2: Chemical structure of tocopherols and tocotrienols.

The benefits of VTE for human health are related to its antioxidant and anti-inflammatory properties (Rizvi *et al.* 2014) and includes decreased risk of mortality from thromboembolism in weman (Booth *et al.* 2004), inhibition of cancer growth (Stone *et al.* 2004; Jiang *et al.* 2004), protection against neurodegenerative disorders, such as Alzheimer's disease (Morris *et al.* 2015) and dementia (Cherubini *et al.* 2005), among others. Tocopherol forms have different bioavailability and bioactivity, being α-tocopherol the form with the highest VTE activity in mammals (Mène-Saffrané & Dellapenna 2010). However, it is worth to mention that γ-tocopherol is also well absorbed in human tissues, and has properties that are important to human health that are not shared with α-tocopherol, with epidemiologic studies describing positive relations between increased γ-tocopherol serum concentration and lower risk of prostate cancer and cardiovascular diseases (Jiang *et al.* 2001)

In plants, tocopherols are fundamental players of the photoprotective machinery particularly involved in controlling the level of singlet oxygen ($^1O_2$) in photosystem II (PSII), and the extent of lipid peroxidation in thylakoid membranes (Triantaphylidès & Havaux 2009;

Rastogi *et al.* 2014; Miret & Munné-Bosch 2015). Beyond photoprotective roles, tocopherol is also involved in seed longevity, seedling germination (Sattler *et al.* 2004; Mène-Saffrané *et al.* 2010), and photoassimilate export regulation (Almeida *et al.* 2016).

Tocopherol metabolism (Figure 3) is highly linked to chlorophyll and carotenoid metabolic pathways and, in recent years, it has been characterized in tomato (Almeida *et al.* 2011; Almeida *et al.* 2016; Quadrana *et al.* 2013; Guyer *et al.* 2014; Lira *et al.* 2016). The precursors for tocopherol biosynthesis are derived from two plastidial secondary metabolism pathways, methylerythritol phosphate (MEP) and shikimate (SK) and the description below highlights the main steps for which the catalyzing enzyme encoding genes have shown to be transcriptional regulated and will be studied in the present work (Quadrana *et al*. 2013). The product of two *1-DEOXY-D-XYLULOSE-5-P SYNTHASE* (DXS) paralog genes catalyze the first step of MEP route, *DXS(2)* in green tissues and *DXS(1)*, whose expression is enhanced during ripening. Geranylgeranyl-2P (GGDP) is the MEP intermediate from which carotenoids are synthesized and, in green tissues, is also converted by GERANYLGERANYL DIPHOSPHATE REDUCTASE (GGDR) into phytyl-2P, a precursor of both, chlorophyll and tocopherol biosynthesis.

CHLOROPHYLL SYNTHASE (CHLG) catalyzes the reaction between chlorophyllide *a* and phytyl-2P to produce chlorophyll *a* in photosynthetic organs. While, PHEOPHYTYNASE (PPH) and PHEOPHYTYNASE-LIKE1 (PPHL1) are responsible for chlorophyll degradation and recycling, respectively.

Tocopherols are produced by the condensation of phytyl-2P and the homogentisate (HGA). The latter is synthesized by two possible 4-HYDROXYPHENYLPYRUVATE DIOXYGENASES (HPPD) of SK pathway in tomato, being HPPD2 the most expressed in all tomato tissues/organs (Zouine *et al*. 2017). The HOMOGENTISATE PHYTYL TRANSFERASE (VTE2) produces 2-methyl-6-phytylquinol (MPBQ) from phytyl-2P and HGA. The conversion of MPBQ to 2,3-dimethyl-5-phytylquinol (DPBQ) is done by 2,3-DIMETHYL-5-PHYTYLQUINOL METHYL TRANSFERASE (VTE3), while γ- and δ- tocopherols are synthetized by TOCOPHEROL CYCLASE (VTE1) from DPBQ and MPBQ, respectively. Further, α- and β- tocopherols are converted from γ- and δ- forms, respectively, by TOCOPHEROL γ-METHYL TRANSFERASE (VTE4). During tomato fruit ripening, GGDR is downregulated and the GGDP is directed towards carotenoid biosynthesis (Quadrana *et al*. 2013; Almeida *et al*. 2015). However, tocopherol content increases during ripening, fed by the recycling of chlorophyll degradation-derived phytol by PHYTOL KINASE (VTE5) and PHYTYL-PHOSPHATE KINASE (VTE 6), which produce phytyl-2P for further condensation with HGA (Almeida *et al*. 2011, Almeida *et al*. 2016).

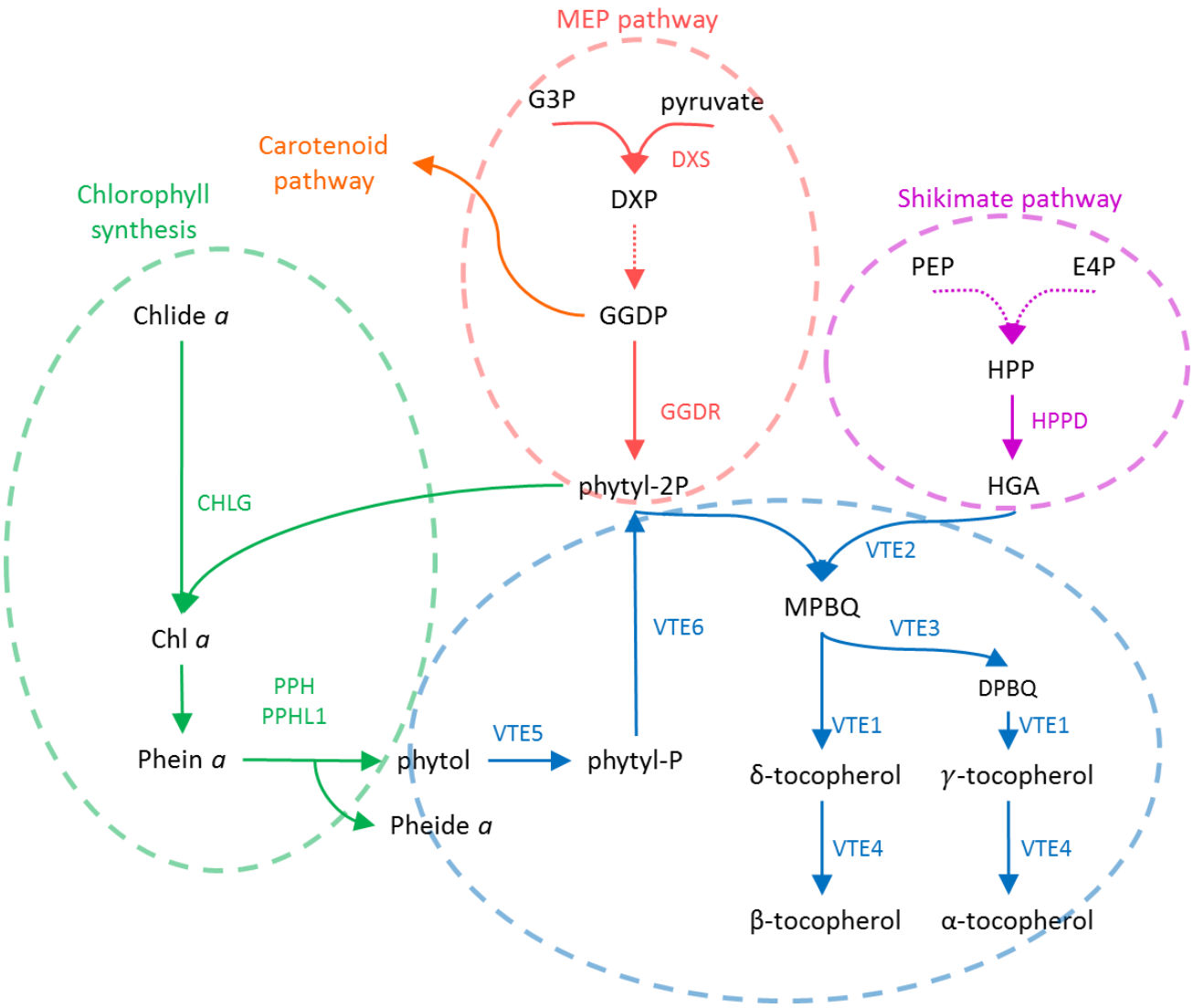

Figure 3: Simplified tocopherol biosynthetic pathway.
MEP, shikimate, chlorophyll and tocopherol metabolism are circled in red, purple, green and blue respectively. Dotted arrows indicate that intermediate steps were omitted. Enzymes of interest are indicated next to the arrows. Enzymes: CHLG: CHLOROPHYLL SYNTHASE; DXS: 1-DEOXY-D-XYLULOSE-5-P SYNTHASE; GGDR: GERANYLGERANYL DIPHOSPHATE REDUCTASE; HPPD: 4-HYDROXYPHENYLPYRUVATE DIOXYGENASE; PPH: PHEOPHYTINASE; PPHL1: PHEOPHYTINASE LIKE-1; VTE1: TOCOPHEROL CYCLASE; VTE2: HOMOGENTISATE PHYTYL TRANSFERASE; VTE3: 2,3-DIMETHYL-5-PHYTYLQUINOL METHYL TRANSFERASE; VTE4: TOCOPHEROL Γ -METHYL TRANSFERASE; VTE5: PHYTOL KINASE; VTE6: PHYTYL-PHOSPHATE KINASE. Metabolites: Chlide *a*: chlorophyllide *a*; Chl *a*: chlorophyll *a*; DPBQ: 2,3-Dimethyl-5-phytylquinol; DXP: 1-Deoxy-D-xylulose-5P; GGDP: geranylgeranyl-2P; HGA: Homogentisate; HPP: hydroxyphenylpyruvate; MPBQ: 2-Methyl-6-phytylquinol; Pheide *a*: pheophorbide *a*; Phein *a:* pheophytin.

1.3. The role of GOLDEN 2-LIKE genes in chloroplast maintenance and activity.

Several transcriptional factors are involved in chloroplast differentiation. Among them, GLK proteins are one of the key factors, with great importance for both, plastidial biogenesis and activity maintenance (Fitter *et al*. 2002). In *A. thaliana*, there are 2 *loci* that encodes for GLK proteins, *AtGLK1* and *AtGLK2*. Although they have a slightly different transcriptional pattern, they are functionally redundant since only the double mutant, *Atglk1Atglk2*, is deficient in plastid

development. AtGLK1 and AtGLK2 proteins induce expression of several genes involved in the formation of the photosynthetic apparatus, and respond to retrograde signals of chloroplasts, being able to coordinate the expression of nuclear genes related to photosynthesis and optimize this process according to environmental conditions (Waters *et al.* 2009).

In *S. lycopersicum* genome there are also two copies of *GLKs*: *SlGLK1* and *SlGLK2*. While *SlGLK1* is mostly expressed in cotyledons, sepals and leaves, *SlGLK2* is predominantly expressed in fruits, concentrated at the pedicelar region, resulting in a phenotype called "green shoulder", decreasing in a longitudinal gradient until the base of the fruit (Powell *et al*. 2012; Nguyen *et al*. 2014).

Characteristics that facilitate harvesting and shipping, and increase shelf-life had great importance during tomato domestication (Giovannoni 2001). In this context, in order to select fruits that ripen evenly, the *uniform ripening* mutation was fixed, selecting the mutant allele of *SlGLK2* (*Slglk2*), which is found in most cultivated tomato varieties nowadays. *Slglk2* allele has a single base insertion at the coding region, originating a premature stop codon and a truncated protein with only 80 amino acids (Figure 4), while the wild protein encoded by the wild allele has 310 amino acids (Powell *et al.* 2012).

Fixation of *Slglk2* mutation had metabolic consequences, as mutant fruits has lower amount of chlorophyll and soluble sugars (Powell *et al.* 2012; Nguyen *et al.* 2014). Also, overexpression of *SlGLK2* in mutant background results in fruits with higher content of starch, soluble sugars and carotenoids (Powell *et al.* 2012; Nguyen *et al.* 2014). There are no reports of *SlGLK2* effect on other nutraceutical compounds, such as VTE.

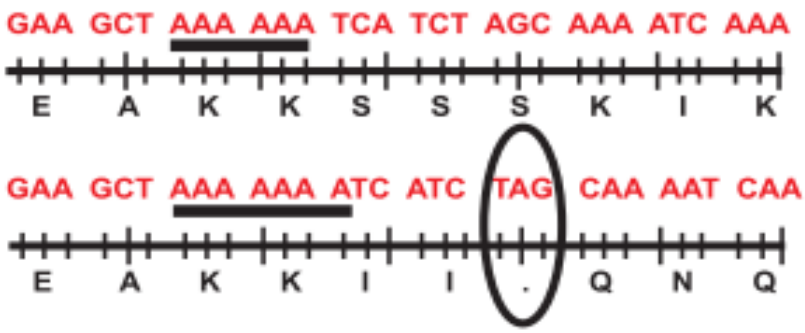

Figure 4: Comparison between wild *SlGLK2* and mutant *Slglk2* alleles. Detail from nucleotide number 210 of the coding region of wild (above) and mutant (below) alleles. The insertion of an adenine caused a frameshift, resulting in a premature stop codon (circled), creating a non-functional truncated protein. Adapted from Powell *et al.* (2012).

Regarding *SlGLKs* expression regulation, it has been shown that *SlGLK2* expression is higher in fruits that developed in the presence of light when compared to dark grown fruits (Powell *et al.* 2012). This observation is in agreement with the results obtained in *A. thaliana*, which demonstrated the transcriptional downregulation and post translational inactivation of AtGLK

proteins triggered by dark-induced senescence (Garapati *et al.* 2015; Rauf *et al.* 2013; Sakuraba *et al.* 2014). Kobayashi *et al.* (2012) demonstrated that auxins repress, while cytokinins induce chloroplast development in *A. thaliana* roots. The mechanism involves cytokinin-mediated transcriptional induction of *HY5* and *AtGLK2*, which in turn coordinate the expression of key genes of chloroplast biogenesis. In tomato, Sagar *et al.* (2013) demonstrated that the downregulation of *SlARF4* expression, an auxin induced repressor of auxin response, leads to the upregulation of *SlGLK1*, resulting in the increment of chloroplast number and chlorophyll accumulation. Additionally, senescence delay and maintenance of plastid activity has been largely described in "evergreen" plants with high endogenous cytokinin content, but the role of *GLK* genes has not been addressed in these studies (Thomas & Ougham 2014).

In this context, the importance of *GLK* genes for plastid function is evident, however, data on the effect of *SlGLKs* on fruit quality and their regulatory mechanisms are fragmented, and the studies were mostly restricted to the model species *A. thaliana*. Thus, the present work intended to improve the knowledge about *SlGLK2*, specially about their role on tomato fruit development and ripening.

II. Objectives

Knowing that several nutraceutical compounds that are important in the human diet are produced in tomato fruit plastids, and that light and phytohormones are important factors that regulates chloroplast biogenesis and activity, this work intended to study the role of PHY-mediated light perception and phytohormones on the regulation of tomato *GOLDEN 2-LIKE2 (SlGLK2)* transcription factor and its effect on fruit nutritional quality, focusing on carbon metabolism and VTE.

In order to achieve this objective, this dissertation was organized in three specific objectives that proposed the following activities:

I) Analyze *GLK* genes diversity in Viridiplantae.

II) Investigate the effect of PHY-mediated light perception on *SlGLK2* expression and its effect on fruit quality.

   a. Evaluate *SlGLK*s gene expression in fruits of wild type plants (*SlGLK2*), *Slglk2* mutant and PHY-deficient mutant (*aurea-SlGLK2*).

   b. Evaluate the effect of SlGLK2 on fruit nutritional quality.

   c. Obtain and characterize transgenic lines overexpressing *SlGLK2* in *aurea-Slglk2* genetic background.

III) Investigate the crosstalk between *SlGLK2* and the production and signaling of auxins and cytokinins.

   a. Evaluate temporal and spatial correlation between hormonal activity and SlGLK2 presence.

   b. Evaluate the influence of altered hormonal metabolism or signaling over the abundance of *SlGLK2* transcripts.

III. Material and Methods

3.1. Plant material, growth conditions and sampling

The model species used in this work was *Solanum lycopersicum*, cv. Micro-Tom. Depending on the experiment, different mutants in *SlGLK2* (wild allele) and the *uniform ripening Slglk2* (mutant allele) backgrounds were used. All the genotypes are described in Table 1.

Table 1. Genotypes used.

SlGLK2/SlGLK2 background	Homozygotes for wild allele SlGLK2
SlGLK2	Wild type Micro-Tom.
aurea-SlGLK2	Micro-Tom mutant deficient in PHY chromophore synthesis. **Obtained in this work.**
dgt	Micro-Tom mutant deficient in DIAGEOTROPICA cyclophilin biosynthesis. **Obtained in this work.**
35S::CKX2	Micro-Tom transgenic overexpressing cytokinin oxidase. **Obtained in this work.**
***Slglk2/Slglk2* background**	**Homozygotes for mutant allele *Slglk2***
Slglk2	Micro-Tom mutant for transcription factor SlGLK2.
aurea-Slglk2	Micro-Tom mutant deficient in PHY chromophore synthesis.
DR5::GUS	Micro-Tom transgenic expressing *uidA* gene under control of the promotor *DR5*, responsive to auxin.
ARR5::GUS	Micro-Tom transgenic expressing *uidA* gene under control of the promotor *DR5*, responsive to cytokinin.
DR5::GUS-Slglk2 ***ARR5::GUS-Slglk2***	Micro-Tom transgenic with transgenes in hemizygosis. **Obtained in this work.**
dgt-Slglk2	Micro-Tom mutant deficient in DIAGEOTROPICA cyclophilin biosynthesis.
35S::CKX2-Slglk2	Micro-Tom transgenic overexpressing a cytokinin oxidase.
***SlGLK2/ Slglk2* background**	**Heterozygotes for wild allele *SlGLK2***
DR5::GUS-SlGLK2 ***ARR5::GUS-SlGLK2***	Micro-Tom transgenic with transgenes in hemizygosis. **Obtained in this work.**

In order to understand the effect of PHY-mediated light perception on the regulation of *SlGLK2*, the *aurea* mutant was chosen. This genotype is deficient in functional PHY (Parks *et al.* 1987). Although it synthetizes normally all the apoproteins, a mutation on *PHYTOCHROMOBILIN SYNTHASE* gene prevents the correct synthesis of the chromophore, compromising all PHY (Kendrick *et al.* 1997). Consequently, *aurea* mutant presents elongated hypocotyls, reduced levels of chlorophyll and anthocyanins, resulting in chlorotic leaves and fruits (Figure 5A). The *aurea* chloroplasts show impaired ultrastructure, presenting reduced thylakoids that do not organize into *grana* (Koornneef *et al.* 1985). Originally in *Slglk2* background, *aurea* mutation was introgressed into *SlGLK2* background to perform the experiments (Table 1). The mutation, a CG deletion on sites

945-946 of the coding region (Muramoto *et al*. 2005), was confirmed by sequencing with the primers aurea (F/R) and aurea mid (F/R), described in Supplemental Material I.

To evaluate the influence of SlGLK2 in hormonal activity, transgenic plants expressing reporter gene *uidA* (encoding for the β-GLUCURONIDASE enzyme, GUS) under control of cytokinins (*ARR5::GUS*) and auxins (*DR5::GUS*) responsive promoters were used. Originally obtained in *Slglk2* background, these genotypes were crossed with *SlGLK2* and *Slglk2* plants in order to obtain hemizygotes for *ARR5::GUS* and *DR5::GUS* in background *SlGLK2*/*Slglk2* or *Slglk2*/*Slglk2* for further experiments (Table 1).

To study the influence of auxins and cytokinins on the regulation of *SlGLK2*, the following genotypes were used: *diageotropica* (*dgt*) mutant, a plant with low sensitivity to auxins due to a mutation on DIAGEOTROPICA cyclophilin (Oh *et al*. 2006), characterized by hyponastic leaves, plagiotropic roots with less ramification, slender and elongated stem and smaller fruits (Figure 5B); and a transgenic plant overexpressing *CYTOKININ OXIDASE* (CKX2), *35S::CKX2*, resulting in low endogenous levels of cytokinins (Werner *et al.* 2003), with the plants presenting excessive ramification in roots and shoots, smaller leaves and seeds that take longer to germinate (Figure 5C). This transgenic is also resistant to kanamycin, which was used for selection. The mutation and the transgene were originally in *Slglk2* background, and were introgressed into *SlGLK2* background (Table 1). Three generations were needed to obtain these plants: (i) *dgt-Slglk2* and *35S::CKX2-Slglk2* X *SlGLK2*: all homogenous heterozygous F1 seeds were collected; (ii) F1 self-fertilization: all segregating F2 seeds were collected individually for each plant; (iii) F2 seeds were sown and homozygous plants were selected according to: *dgt* mutation phenotype because the mutation is recessive; *35S::CKX2* in homozygosity by progeny test with kanamycin treatment; and *SlGLK2* homozygosity by sequencing. Homozygous F3 plants were grown for the experiments.

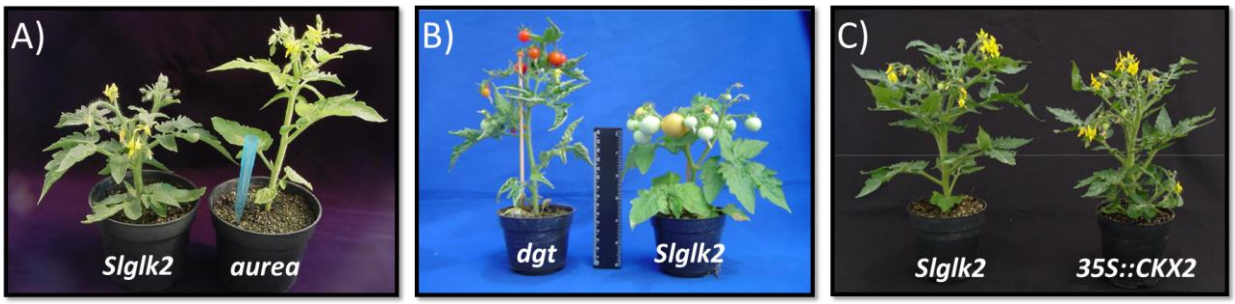

Figure 5: Phenotype of *aurea-Slglk2*, *dgt-Slglk2* and *35S::CKX2-Slglk2* in comparison to *Slglk2* genotype. Aspect of the different genotypes used in this work comparing to Micro-Tom *Slglk2*. **(A)** *aurea-Slglk2* mutant has elongated and narrower stem, and chlorotic leaves and fruits. **(B)** *dgt-Slglk2* mutant has elongated stem and hyponastic leaves. **(C)** Transgenic *35S::CKX2-Slglk2* has greater ramification. Images adapted from http://esalq.usp.br/tomato/index.html.

All genotypes were originally obtained from *Laboratory of Hormonal Control of Plant Development* (ESALQ-USP). Plants were cultivated in 2L rectangular plastic pots containing a 1:1 mixture of substrate and vermiculite supplemented with NPK 10:10:10, dolomite limestone ($MgCO_3$ + $CaCO_3$) and magnesium thermophosphate (Yoorin®), under controlled temperature (25 ± 3 ºC), daily automatically irrigation by capillarity, and under natural light conditions (11.5 h/13 h photoperiod on winter/summer, respectively, and 250–350 µmolm−2 s−1 of incident photo-irradiance) in a biosafety level 1 greenhouse (NBI) at the Instituto de Biociências, Universidade de São Paulo.

Fruit pericarp (without placenta and locule walls) were used for biochemical and gene expression analysis in different stages: (i) immature green 3 (IG3, about 15-17 mm diameter for most genotypes and 14-16 mm for *aurea-SlGLK2* genotype); (ii) immature green 5 (IG5, fruit maximum size before it starts the ripening process, about 22 mm for most genotypes, 19 mm for *aurea-SlGLK2* and *aurea-Slglk2* and 16 mm for *dgt*); (iii) mature green (MG, when the placenta displays a gelatinous aspect); (iv) breaker (Br, beginning of ripening process, the fruit begins to present a yellowish coloration); (v) orange (Br+3, three days after breaker stage, the fruits presents orange coloration); (vi) red ripe in two different points (Br+5 and Br+6, 5 and 6 days after breaker stage, respectively). Different stages are presented in Figure 6. Fruits were sectioned in 3 parts, and the most proximal and distal portions to the petiole were used, while the middle region was discarded (Figure 7). Different experiments used different sets of fruit sections and development and ripening stages as indicated. For all the experiments, at least four pools of fruits (biological replicates) were harvested from at least five plants. Samples were frozen in liquid nitrogen and stored at -80ºC freezer until processing. Due to problems in determining fruit stage on L2 green fruits, most biochemical analyses were performed only in ripe fruits, but immature green fruits were used for chlorophyll quantification and qPCR analysis.

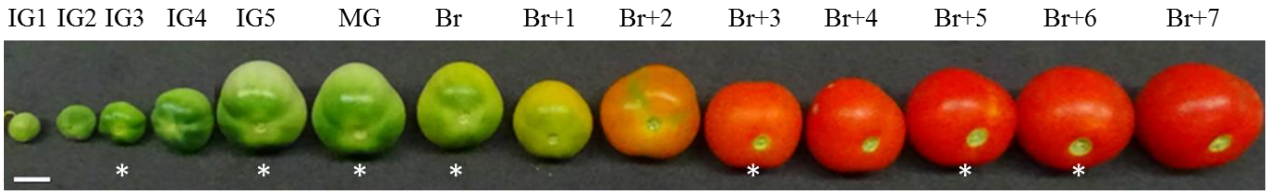

Figure 6: Flower and fruit development stages of wild tomato (*SlGLK2*).
Stages used for the analyses are marked with asterisk (*). UF: unopen flower; OF: open flower; IG: immature green; MG: mature green; Br: breaker; Br+n: n days after breaker. Scale bar: 1 cm.

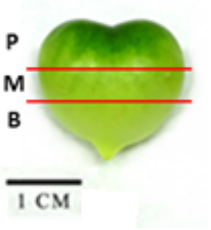

Figure 7: Fruit section scheme.
Fruits were sectioned in 3 parts, being one proximal to the petiole (P), region encompassing the "green shoulder", one basal (B), and the middle (M) region that wasn't used for analyses.

3.2. GLK genes diversity analysis

Phylogenetic analysis of *GLK* genes was performed using 25 protein sequences representing 11 species of Viridiplantae (Supplemental Material II) retrieved from Phytozome V.12.0 database (Goodstein *et al*. 2011), using AtGLK1 sequence, obtained from TAIR (Lamesch *et al*. 2011), as query. Amino acid sequences were aligned in the program T-COFFEE, using the structural alignment method (Expresso) (Notredame *et al*. 2000). Phylogenetic reconstruction was performed with the program PHYML with substitution model LG and proportion of invariable sites and gamma shape parameter estimated from data. Clades were corroborated through bootstrap analysis from 100 replicates (http://www.hiv.lanl.gov/content/sequence/PHYML/interface.html).

3.3. Analysis of SlGLK1 and SlGLK2 genes expression

3.3.1. Total RNA extraction and cDNA synthesis

RNA extraction and cDNA synthesis were performed as described in Quadrana *et al*. (2013). The absence of genomic contamination was verified by PCR, using primers for actin gene that anneal to different exons (Act-F and Act-R, Supplemental Material I). For these reactions were used 0,2 mM of each dNTP, 0,2 mM of each primer, 50 ng of cDNA and 1 U of Taq DNA polymerase® (Invitrogen) enzyme. Amplification conditions were 94ºC for 10 min; 35 cycles of 94ºC for 30 s, 55ºC for 30 s, 72ºC for 1 min; final extension at 72ºC for 10 min. Amplicons were analyzed by electrophoresis in 1% agarose gel in TBE 0,5X. The expected fragment sizes were 818 bp and 521 bp for genomic DNA or cDNA, respectively. Finally, cDNA samples were diluted in 1:10, obtaining final concentration of approximately 5 ng of cDNA/µL.

3.3.2. Real Time quantitative PCR (qPCR)

Reactions were performed using 2,8 µL of diluted cDNA, primer concentration from 200 µM to 800 µM (Supplemental Material I) and 7 µL 2X SYBR Green Master Mix (Qiagen), using thermocycler 7500 PCR Real Time (Applied Biosystems), following amplification program of 95ºC for 10 min and 40 cycles of 95ºC for 15 s, 60ºC for 30 s and 72 ºC for 30 s (moment at which the acquisition of SYBR Green signal occurs). Expression values were normalized against the geometric mean of two constitutively expressed genes, *EXPRESSED* and *TIP41* according to Quadrana *et al*. (2013). Cycle threshold values (Cts) and primer efficiency were obtained with LinRegPCR software (Ruijter *et al*. 2009). Statistical differences in expression values (P>0,05) were calculated with a permutation test, which lacks sample distribution assumptions (Pfaffl *et al*. 2002), using the algorithms in the fgStatistics software (Di Rienzo 2009). Gene expression patterns were presented in the form of heat maps, constructed with Morpheus program

(https://software.broadinstitute.org/morpheus/). Primer sequence and primer concentration for all analyzed genes are described in Supplemental Material I.

3.4. Transgenic plant generation

3.4.1. Bacterial strains and vectors

To obtain transgenic plants overexpressing *SlGLK2*, the following bacterial strains and plasmid vectors were used:

***Escherichia coli* strain DH10B:** All cultures were performed in LB medium (Luria-Delbrück medium) at 37ºC. Liquid cultures were performed under agitation speed of 180 rpm. Depending on the plasmid vector, the selection of transformants was performed by adding the adequate antibiotic to the culture medium.

***Agrobacterium tumefaciens* strain EHA105:** This strain is resistant to rifampicin (25 mg/L) and streptomycin (300 mg/L). Bacteria were cultivated in YEP medium with antibiotic at 28ºC. Liquid cultures were performed under agitation speed of 180 rpm.

Plasmids: Vectors used for construct obtainment and plant transformation were pENTR/D-TOPO and pK7WG2D,1, respectively (Table 2, Supplemental Material III).

Table 2. Vectors used.

Vectors	Resistance in bacteria	Resistance in plants	Characteristics	Origin
pENTR/D-TOPO	Kanamycin	-	Vector linearized with directional cloning site for blunt-end PCR products. Contains *attL1* and *attL2 sites* for site-specific recombination of entry clone with Gateway® system destination vector.	Invitrogen
pK7WG2D,1	Spectinomycin Streptomycin	Kanamycin	Binary destination vector. Contains CaMV 35S promoter; *attL1* and *attL2* sites for Gateway® recombination; 35S terminator; independent promoter associated to GFP marker coding region; *ccdB* gene for negative selection.	Karimi *et al.* (2002) (Supplemental Material III)

3.4.2. Vector construction

For *SlGLK2* coding sequence amplification, cDNA was synthesized following the protocol described in section 3.3.1., in this case oligo-dT were used instead of random primers.

PCR reaction was performed using 50 ng of cDNA, 0,2 mM of each dNTP, 0,2 mM of each primer (GLK2_seq_F and OE_GLK2-R, Supplemental Material I), 1,5 mM of $MgCl_2$ and 1 U of Platinum® Pfx DNA polymerase enzyme (Invitrogen). Amplification program comprised 94ºC for 3 min; 35 cycles of 94ºC for 30 s, 55ºC for 30 s, 68ºC for 1 min; final extension at 68ºC for 10 min. PCR products were verified by electrophoresis in 1% agarose gel in TBE 0,5X. Fragments were

purified using GFX PCR DNA and gel purification kit (GE Healthcare #28903470) and inserted in pENTR/D-TOPO (Invitrogen #450218) entry vector following manufacturer protocol.

An aliquot of 50 µL of competent *E. coli* DH10B was transformed with 2 µL of ligation product. Bacteria were kept in ice for 30 min and submitted to heat shock at 42ºC for 45 s, followed by 2 min on ice. Then, bacteria were incubated in 500 µL of SOC medium at 37ºC and 180 rpm for 45 min. Samples were centrifuged for 3 min at 5000 rpm at room temperature and 300 µL of supernatant were discarded. Bacteria were resuspended in the remaining supernatant and plated in LB agar medium with kanamycin, and incubated at 37ºC for 16 hours. Isolated colonies were grown in 4 mL LB liquid medium with kanamycin for 16 hours at 37ºC with 180 rpm agitation speed. The presence of the desired fragment was confirmed from liquid cultures by PCR using universal primers M13-F and M13-R (Supplemental Material I). Plasmids of positive colonies were purified with QIAprep Spin Miniprep Kit (QIAGEN #27106). The integrity of the clones was confirmed by sequencing using the same primers.

For fragment insertion in the destination binary vector, the entry and the pK7WG2D,1 (Supplemental Material III) plasmids were recombined with LR clonase enzyme (Invitrogen #11791020). 2 µL of recombination product were used for competent E. coli DH10B transformation as described above. Positive clones were identified by PCR, and confirmed by sequencing and endonuclease restriction with HindIII and XbaI. Clones were introduced in *A. tumefaciens* strain EHA105 following protocol described in Shen & Forde (1989).

3.4.3. Plant transformation

Transformation of *S. lycopersicum* (cv. Micro-Tom) *aurea-Slglk2* was performed via *A. tumefaciens*, following protocol described by Pino *et al.* (2010).

3.4.4. Genotyping transgenic lines

Genomic DNA of transgenic lines were extracted from 100 mg of fresh leaves, using GeneJetTM Plant Genomic DNA Purification Mini Kit (Fermentas K0792), following manufacturer protocol. The presence of the transgene was verified by PCR using 50 ng of gDNA 0,2 mM of each dNTP, 0,2 mM of each primer (35S-F and GLK2_seq_R, Supplemental Material I), 1,5 mM of $MgCl_2$ and 2,5 U of Taq DNA polymerase® (Invitrogen) enzyme. Amplification conditions were 94ºC for 10 min; 35 cycles of 94ºC for 30 s, 55ºC for 30 s, 72ºC for 1 min; final extension at 72ºC for 10 min. Amplified products were verified via electrophoresis in agarose gel (1%, TBE 0,5%).

3.4.5. Transgene expression level

SlGLK2 overexpression level in transgenic lines was confirmed by qPCR as described in section 3.3. by using RT-GLK2 F and RT-GLK2 R primers (Supplemental Material I).

3.4.6. Total protein extraction, quantification and Western Blot

Approximately 400 mg of immature green fruits were frozen in liquid nitrogen, grounded and lyophilized. The homogenized tissue was resuspended in extraction buffer (1:1 w/v ratio) containing 10 mM KCl, 5 mM MgCl 2, 400 mM sucrose, 10 mM β-mercaptoethanol, 100 mM Tris-HCl, pH 8, 10% glycerol, 1 mM PMSF (Isogai *et al.* 1998) and 1:100 Protease Inhibitor Cocktail (Sigma-Aldrich # P9599) and centrifuged twice at 12000 RPM for 15 min at 4°C. The supernatant was collected and quantified using the Bradford assay (Bradford 1976). 80 µg of total protein extracts were separated by SDS/PAGE on a 12% (w/v) acrylamide (30% acrylamide/Bis Solution, 29:1; Bio-Rad) gel, and transferred on a 0.45-mm nitrocellulose membrane (Bio-Rad # 1620115). The membrane was stained with Ponceau Red to assess equal transfer. Blotted membrane was blocked in Tris-buffered saline (TBS) containing 0.1% Tween 20 (TBS-T) with 5% dry milk (Biorad # 1706406) for 1 h and 30 min at 37°C, and then washed three times for 5 min with TBS-T and incubated with a specific polyclonal antibody raised against synthetic peptide based on specific amino acid sequence of SlGLK2 (peptide sequence: CSLSYKNERENYD) (FastBio, Brazil). After incubation with the primary antibody the membrane was washed and subsequently incubated with Alkaline phosphatase-coupled anti-rabbit secondary antibody (Sigma-Aldrich # A-3687) for 3 h at room temperature. AP Conjugate Substrate Kit (Bio-Rad # 1706432) was used for detection.

3.5. Biochemical and plant growth analyses

3.5.1. Evaluation of growth and yield parameters in the transgenic lines

Regarding growth analysis, all the ripe fruits on Br+6 stage were harvested from 12 plants of each line and individually weighted. By the end of the harvest, the aerial part of each plant was also individually weighted. Total number of fruits per plant and total aerial weight (vegetative portion + total fruit weight per plant) were used for calculation of harvest index, using the formula:

Harvest index = total fruit weight*100/aerial biomass

3.5.2. Chlorophyll quantification

Chlorophyll quantification was performed from 100 mg of grounded leaf tissue and 200 mg fruit pericarp tissue. Extraction was conducted as described in Porra *et al*. (1989). The absorbance of the supernatants was read in spectrophotometer at 664 and 647 nm. Based on obtained

absorbance, chlorophyll *a* and *b* concentrations were calculated using equations below (Porra *et al*. 1989). Total chlorophyll content was normalized by fresh weight.

Chlorophyll *a*= 12 * Abs 664 – 3,11 * Abs 647

Chlorophyll *b*= 20,78 * Abs 647 – 4,88 * Abs 664

3.5.3. Quantification of starch and soluble sugars

For soluble sugars quantification 200 mg of grounded fruit pericarp were used for extraction with ethanol 80% (v/v) four times as described by Freschi *et al*. (2010). The total supernatant was centrifuged and filtered through 0.45 µm membrane, and 1 mL of extract was dried under vacuum in a SpeedVac system and resuspended in 1 mL of ultra-pure water. Glucose, fructose and sucrose were quantified by high performance anion exchange chromatography with pulsed amperometric detection (HPAEC-PAD; Dionex, Sunnyvale, CA, USA) using a Carbopac PA1 column (250 x 4 mm, 5 µm particle size, Dionex) in an isocratic run with 18 mM NaOH as mobile phase. Content of each sugar was calculated using standard curves made with pure glucose, fructose and sucrose.

The pellets were used for starch extraction and quantification, performed according to protocol described by Freschi *et al*. (2010).

3.5.4. Tocopherol extraction and quantification

Tocopherol extraction and quantification was performed following protocol described in Lira *et al*. (2017).

3.5.5. Quantification of GUS activity by fluorometric assay

Fruits of genotypes *DR5::GUS* and *ARR5::GUS* in *SlGLK2/Slglk2* or *Slglk2/Slglk2* background were ground in liquid nitrogen and analyzed through *in vitro* GUS activity quantitative assay, using methylumbelliferyl-β-D-glucuronide (MUG), as described by Jefferson *et al.* (1987).

3.5.6. Transmission electron microscopy

Samples of immature green fruits at IG5 stage from transgenic lines and controls were fixed in glutaraldehyde 2,5% in sodium phosphate buffer (0,1 M pH 7,2) for 2 hours, post-fixed in sodium tetroxide 2% in same buffer for 2 hours and treated with tannic acid 1% in sodium phosphate buffer (0,05 M pH 7,2) for 16 hours. Dehydration was performed gradually in acetone and, finally, samples were included in Spurr resin (Electron Microscopy Science #14300). For plastid ultrastructure analysis, ultra-thin sections were stained with uranyl acetate (Watson, 1958) and citrate (Reynolds, 1963), and finally visualized under transmission electron microscopy Zeiss EM 900.

3.5.7. Chloroplast number

Slides from immature green fruits at IG5 stage from transgenic lines were prepared as described by Pyke (2011) and analyzed in optical microscopy Axio Imager M2. Chloroplast number were counted manually.

3.6. Data analysis

Differences in parameters were statistically evaluated using Infostat software v. 2016 (Di Rienzo *et al*. 2016). When data set showed homoscedasticity, ANOVA analysis was performed to compare values along development in the same genotype ($P<0,05$). In the absence of homoscedasticity, non-parametric analysis was performed using the Krustal Wallis test ($P<0,05$). To compare values between transgenic lines and controls, Student's t-test was performed ($P>0,05$).

IV. Results

4.1. GLK gene diversity analysis in Viridiplantae

A phylogenetic reconstruction of GOLDEN 2-LIKE protein family was performed with 25 protein sequences (Supplemental Material II) representing 11 species of Viridiplantae (Figure 8).

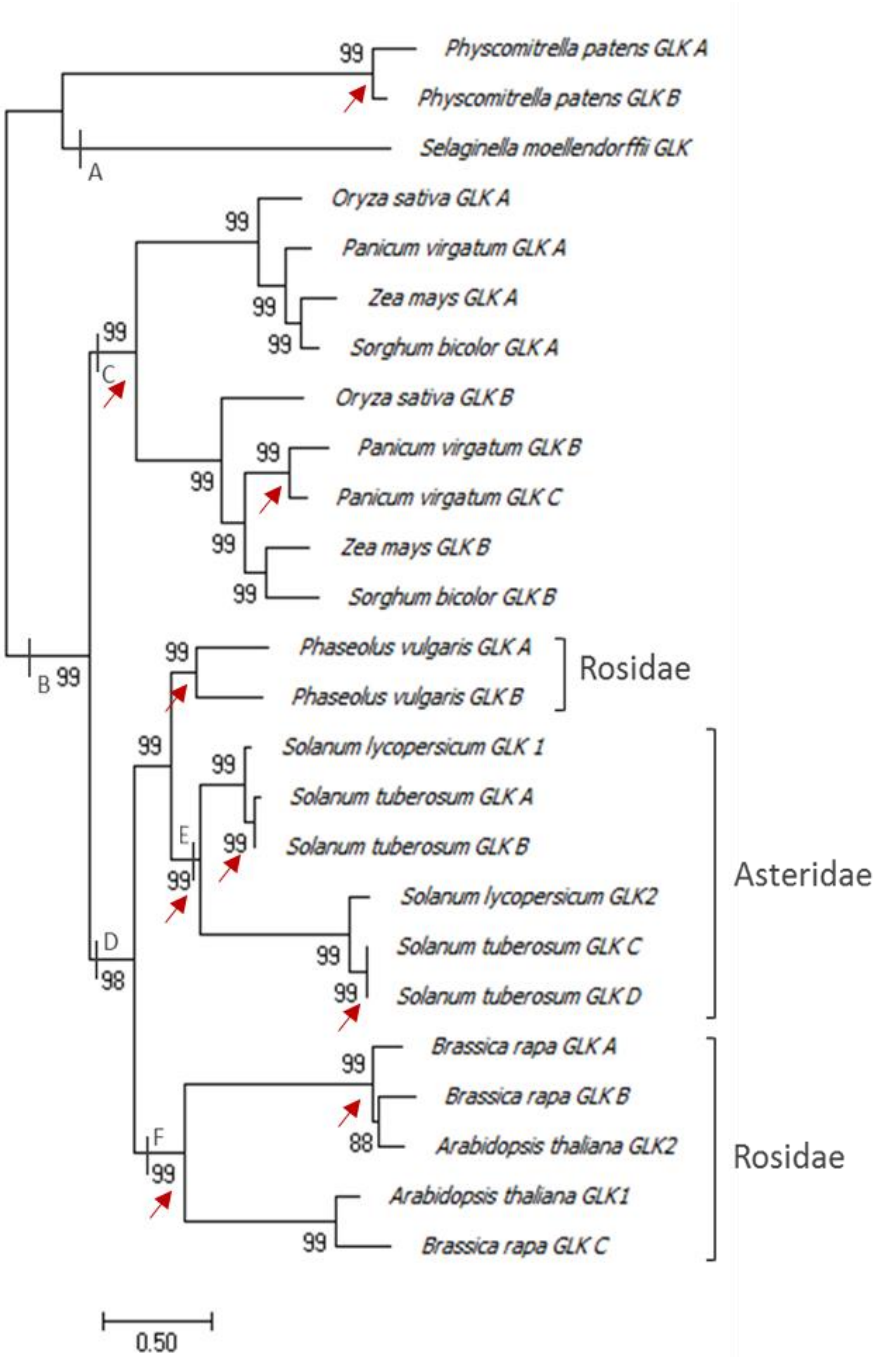

Figura 8: Phylogenetic analysis from GOLDEN 2-LIKE family.
Twenty-five GOLDEN 2-LIKE protein sequences retrieved from Phytozome V.12.0 database, representing 11 species whose genomes were completely sequenced, were used for phylogenetic reconstruction. Numbers in nodes represent bootstrap analysis from 100 replicates. A: Lycopodiopsida; B: Magnoliophyta; C: Liliopsida; D: Rosopsida; E: Solanaceae; F: Brassicaceae. Independent duplication events are indicated by red arrows.

The tree displayed a complex topology, revealing nine independent duplications. The number of paralogs varies between one, in *Selaginella moellendorffii*, to four, in *Solanum tuberosum*, with most species harboring two paralog genes. Independent duplication events originated the monocotyledons and eudicotyledons *GLK* copies. Terminal duplications occurred in *Physcomitrella patents*, *Panicum virgatum*, *Phaseolus vulgaris*, *S. tuberosum* and *Brassica rapa*. In agreement to that previously reported by Powell *et al*. (2012), Brassicaceae species (*Brassica rapa* and *A. thaliana*) did not group together with *Phaseolus vulgaris*, which also belongs to Rosideae clade.

The duplication that originated *SlGLK1* and *SlGLK2* occurred in Solanaceae lineage previous to the divergence between *S. lycopersicum* and *S. tuberosum.* Additionally, in potato, each *GLK* gene duplicated again giving rise to the four paralogs found in this species. New sequences in *S. lycopersicum* were not identified beyond previously reported *SlGLK1* and *SlGLK2*.

The most basal species that contains *GLK* genes in this analysis is the moss *Physcomitrella patens* that has two paralogs result from an exclusive duplication (Bravo-Garcia *et al.* 2009).

4.2. Effect of PHY-mediated light perception on SlGLK2 expression and its effect on fruit quality

4.2.1. SlGLKs gene expression in fruits of wild type plants (SlGLK2), Slglk2 and PHY-deficient (aurea-SlGLK2) mutants.

In accordance with previous report (Powell *et al*. 2012), *SlGLK2* expression levels in fruits were much higher (at least 7 times) than *SlGLK1* in all stages (IG: immature green, MG: mature green, Br: breaker, Br+3: three days after breaker and Br+5: five days after breaker; see material and methods for details) and genotypes analyzed (Table 3), and for this reason, all further analyses were performed only with *SlGLK2*.

Table 3. *SlGLK2* expression levels relative to *SlGLK1* in fruits along development and ripening.
Bold values represent statistically significant values (P<0,05). Values represent mean of at least four biological replicates. nd: non-detected.

	IG3		IG5		MG		Br		Br+3	
	SlGLK1	SlGLK2	SlGLK1	SlGLK2	SlGLK1	SlGLK2	SlGLK1	SlGLK2	SlGLK1	SlGLK2
SlGLK2	1.00 ± 0.13	**33.94 ± 05.43**	1.00 ± 0.31	**21.25 ± 03.67**	1.00 ± 0.34	**82.07 ± 08.05**	1.00 ± 0.35	**160.8 ± 24.80**	1.00 ± 0.12	**34.43 ± 5.51**
Slglk2	1.00 ± 0.10	**17.39 ± 01.73**	1.00 ± 0.06	**07.42 ± 01.03**	1.00 ± 0.11	**41.71 ± 22.26**	1.00 ± 0.27	**79.15 ± 12.84**	nd	nd
aurea-SlGLK2	1.00 ± 0.09	**444.8 ± 49.37**	1.00 ± 0.74	**3642 ± 425.9**	1.00 ± 0.18	**101.4 ± 30.09**	1.00 ± 0.32	**138.8 ± 26.26**	1.00 ± 0.29	**09.23 ± 1.55**

Comparing transcript relative abundance in the pedicelar region to that observed in the basal region of the fruit, it was evident that *SlGLK2* is more expressed in pedicelar region in all three genotypes analyzed (Figure 9A). This observation corroborates previous reports describing that *SlGLK2* expression increases from the bottom to the top of the fruits (Powell *et al*. 2012). Interestingly, the mutant allele, *Slglk2*, is also expressed with the same pattern, although with lower values when compared to SlGLK2 genotype. Thus, the subsequent analyses were focused only on the pedicelar region of the fruits.

During fruit development and ripening, *SlGLK2* displayed different expression patterns in the three genotypes analyzed. While the wild type *SlGLK2* showed the maximum expression level at IG5 stage, the mutant allele, *Slglk2*, peaked latter at MG, decaying after Br stage. Interestingly, *SlGLK2* in *aurea-SLGLK2* mutant showed the highest expression levels at IG3 stage (Figure 9B).

Finally, comparing relative transcript abundance between genotypes, it was possible to observe that compared to wild type genotype, *Slglk2* mutant showed lower transcript levels in all stages, while *aurea-SlGLK2* genotype accumulated higher *SlGLK2* transcript levels during immature stages that rapidly decreased from Br stage onwards (Figure 9C).

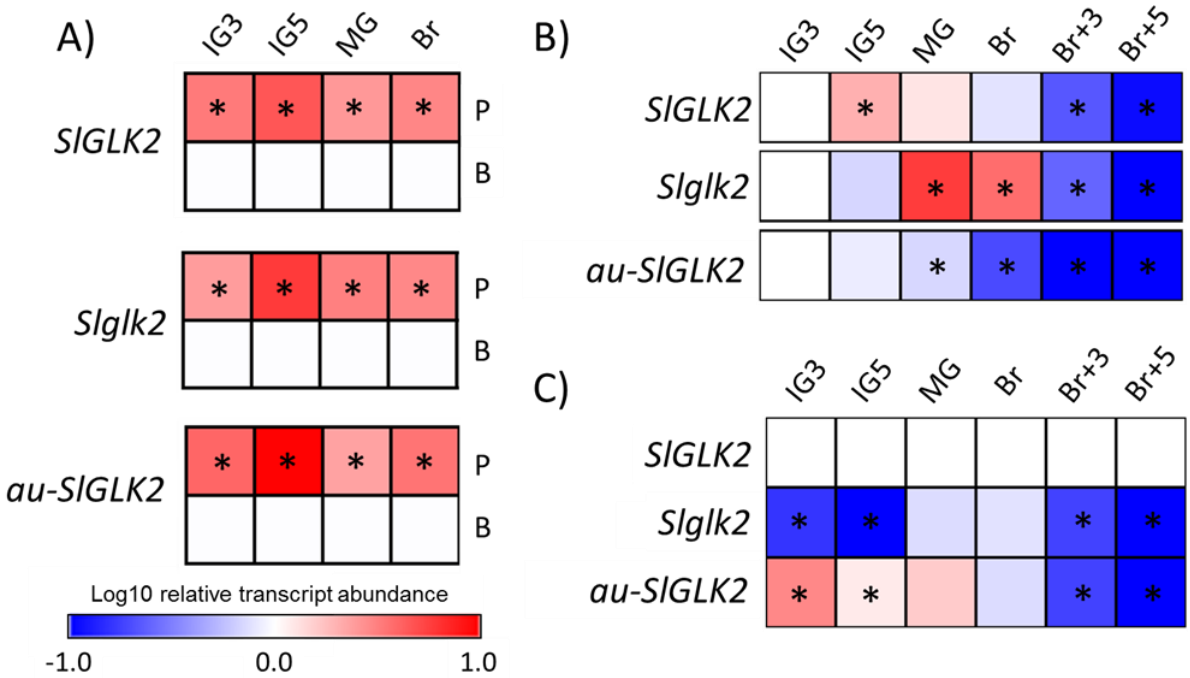

Figure 9: *SlGLK2* expression pattern.
Heat map representation of *SlGLK2* relative abundance obtained by qPCR in wild type (*SlGLK2*), *uniform ripening* (*Slglk2*) and *aurea-SlGLK2* mutant genotypes. **A)** Expression level comparison between pedicelar (P) and basal (B) regions of the fruit in all three genotypes, in all analyzed stages; **B)** Expression level along fruit development and ripening in relation to IG3 in pedicelar region; **C)** *SlGLK2* expression levels in *Slglk2* and *aurea-SlGLK2* in relation to *SlGLK2* wild type genotype. Asterisks (*) represent statistically significant values (P<0,05). Values represent mean of at least four biological replicates.

Thus, these results showed that the mutant allele *Slglk2* is also expressed, although in much less amount that the wild type, and that PHY-mediated light perception impairment alters the pattern of *SlGLK2* expression along fruit development and ripening enhancing the levels of transcript during the immature stages.

4.2.2. Effect of SlGLK2 on fruit nutritional quality.

Being demonstrated that PHY-mediated light perception modifies the expression of *SlGLK2*, we further explored the effect of PHY deficiency and the presence of SlGLK2 on nutritional quality. To accomplish this aim, chlorophylls, tocopherol, starch and soluble sugars were quantified in wild type (*SlGLK2*), *uniform ripening* mutant (*Slglk2*) and *aurea-SlGLK2* mutant genotypes. Although chlorophyll is absent in the edible fruit, its content was measured because of its metabolic link with tocopherol biosynthesis.

Fruits from *SlGLK2* plants showed higher amounts of total chlorophyll than the mutant genotypes, revealing that light and SlGLK2 are key factors for chlorophyll accumulation. There was no significant difference between *Slglk2* and *aurea-SlGLK2* genotypes (Figure 10).

Tocopherol analysis in these fruits resulted in significant difference between genotypes as well. The amount of tocopherol in Br+5 stage (red ripe fruit) correlated with chlorophyll content at IG3 stage. While *aurea-SlGLK2* mutant displayed the lowest levels of tocopherol in all analyzed stages, the difference between *SlGLK2* and *Slglk2* was evident only at the Br+5 stage (Figure 10). Noteworthy to mention, the increments in γ- and δ-tocopherol content were responsible for the significant difference in total-tocopherol between *SlGLK2* and *Slglk2* genotypes at Br+5 stage (Figure 11).

Soluble sugar contents, *i.e.* glucose, fructose and sucrose, was profiled in *SlGLK2*, *Slglk2* and *aurea-SlGLK2* genotypes. *SlGLK2* and *Slglk2* have very similar values for glucose and fructose, but sucrose levels are significant higher in *SlGLK2* genotype. Regarding *aurea-SlGLK2* mutant, higher levels of the three soluble sugars were observed in almost all the stages analyzed in comparison with the control *SlGLK2* genotype, which agreed to *SlGLK2* expression profile, which showed higher levels in *aurea-SlGLK2* background (Figure 12).

Starch content analysis revealed that *aurea-SlGLK2* is the genotype that accumulated the highest amount of starch, while the wild type *SlGLK2* showed the lowest starch content at MG stage (Figure 12).

In summary, the lack of *SlGLK2* and the impairment of light perception in *aurea-SlGLK2* mutant compromised the content of tocopherol. Regarding sugars and starch, the mutations resulted in a general trend of increment compared to wild type genotype, in particular in *aurea-SlGLK2*.

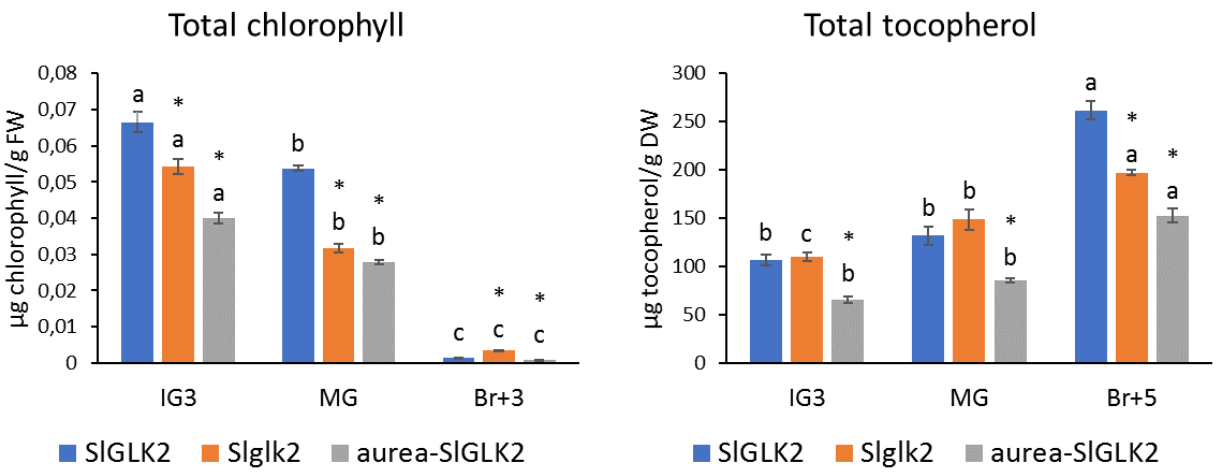

Figure 10: Chlorophyll and tocopherol content in fruits of wild type *(SlGLK2), uniform ripening* (*Slglk2*) and *aurea-SlGLK2* mutant genotypes.
Different letters indicate statistically significant values between stages within each genotype. Asterisk (*) indicates significant difference compared to *SlGLK2* genotype within each stage. Values represent mean ± SE of at least three biological replicates (P<0,05).

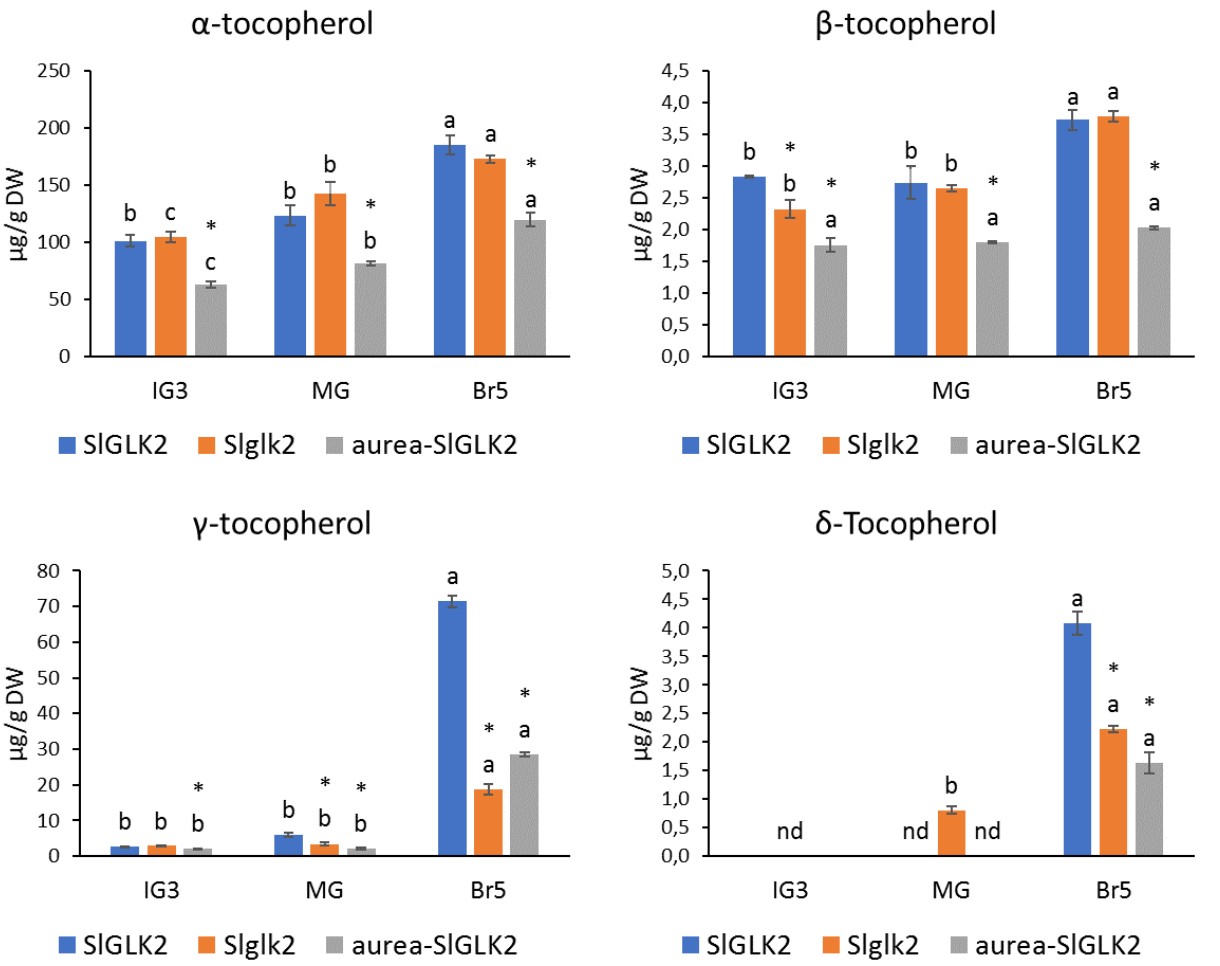

Figure 11: Tocopherol composition.
α, β, γ and δ-tocopherol forms were quantified. Different letters indicate statistically significant values between stages within each genotype. Asterisk (*) indicates significant difference compared to *SlGLK2* genotype within each stage. Values represent mean ± SE of at least three biological replicates (P<0,05). nd: non-detected.

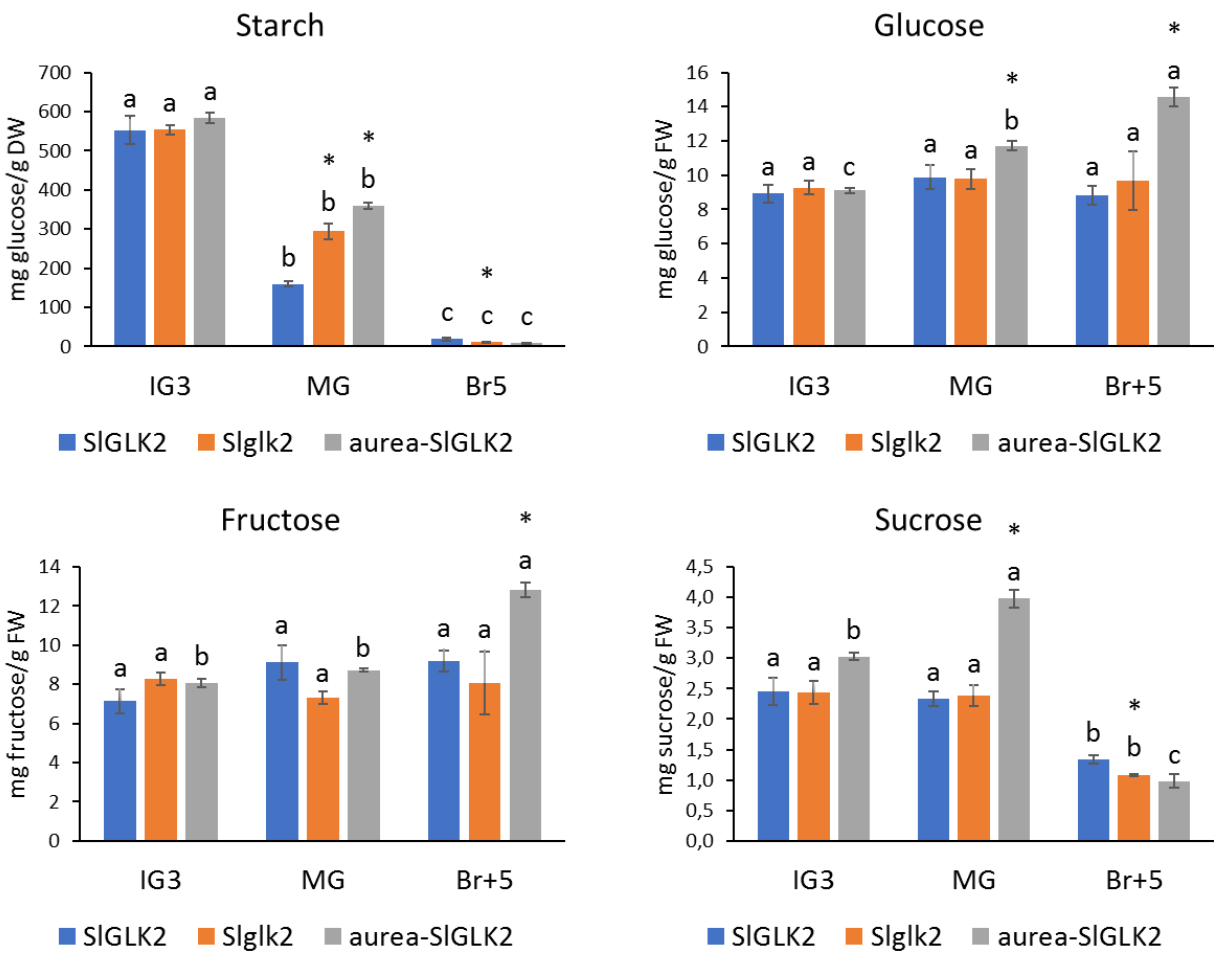

Figure 12: Starch and soluble sugars profile in fruits of wild type (*SlGLK2*), *uniform ripening* (*Slglk2*) and *aurea-SlGLK2* mutant genotypes.
Different letters indicate statistically significant values between stages within each genotype. Asterisk (*) indicates significant difference compared to *SlGLK2* genotype within each stage. Values represent mean ± SE of at least three biological replicates (P<0,05).

4.2.3. Expression profile of isoprenoid biosynthetic genes

To evaluate whether the differences in chlorophyll and tocopherol content were consequence of the differential transcriptional regulation of the biosynthetic enzyme encoding genes, the mRNA amount of eight genes (*DXS(1)* and *GGDR* participate in the production of phytyl-2P, precursor of both chlorophyll and tocopherol synthesis; *VTE1*, *VTE2*, *VTE3(1)* and *VTE4* involved in tocopherol biosynthetic core pathway; and *VTE5* and *VTE6* responsible for phytol recycling providing phytyl-2P for tocopherol core pathway during ripening) was profiled. These genes were chosen because in previous studies they showed to be regulated at transcriptional level and contribute in determining ripe fruit tocopherol content (Almeida *et al.* 2015, Almeida *et al.* 2016). The relative transcript values are detailed in Supplementary Material IV.

The absence of an active SlGLK2 resulted in the decrease of *DXS* and *GGDR* expression at immature fruit stage that might explain the reduced level of chlorophyll observed from early stages

of fruit development in *Slglk2* genotype. Else, the deficiency in light perception in *aurea-SlGLK2* led to the expression reduction in *DXS*, *GGDR*, *VTE2*, *VTE4* and *VTE6* explaining the reduction of tocopherol content in ripe fruits (Figure 13).

Hence, the mRNA profile revealed that the gene expression pattern explains, at least in part, the deficiency in chlorophyll and tocopherol forms observed in both mutant genotypes analyzed.

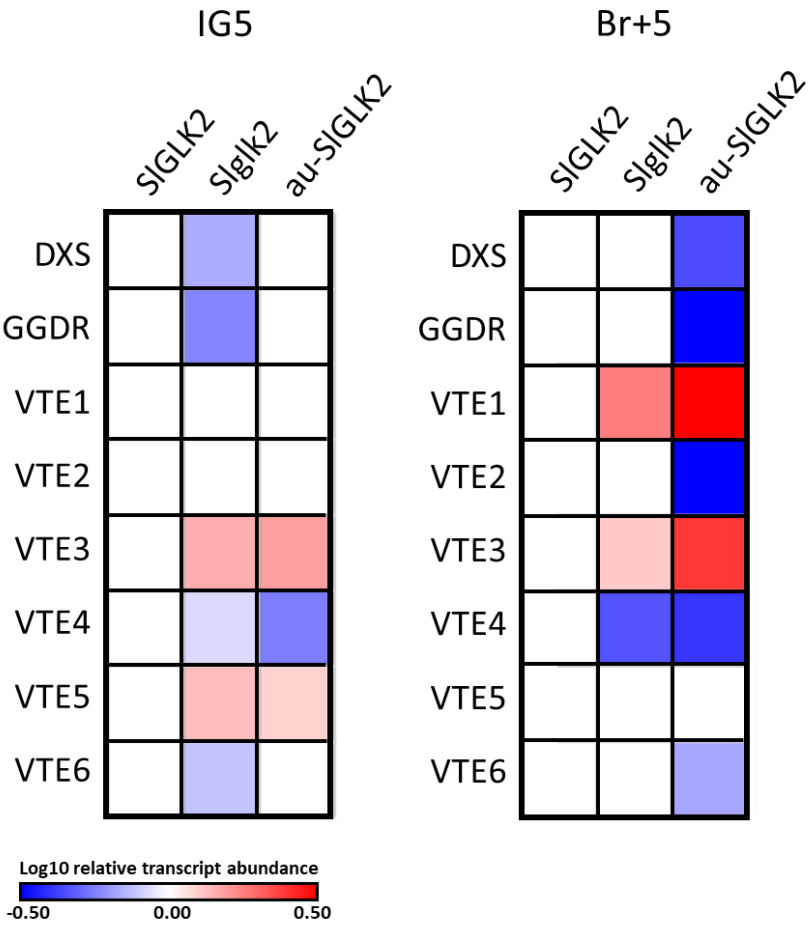

Figure 13: Expression profile of tocopherol biosynthetic enzyme encoding genes in fruits of wild type (*SlGLK2*), *uniform ripening* (*Slglk2*) and *aurea-SlGLK2* mutant genotypes.
The expression profile was obtained by RT-qPCR. The heatmap represents statistically significant differences in relative transcript levels detected *Slglk2* and *aurea-SlGLK2* mutant genotypes compared to wild type (*SlGLK2*) ($P<0.05$). Values represent mean of at least three biological replicates. Relative transcript values are detailed in Supplementary Material IV. DXS: 1-DEOXY-D-XYLULOSE-5-P SYNTHASE; GGDR: GERANYLGERANYL DIPHOSPHATE REDUCTASE; VTE1: TOCOPHEROL CYCLASE; VTE2: HOMOGENTISATE PHYTYL TRANSFERASE; VTE3: 2,3-DIMETHYL-5-PHYTYLQUINOL METHYL TRANSFERASE; VTE4: TOCOPHEROL Γ -METHYL TRANSFERASE; VTE5: PHYTOL KINASE; VTE6: PHYTYL-PHOSPHATE KINASE

4.2.4. Obtainment and characterization of transgenic lines overexpressing SlGLK2 in aurea-Slglk2 genetic background.

In order to evaluate whether the SlGLK2 protein is able to complement the chlorotic phenotype of the PHY-deficient mutant *aurea*, transgenic plants overexpressing *SlGLK2* in *aurea-Slglk2* genetic background were obtained and characterized.

Eight regenerated lines were positive for the presence of the transgene by PCR. Out of those, five showed higher *SlGLK2* expression levels compared to the control *aurea-Slglk2*. The three lines that exhibited the highest relative transcript abundances were selected for further phenotypic characterization (Figure 14), hereafter named as L2, L7 and L8, in T1 generation. Although, L7 and L8 accumulated up to 8-fold more *SlGLK2* mRNA than *aurea-Slglk2* control in IG5 fruits, the amount of SlGLK2 protein was mostly similar than the wild type genotype *SlGLK2* (Figure 15). Differently, L2 line exhibited an increase of *SlGLK2* transcript amount up to 20-fold in fruits, compared to L7 and L8 lines, which reflected in a conspicuous increment in protein content (Figure 15). Thus, it is possible to conclude that the only line that really overexpresses SlGLK2 protein is L2.

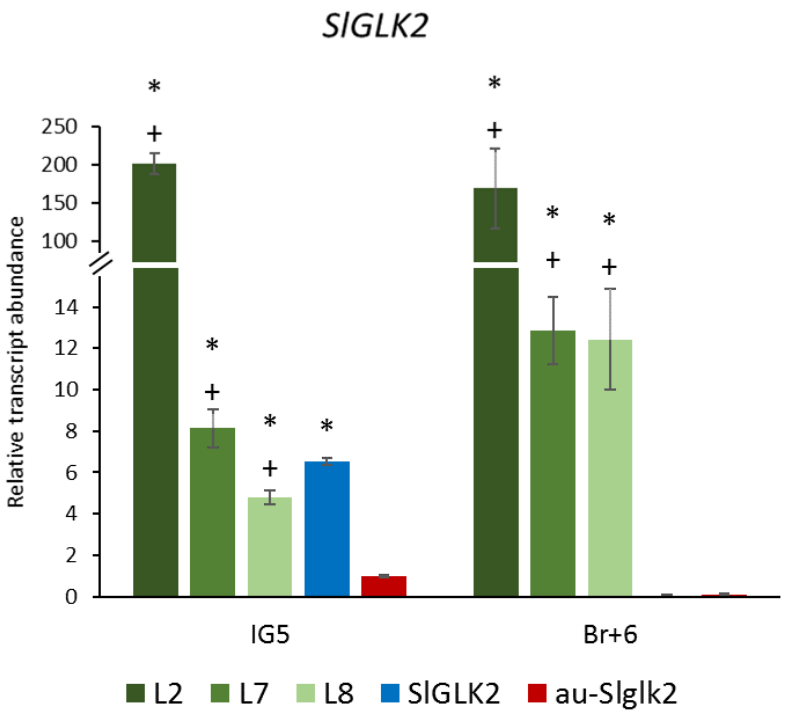

Figure 14: *SlGLK2* expression profile in fruits of transgenic plants.
The expression profile was obtained by qPCR from fruits of the transgenic lines (L2, L7 and L8) and the control genotypes, *SlGLK2* and *aurea-Slglk2*. Asterisk (*) indicates statistically significant differences compared to control *aurea-Slglk2* (P<0,05). Plus signal (+) indicates statistically significant difference between transgenic lines and control *SlGLK2* genotype (P<0,05). Relative transcript abundance values are relative to IG5 *aurea-Slglk2* mutant samples and represent mean ± SE of at least three biological replicates.

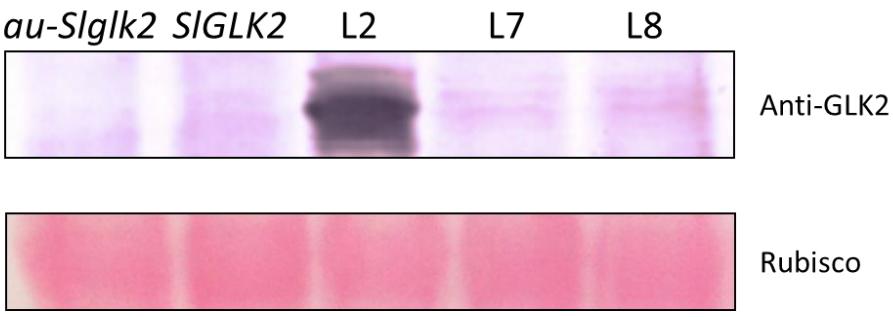

Figure 15: *SlGLK2* protein profile in transgenic lines.
Detection of SlGLK2 protein by Western blot was performed from fruits at IG5 stage of the transgenic lines (L2, L7 and L8) and the control genotypes, *SlGLK2* and *aurea-Slglk2*, using a polyclonal antibody anti-SlGLK2.

4.2.5. Visual phenotyping and productivity parameters of transgenic lines

Transgenic lines L7 and L8 were very similar to each other. The fruits were slightly greener than the control *aurea-Slglk2*, while L2 presented darker green fruits even compared to control *SlGLK2*, exhibiting a wide size variation that hindered the stage determination. Although L7 and L8 lines had leaves with lighter green color than L2, in general, the leaves of transgenic lines showed similar color to control *aurea-Slglk2*, while *SlGLK2* leaves exhibited darker green color. The visual phenotype of transgenic lines and controls are shown in Figure 16.

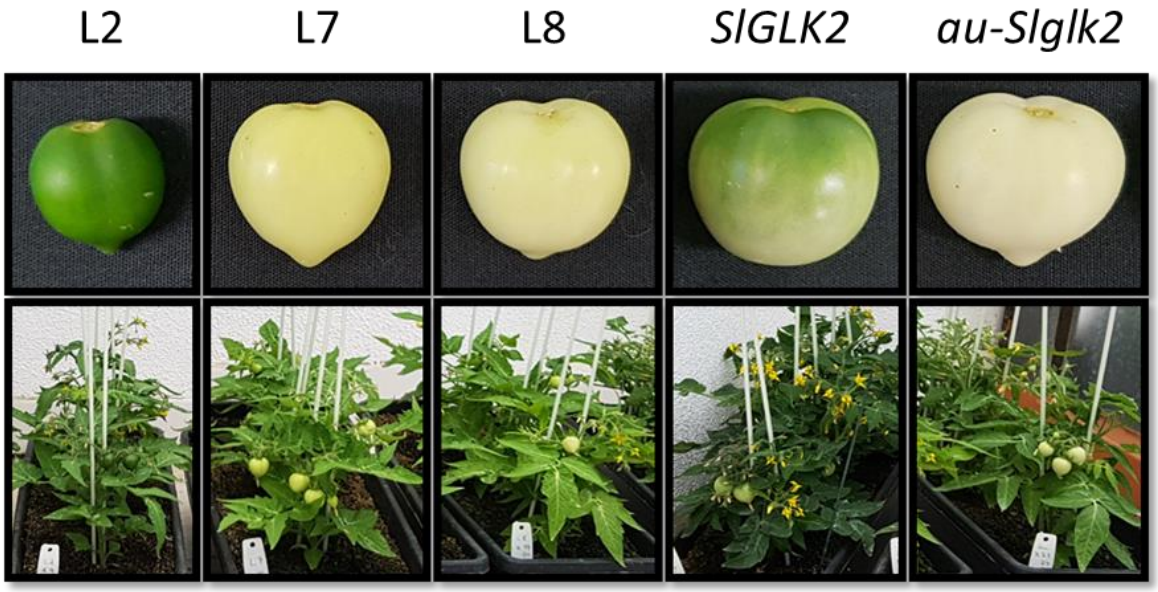

Figure 16: Phenotype of transgenic lines and controls.

As a parameter of industrial quality, the °Brix was measured, which is an estimative of total soluble solids, *i.e.* mainly amino acids, organic acids and soluble sugars. L2 line exhibited higher °Brix in ripe fruits (Br+6 stage) than all the other genotypes. Interestingly, *SlGLK2* control showed significant lower °Brix than *aurea-Slglk2* (Figure 17).

Harvest index, calculated through formula [Harvest index = total fruit weight*100/aerial biomass], did not show significant differences between none of the analyzed genotypes (Figure 18A). Interestingly, transgenic lines produced lighter or fewer fruits (Figure 18B and 18C) but, since the aerial vegetative part (Figure 18D) was lighter than controls as well, no differences in harvest index were observed.

In summary, *SlGLK2* overexpression resulted in considerable penalty in plant growth resulting in less vegetative biomass accumulation and the production of lighter fruits that showed higher content of soluble solids.

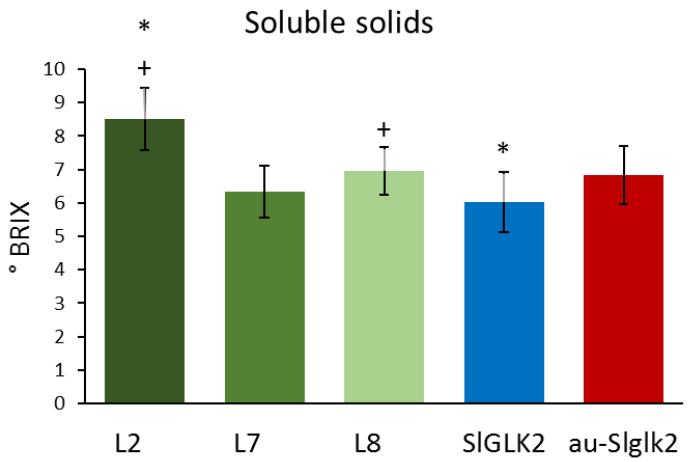

Figure 17: Impact of *SlGLK2* overexpression on total soluble solids content.
Total soluble solids (°Brix) was measured in ripe fruits at Br+6 stage. Asterisk (*) indicates significant differences between transgenic lines and control *aurea-Slglk2*; Plus signal (+) indicates significant differences between transgenic lines and control *SlGLK2* (P<0,05). Values represent mean ± SE of at least 12 biological replicates per genotype.

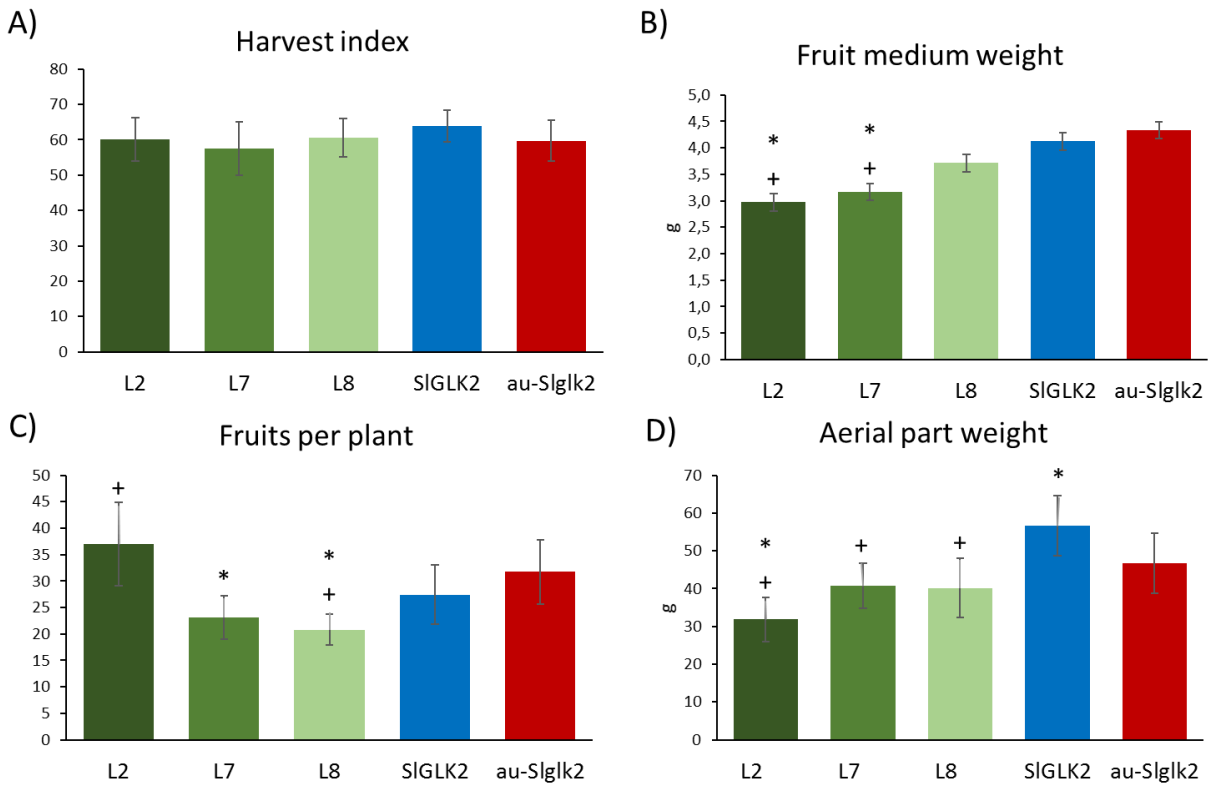

Figure 18: Impact of *SlGLK2* overexpression on productivity parameters.
A) Harvest index was calculated with the formula [total fruit weight*100/aerial biomass]. **B)** Fruit medium weight of Br+6 fruits per plant. **C)** Total number of fruits per plant. **D)** Total vegetative aerial biomass, individually measured after fruit harvesting. Asterisk (*) indicates significant differences between transgenic lines and control *aurea-Slglk2*; Plus signal (+) indicates significant differences between transgenic lines and control *SlGLK2* (P<0,05). Values represent mean ± SE of at least 12 biological replicates per genotype.

4.2.6. *Biochemical analysis*

The measurement of total chlorophyll content in fruits revealed that L2 accumulated 9-fold and 3-fold more chlorophyll than the *aurea-Slglk2* and *SlGLK2* controls, respectively; whereas L7 and L8 revealed similar chlorophyll levels to control *aurea-Slglk2* (Figure 19).

Fruits from L7 and L8 transgenic lines showed similar contents of total tocopherol to control *aurea-Slglk2* genotype, with the exception of the Br+6 fruits from L8 that displayed a discrete increment. On the contrary, ripe fruits of L2 line displayed higher content than *aurea-Slglk2* and similar amount of total tocopherol compared to the wild type control *SlGLK2* (Figure 19). Analyzing the different tocopherol forms, it is evident that the increment in total tocopherol observed in Br+6 fruits of L2 line compared to *aurea-Slglk2* control is due to the increased levels all tocopherol forms, although only γ and δ forms reached levels even higher than control *SlGLK2* (Figure 20).

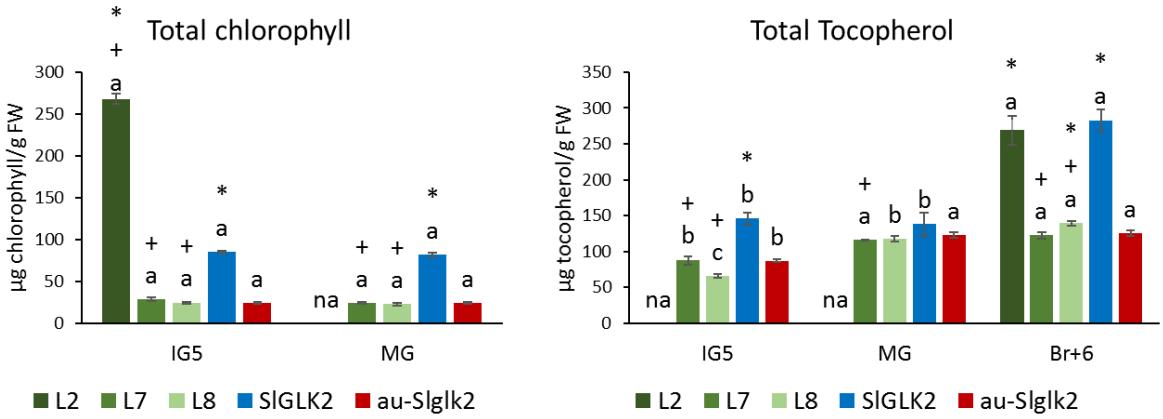

Figure 19: Total chlorophyll and tocopherol content in fruits from transgenic lines.
The chlorophyll and tocopherol content was quantified from fruits of the transgenic lines (L2, L7 and L8) and the control genotypes, *SlGLK2* and *aurea-Slglk2*. Different letters indicate statistically significant differences between stages within each genotype. Asterisk (*) indicates statistically significant differences compared to control *aurea-Slglk2* (P<0,05). Plus signal (+) indicates statistically significant difference between transgenic lines and control *SlGLK2* genotype (P<0,05). Values represent mean ± SE of at least three biological replicates. na: non-analyzed due to the lack of enough fruits.

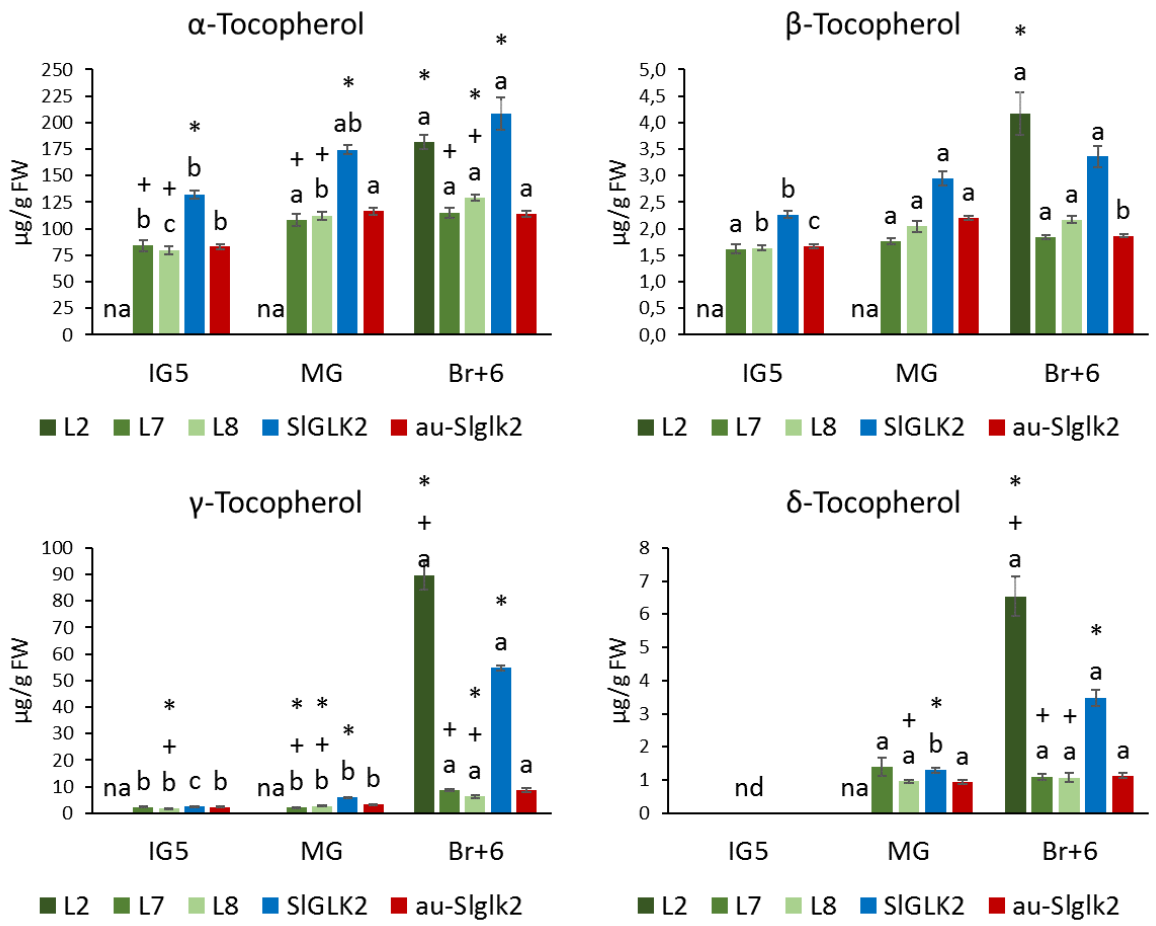

Figure 20: Tocopherol composition in fruits from transgenic lines.
α, β, γ and δ-tocopherol forms were quantified. Different letters indicate statistically significant differences between stages within each genotype. Asterisk (*) indicates statistically significant differences compared to control *aurea-Slglk2* (P<0,05). Plus signal (+) indicates statistically significant difference between transgenic lines and control *SlGLK2* genotype (P<0,05). Values represent mean ± SE of at least three biological replicates. na: non-analyzed due to the lack of enough fruits; nd: non-detected.

Intriguingly, immature green fruits from L7 and L8 lines showed lower content of starch than *aurea-Slglk2* control. Quantification of soluble sugars revealed that L2 had higher glucose, fructose and sucrose content in ripe fruits when compared to *aurea-Slglk2*, with values even greater than *SlGLK2* control for glucose and sucrose. L7 and L8 showed similar values of soluble sugar to *aurea-Slglk2*, except for fructose and glucose in MG stage of L7 that exhibited lower content and higher sucrose amount in Br+5 of L8 line (Figure 21).

These results show that SlGLK2 overexpression reverted the deficiency in chlorophyll, tocopherol and soluble sugar of *aurea-Slglk2* fruits.

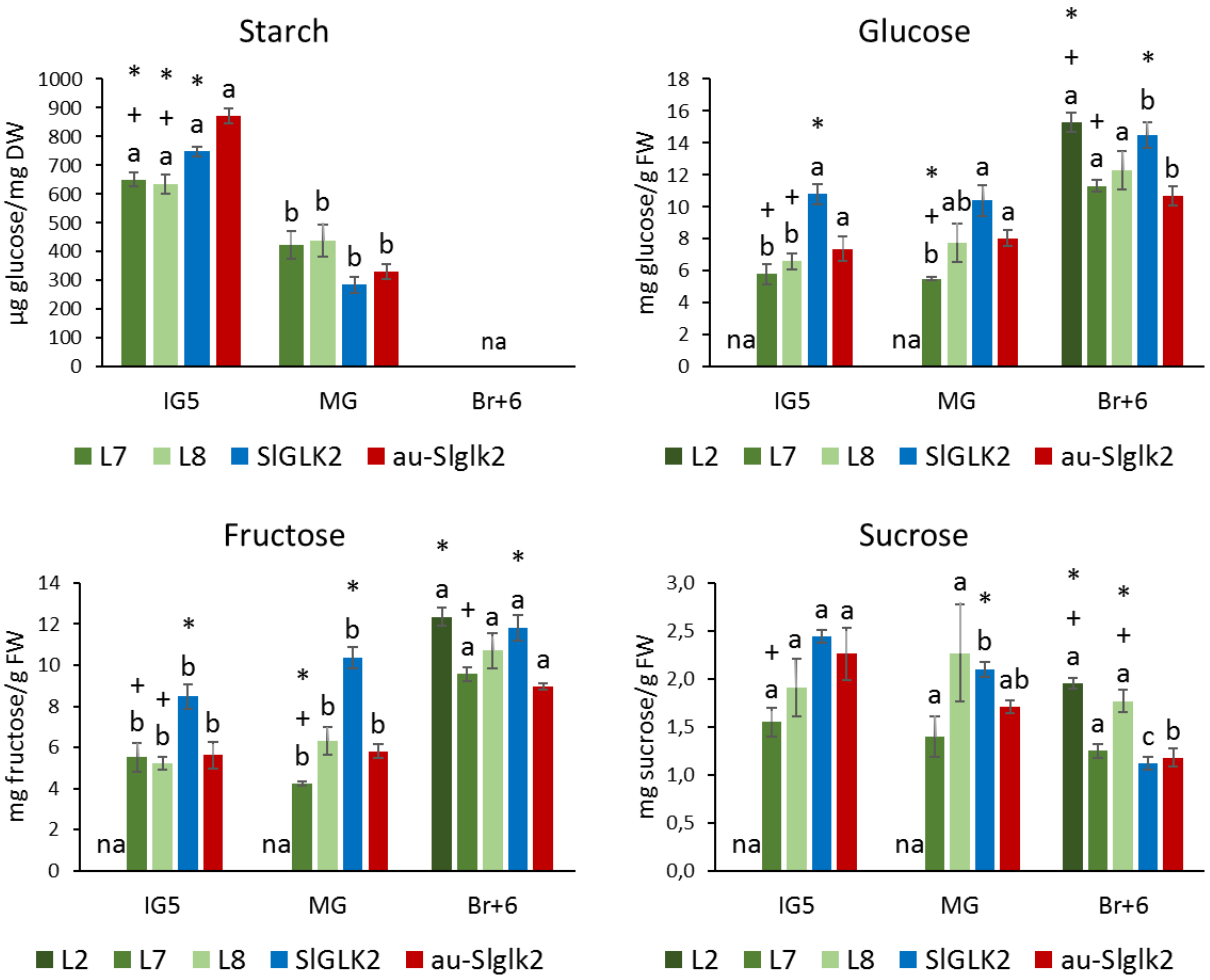

Figure 21: Starch and soluble sugars content in fruits from transgenic lines.
Starch and soluble sugars were quantified from fruits of the transgenic lines (L2, L7 and L8) and the control genotypes, *SlGLK2* and *aurea-Slglk2*. Different letters indicate statistically significant differences between stages within each genotype. Asterisk (*) indicates statistically significant differences compared to control *aurea-Slglk2* (P<0,05). Plus signal (+) indicates statistically significant difference between transgenic lines and control *SlGLK2* genotype (P<0,05). Values represent mean ± SE of at least three biological replicates. na: non-analyzed due to the lack of enough fruits.

4.2.7. Expression profile of isoprenoid biosynthetic genes

To better understand the origin of the differences observed in chlorophyll and tocopherol biochemical profile observed in the transgenic lines, the expression of some of the metabolic enzyme encoding genes were profiled by qPCR. Interestingly, all of the analyzed genes showed to be upregulated in L2 when compared to control *aurea-Slglk2* in at least one of the analyzed stages, with the exception of *HPPD2* gene, which is downregulated in *aurea-Slglk2* control and all of the transgenic lines compared to *SlGLK2*. Both L7 and L8 presented very few differences when compared to *aurea-Slglk2*, exhibiting mostly downregulated genes (Figure 22).

It is noteworthy mentioning that all enzymes coding genes that were upregulated in *SlGLK2* in comparison to *Slglk2* (Figure 14) were also found upregulated in L2, which suggest that they are indeed directly or indirectly regulated by SlGLK2 transcription factor.

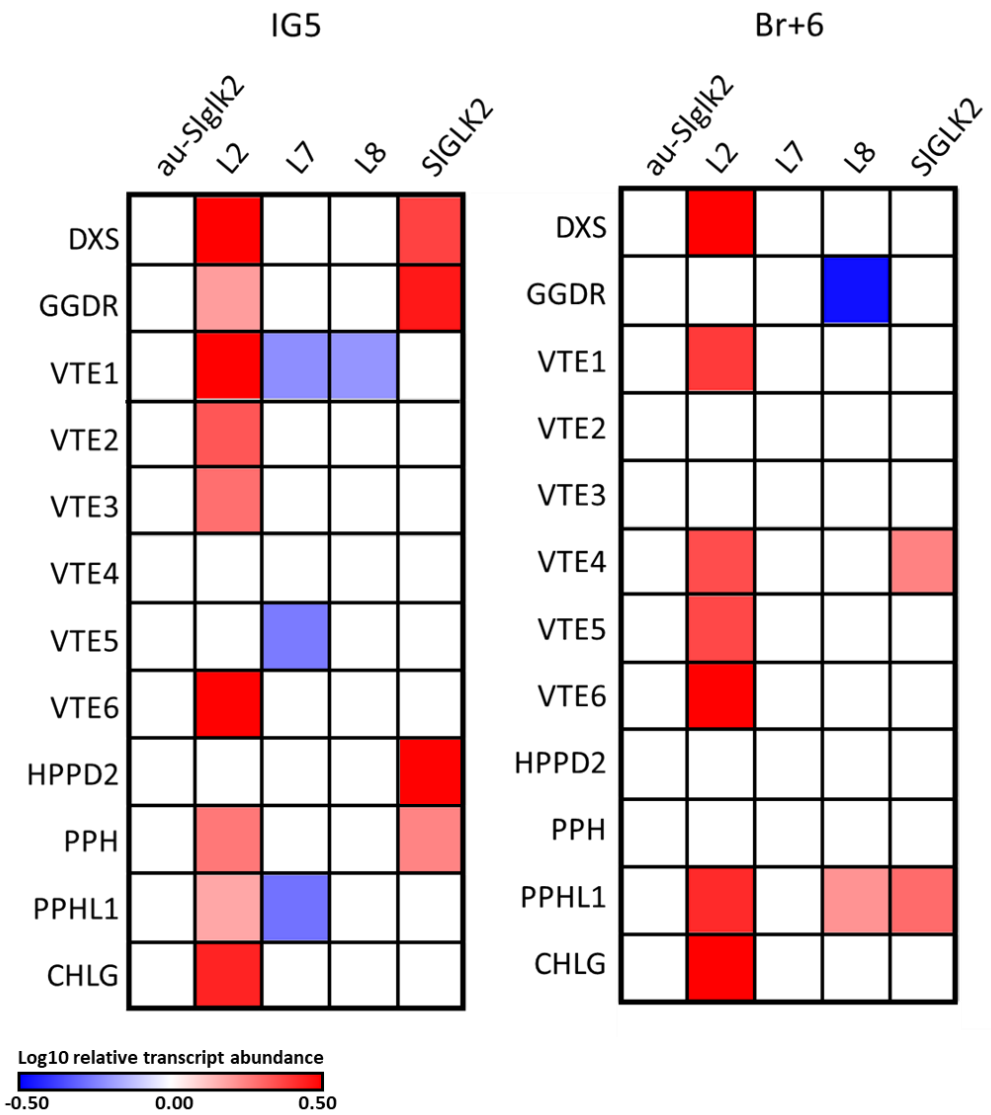

Figure 22: Expression profile of tocopherol and chlorophyll metabolic enzyme encoding genes in fruits of transgenic lines.

The expression profile was obtained by qPCR from fruit at IG5 and Br+6 stages. The heatmap represents statistically significant differences in relative transcript levels detected in L2, L7, L8 and *SlGLK2* wild type genotypes compared to *aurea-Slglk2* control (P<0.05). Values represent mean of at least three biological replicates. Relative transcript values are described in Supplementary Material IV. DXS: 1-DEOXY-D-XYLULOSE-5-P SYNTHASE; HPPD2: 4-HYDROXYPHENYLPYRUVATE DIOXYGENASE (2); GGDR: GERANYLGERANYL DIPHOSPHATE REDUCTASE; VTE1: TOCOPHEROL CYCLASE; VTE2: HOMOGENTISATE PHYTYL TRANSFERASE; VTE3: 2,3-DIMETHYL-5-PHYTYLQUINOL METHYL TRANSFERASE; VTE4: TOCOPHEROL Γ -METHYL TRANSFERASE; VTE5: PHYTOL KINASE; VTE6: PHYTYL-PHOSPHATE KINASE; PPH: PHEOPHYTINASE; PPHL1: PHEOPHYTINASE LIKE-1; CHLG: CHLOROPHYLL SYNTHASE.

4.2.8. Chloroplast number and ultrastructure

Chloroplast number was analyzed in immature green fruits of transgenic and controls lines. Significant increase in chloroplast number was observed in L2 and L7 in comparison to control *aurea-Slglk2*, but no significant difference was found for L8 (Figure 23).

The ultrastructure analysis of IG5 fruit chloroplasts revealed that in L2 the thylakoid membranes are organized into grana with more stacks than control *aurea-SlGLK2*. There were few plastoglobuli per cell in L2 compared to *SlGLK2*, although more than found in *aurea-Slglk2* (Figure 24). It was also possible to see smaller starch grains in L2 than in control *aurea-Slglk2* (Figure 25).

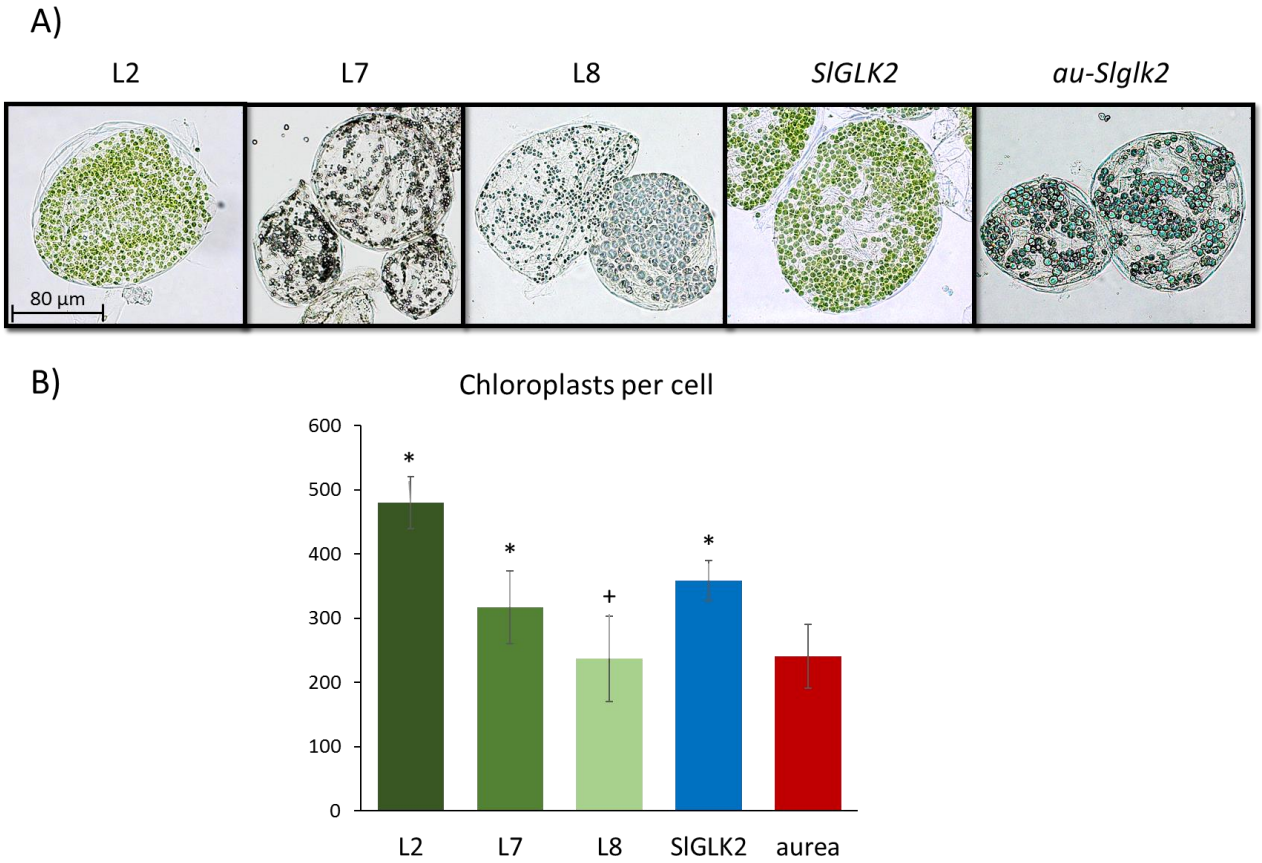

Figure 23: Impact of *SlGLK2* overexpression on fruit chloroplast number.
(A) Optical microscopy of IG5 fruits in transgenic and control lines *aurea-Slglk2* and *SlGLK2*. **(B)** Graphic representation of chloroplast number per cell in IG5 fruits. Asterisk (*) indicates significant difference between transgenic lines and control *aurea-Slglk2*; Plus signal (+) indicates significant difference between transgenic lines and control *SlGLK2* (P<0,05). Values represent mean ± SE of 10 cells.

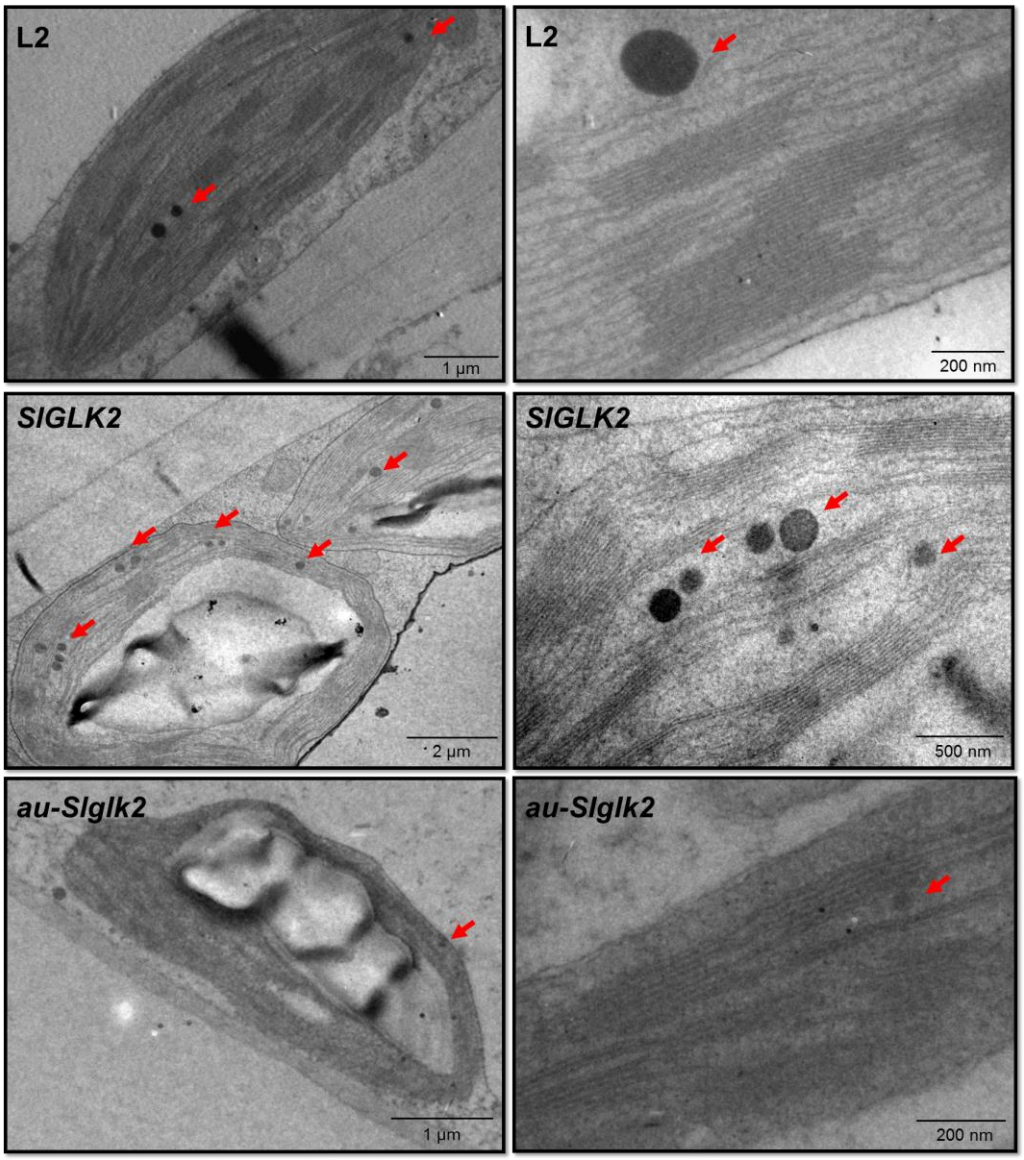

Figure 24: Fruit chloroplast ultrastructure
Images obtained by transmission electron microscopy. Red arrows indicate plastoglobuli.

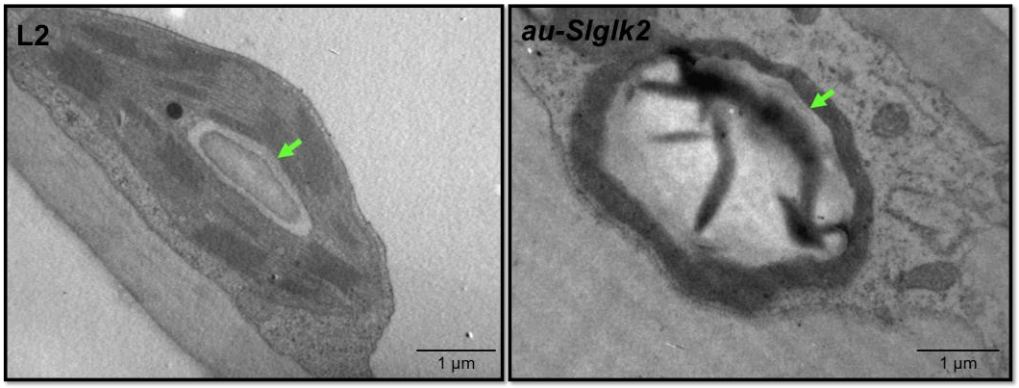

Figure 25: Starch grains in fruit chloroplasts.
Images obtained by transmission electron microscopy. Starch grains are indicated by green arrows.

4.3. Crosstalk between SlGLK2 and the production and signaling of auxins and cytokinins.

4.3.1. Evaluation of temporal and spatial correlation between hormonal activity and SlGLK2 presence.

The eventual impact of SlGLK2 on hormonal activity was evaluated by analyzing the activity of GUS reporter enzyme expressed under the control of the *DR5* and *ARR5* promoters, which are responsive to auxin and cytokinin, respectively.

While no significant differences were observed between *DR5::GUS-SlGLK2* and *DR5::GUS-Slglk2*, GUS activity was higher in the fruits from *ARR5::GUS-SlGLK2* than those from *ARR5::GUS-Slglk2* in all stages of development analyzed (Figure 26). This data suggests that SlGLK2 has a positive influence on cytokinins signaling, evidenced by the increment in ARR5 promoter activity in the presence of the wild allele.

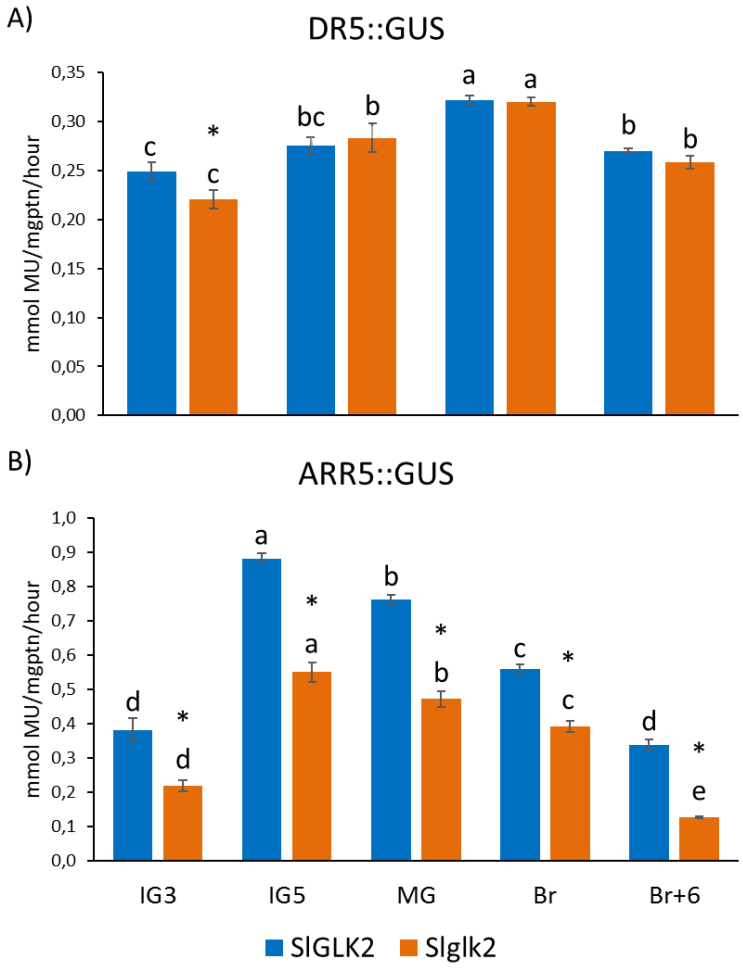

Figure 26: SlGLK2 influence on hormonal signaling.
Hormonal activity was analyzed by GUS assay in genotypes expressing the reporter gene *uidA* under control of the promoters *DR5* **(A)** or *ARR5* **(B)**, which are responsive to auxins and cytokinins, respectively. Different letters indicate statistically significant differences between stages within each genotype. Asterisk (*) indicates significant differences between genotypes within the same fruit stage (P<0,05). Values represent mean ± SE of at least three biological replicates. After *DR5::GUS* analysis, *SlGLK2* transcriptional profile revealed that this gene expression peaks in IG5 stage (Figure 9B), hence this stage was included for *ARR5::GUS* analysis.

4.3.2. Effect of altered hormonal metabolism or signaling over the abundance of SlGLK2 transcripts.

To address whether *SlGLK2* expression is regulated by auxins or cytokinins, its relative transcript abundance was evaluated by qPCR in hormonal signaling deficient plant, the *dgt* mutant, which has low sensitivity to auxins, and transgenic *35S::CKX2*, with low levels of endogenous cytokinins. The *dgt* mutant showed higher levels of *SlGLK2* expression, both in immature and mature green fruits. Transgenic line *35S::CKX2* did not show any significant difference from control *SlGLK2* (Figure 27).

These results suggest that auxins negatively regulate *SlGLK2*, since *dgt* plants, with low sensitivity to this hormone, have lower transcript relative abundance of *SlGLK2* compared to wild type *SlGLK2*.

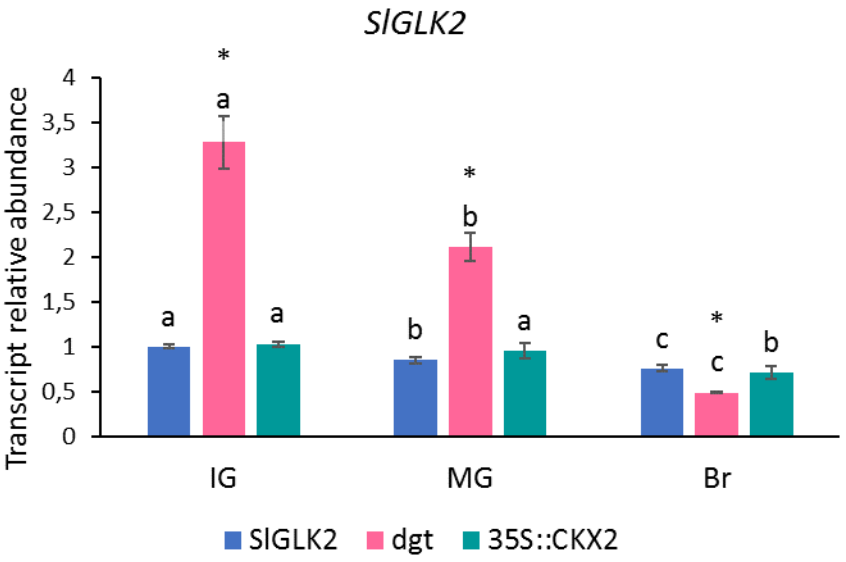

Figure 27: Effect of cytokinins and auxins on *SlGLK2* transcript relative abundance
The expression profile was obtained by qPCR from fruits of cytokinin deficient and auxin insensitive mutant plants. Different letters indicate statistically significant differences between stages within each genotype. Asterisk (*) indicates statistically significant differences compared to control *SlGLK2* genotype ($P<0.05$). Relative transcript abundance values represent mean ± SE of at least three biological replicates.

V. Discussion

5.1. GLK-mediated regulation of chloroplast development is an ancient mechanism conserved across all land plants

Several studies have demonstrated that during evolution, different lineages of photosynthetic organisms have suffered whole genome duplication events. Polyploidization events provide the basis for the evolution of novel functions and, in particular, the expansion of genes encoding transcription factors correlates with the evolutionary gain of morphological and physiological complexity (Rensing 2014). In this sense, the evaluation of gene diversity is fundamental to establish orthology relations and to distinguish functional diversification of duplicate genes.

A dedicated phylogenetic analysis encompassing 11 species allowed us to propose that *GLK* genes play a highly-conserved function in plastidial biogenesis and maintenance. As no copies of *GLK* genes were retrieved for any fully sequenced algae genome, we are confident to further propose that GLK function is a novelty that arose in Embryophyta, in agreement with that reported by Wang *et al.* (2013). The most basal species analyzed here that harbors these genes is the moss *Physcomitrella patens*, which displayed a recent gene duplication (Yasumura *et al*. 2005). So, we can presume that GLK-mediated regulation of chloroplast development defines one of the most ancient conserved regulatory mechanisms identified in the plant kingdom (Yasumura *et al*. 2005). Several specific lineage duplication events and species with only one copy of *GLK* (*e.g*. *Selaginella moelendorffii*) indicates that Embryohpyta ancestor had a single copy gene. In monocotyledons, the gene suffered an ancestral duplication event that originated two *GLK* copies. In some species, such as maize, functional diversification has occurred, with *GLK* genes regulating C_4 dimorphic chloroplast differentiation either in bundle sheath or in mesophyll cells. In others such as rice, a C3 species, both *GLKs* are functionally redundant (Wang *et al.* 2013).

Solanum lineage have been affected by two whole-genome triplications; the first occurred before the divergence between *Arabidopsis* and *Solanum* more than 120 MYA, while the second preceded the divergence between tomato and potato estimated at 71 (± 19.4) MYA. It has been proposed that these genome triplications contributed with fruit-specific functions in tomato, such as the ripening master transcription factor *RIPENING INHIBITOR* (*RIN*) and *PHYs* that influence fruit quality (The Tomato Genome Consortium 2012). In *Solanum*, both *GLK* copies seem to be originated during the second whole genome duplication since the duplication occurred after the divergence between Rosidae and Asteridae. Later, a *S. tuberosum* specific duplication gave rise to the four copies found in potato genome. Interestingly, in *S. lycopersicum*, *SlGLK1* and *SlGLK2* also

underwent diversification showing specific pattern of expression. While the former is more abundantly expressed in leaves, *SlGLK2* is fruit specific (Powell *et al*. 2012). Differently, in *A. thaliana*, *AtGLK1* and *AtGLK2* are functionally redundant (Fitter *et al.* 2002).

5.2. SlGLK2 expression profile is regulated by the crosstalk between PHY-mediated light perception, auxin and cytokinin signaling.

The crosstalk between light and phytohormones on tomato fruit chloroplast regulation has been approached in several reports (Cocaliadis *et al*. 2014; Sagar *et al*. 2013; Bianchetti *et al*. 2017). Here, we addressed how this intricate signaling network affects the expression of the plastidial biogenesis and maintenance transcription factor encoding gene *SlGLK2*. To gain this objective, the expression pattern of *SlGLK2* was analyzed in fruits from wild type *SlGLK2*, *Slglk2* mutant and PHY (*aurea*), auxin (*dgt*) and cytokinin (*35S::CKX2*) deficient genotypes.

Interestingly, although the difference between the alleles is in the coding region, *Slglk2* showed reduced transcript levels of *SlGLK2* compared to the wild type. Several lines of evidence support the existence of nuclear quality control mechanisms linking transcription, mRNA processing, translation, translocation of the mRNA to the cytoplasm and the elimination of defective transcripts or proteins. For example, transcripts with premature stop codons are eliminated by a nonsense-mediated decay mechanism triggered by the pioneer round of translation in the nucleus (Goff *et al*. 2011).

Powell *et al*. (2012) reported that the expression of *SlGLK2* is induced by light. Interestingly, our results showed that *SlGLK2* in *aurea* mutant background, which is defective in active PHYs, is more abundantly expressed than in wild type plants during immature stages of fruit development. At first glance, this may seem a contradiction, however, the integrated analysis of available data clarifies this observation. A recent publication of our group has demonstrated that *aurea* mutant displays reduced levels of auxins and *SlARF4* expression, an auxin induced repressor of auxin signaling, at early stages of fruit development (Biancheti *et al*. 2017). Additionally, the higher levels of *SlGLK2* mRNA observed in the auxin insensitive *dgt* mutant indicate that this phytohormone inhibits the expression of *SlGLK2*. Thus, according to our data it is expectable the upregulation of *SlGLK2* in immature fruits of *aurea* mutant, suggesting that the PHY-mediated light regulation over *SlGLK2* is mediated by auxin. Reinforcing these arguments, *SlARF4* downregulates *SlGLK1* in *Slglk2* mutant genotype probably by the direct interaction with *SlGLK1* promoter (Sagar *et al*. 2013). In support of this hypothesis, we found that the promoter region of the *SlGLK2* gene contains one canonical and two highly conserved ARF binding sites (TGTCTC box) (Supplemental Material V-I).

Interestingly, the temporal expression profile of *SlGLK2* was different in *aurea* background than in wild type genotype. In wild type fruits, *SlGLK2* mRNA accumulation peaks right before the onset of fruit ripening at IG5 stage, while in PHY deficient plants, the highest level of *SlGLK2* was verified earlier in development at IG3, the youngest stage analyzed. Again, this can be explained by the reduced levels of auxin and auxin responsiveness shown in immature stages of fruit development reported in *aurea* mutant (Bianchetti *et al*. 2017).

Less clear is the relationship between cytokinins and *SlGLK2* expression. According to GUS activity assay, the cytokinin responsive *ARR5* promoter drove higher expression levels of *uid* gene in the presence of *SlGLK2* wild type in comparison to mutant *Slglk2* allele in all fruit stages analyzed. This result suggests that SlGLK2 positively regulates cytokinin signaling all along fruit development and ripening. However, the constitutive overexpression of *AtCKX2*, which reduces the content of cytokinin, did not affect *SlGLK2* mRNA levels. This does not confirm the positive effect of cytokinins on *AtGLK2* expression described in *A. thaliana* during root greening (Kobayashi *et al*. 2012), supporting the existence of different regulatory networks in distinct organs. It is worth mentioning that although *AtCKX2* overexpression was confirmed, cytokinin levels were not measured in *35S::CKX2* tomato fruits (Pino *et al*. 2010).

To sum up, the PHY-mediated light regulation over *SlGLK2* is most probably mediated by auxin, while SlGLK2 positively affects cytokinin signaling in fruits (Figure 28).

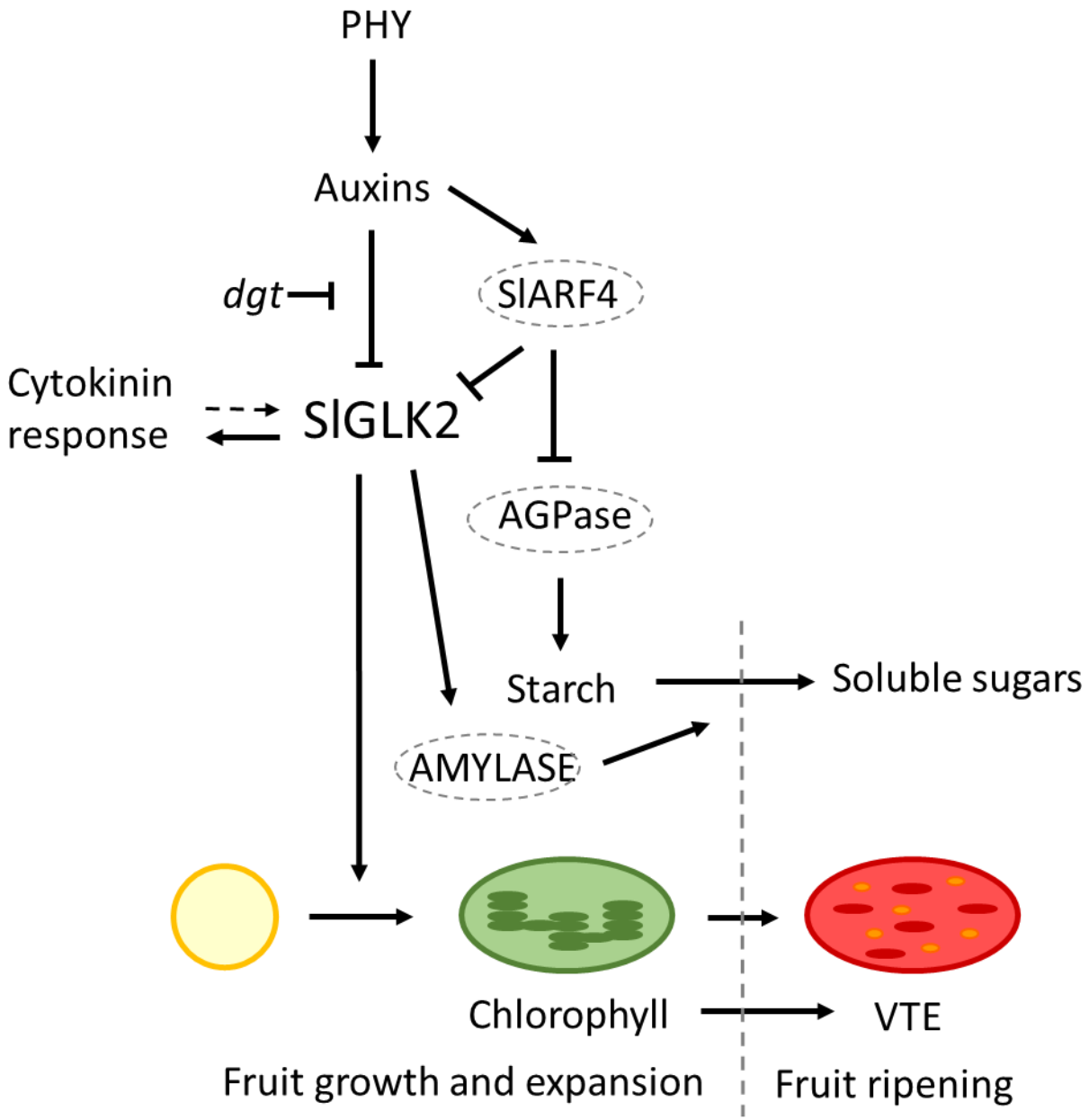

Figure 28: *SlGLK2* expression regulation by PHY-mediated light perception and phytohormones and its impact on carbon metabolism and VTE accumulation.
Schematic representation of the results integrated analysis, where dashed highlighted intermediates were incorporated based on previously published data. Phytochromes (PHY) acts as positive regulators of auxins (Bianchetti *et al*. 2017), which in turn, repress *SlGLK2* expression either directly, or indirectly *via* SlAFR4, a negative regulator of auxin signaling (Sagar *et al.* 2013). In *dgt* background, an auxin response impaired genotype (Oh *et al*. 2006), the negative regulation of auxin over *SlGLK2* gene expression is disrupted. Cytokinin response is upregulated in the presence of SlGLK2. The positive effect of cytokinins over *AtGLK2* expression, described by Kobayashi *et al*. (2012) (dashed arrow), was not verified in tomato fruits. SlGLK2 is a master transcription factor that promotes the differentiation of proplastids into chloroplasts with the corresponding chlorophyll accumulation in green fruits, which is directly proportional to VTE content in ripe fruits. SlARF4 inhibits *AGPase* expression and enzyme activity (Sagar *et al*. 2013). Moreover, auxin is known to inhibit AMYLASE activity, which is associated with ripening inducing starch degradation for soluble sugar accumulation in climacteric ripe fruits (Purgatto *et al*. 2001), probably mediated by *SlGLK2*. The balance between AGPase and AMYLASE enzyme activities determines the starch and, in part, soluble sugar content in green and ripe stages of fruits development.

5.3. SlGLK2 overexpression partially recovers the chlorotic phenotype of aurea mutant

Among many other processes, PHYs are known to regulate the accumulation of photosynthetic pigments (Waters & Langdale 2009). Consistently, immature fruits of the *aurea* mutant exhibited an evident pale-green coloration as consequence of the reduced of total chlorophyll content and approximately 50% in the number of chloroplasts per cell compared to wild type genotype. Additionally, chloroplasts are not only less abundant but also smaller in diameter in *aurea* than in wild type (Bianchetti *et al*. 2017).

Being demonstrated that *SlGLK2* is regulated by PHY-mediated light perception, and to evaluate the role of SlGLK2 in fruit plastid biogenesis, we tested whether *SlGLK2* overexpression could recover the impairment in chlorophyll biosynthesis and chloroplast development in *aurea* mutant. This was addressed by the phenotypic characterization of three independent transgenic lines expressing *SlGLK2* under the control of the constitutive promoter 35S (*i.e.* L2, L7, L8). Interestingly, although L7 and L8 showed 4-fold more *SlGLK2* mRNA levels, this was not reflected in a conspicuous increment in protein amount. The CUL4-DDB1-based E3 ligase (CULLIN4-DAMAGED DNA BINDING PROTEIN 1) is a protein complex that ubiquitinates positive regulators of light signaling mediated by COP1-SPA1 proteins (CONSTITUTIVE PHOTOMORPHOGENIC 1-SUPPRESSOR OF PHYA 1) for further proteasome-mediated-degradation (Lau & Deng 2012). Recently, it has been demonstrated in tomato that the ubiquitin-conjugated degradation of SlGLK2 is mediated by CUL4-DDB1-based E3 ligase (Tang *et al*. 2016). The failure of SlGLK2 overexpression in L7 and L8 lines might be the result of the enhancement in the photomorphogenic repressing mechanisms as a result of the PHY-mediated light perception deficiency in *aurea* background (Lau & Deng 2012), while in L2 line, the extremely high overexpression level overcomes this repression. Indeed, recent data of our group have shown that the relative mRNA levels of genes encoding light signaling repressor proteins, including CUL4, DDB1, COP1 and DETIOLATED1 (DET1) are upregulated in PHY-silenced fruits (Bianchetti 2017). Additionally, different to RNA interference silencing approach that has a well described amplification mechanism (Mello & Conte Jr 2004), when overexpressing a gene, the relationship between mRNA expression and absolute protein levels does not behave as a linear correlation (Sousa Abreu *et al*. 2009). On this regard, the only truly overexpressing line was L2, evidenced by the fact that most of the results obtained for L7 and L8 were not different from those obtained for the control *aurea-Slglk2*.

L7 and L8 fruits showed a discrete color change compared to *aurea-Slglk2* control. On the contrary, L2 fruits were darker than the *SlGLK2* wild type with an even distribution of chloroplasts. Total chlorophyll measurement was in agreement with the visual phenotype, and the immature fruits

from L2 line displayed over 3-fold and 10-fold more photosynthetic pigment than *SlGLK2* and *aurea-Slglk2* controls, respectively. Regarding chloroplast, increased levels of SlGLK2 resulted in fruits with higher number of plastids, which displayed more abundant stacked discs of thylakoids into grana, even under PHY deficiency. So, these results indicate that the overexpression of *SlGLK2* restores *aurea* chloroplast number and ultrastructure, exposing the main role of this gene in fruit chloroplast biogenesis. The impact of *SlGLK2* overexpression on fruit metabolism and quality is discuss in the next section.

Although L2 had approximately 80-fold increase in *SlGLK2* transcript abundance and discrete increment in protein content in source leaves, no reversion in the pale-green phenotype was observed as confirmed by chlorophyll content (Supplemental Material VI), leading us to propose that *SlGLK2* has a limited role in leaf chloroplast biogenesis. Although productivity data were not reported before (Powell *et al*. 2012, Nguyen *et al.* 2014), intriguingly, our data showed that *SlGK2* overexpression led to a significant reduction in whole plant biomass. Similarly, transgenic constitutive repression of the photomorphogenic negative regulator *DET1* has been associated with dwarfism and reduced yield (Davuluri *et al*. 2005).

5.4. SlGLK2 controls plastid metabolism affecting nutritional and industrial quality traits of tomato fruits

Fruits are generally regarded as photosynthate sinks that rely on energy provided by sugars transported from leaves to carry out the highly demanding processes of development and ripening (Lytovchenko *et al*. 2011). However, during the last years, it has been revealed that fruit plastid metabolism has a main role in determining the nutritional and industrial quality of tomato fruits (Cocaliadis *et al*. 2014). Recent reports have shown that transcriptional factors enhancing chloroplast development in fruit may result in higher contents not only of tomato fruit-specialized metabolites (*i.e.* carotenoids) but also of sugars (Pan *et al*. 2013; Powell *et al*. 2012; Sagar *et al*. 2013). *SlGLK2* is within these transcription factors (Nguyen *et al*. 2014) and this work brings new and detailed data to this scenario.

Here, SlGLK2 impact on tocopherol and sugar metabolism has been addressed from two different approaches: (i) comparing the wild and the mutant genotypes, *SlGLK2* vs *Slglk2*, and; (ii) comparing a *SlGLK2*-overexpressing line in the light perception-deficient background *aurea* and the corresponding control genotype, L2 vs *aurea-Slglk2*.

Our experiments have shown that the presence of the wild allele of *SlGLK2* enhanced chlorophyll accumulation in immature fruits compared with those from *Slglk2* genotypes. This effect was evidenced either by the enhancement of *de novo* synthesis of phytyl-2P (*DXS* and

GGDR), chlorophyll biosynthesis (*CHLG*), and/or chlorophyll degradation and recycling (*PPH*, *PPHL1* and *VTE6*). In *A. thaliana*, GLKs induce the expression of photosynthesis related genes by the direct interaction with the promoter sequences of genes that function in light harvesting, such as LIGHT-HARVESTING CHLOROPHYLL-BINDING (LHCB) and key chlorophyll biosynthetic genes (Kobayashi *et al*. 2012; Waters *et al*. 2009). Moreover, GLK proteins influence photosynthetic gene expression independently of the PHYs signaling pathway (Waters *et al*. 2009), in agreement to our results obtained for *SlGLK2*-overexpressing plants in *aurea* background.

During tomato fruit ripening, *DXS* and *GGDR* expression is up and downregulated, respectively, and thus, MEP pathway boost GGDP availability for carotenoid biosynthesis (Quadrana *et al*. 2013). From breaker stage onwards, chlorophyll degradation-derived phytol is recycled to phytyl-2P, which feeds tocopherol biosynthesis (Almeida *et al*. 2016). Thus, there is a positive correlation between chlorophyll levels in green fruits and tocopherol amounts in ripe fruits (Almeida *et al*. 2015). In this regard, higher levels of tocopherol were observed in ripe fruits from *SlGLK2* than in *Slglk2*, although, tocopherol biosynthetic gene expression profile alone does not clearly explain this increment. Even with 3-fold more chlorophyll, ripe fruits from *SlGLK2*-overexpressing plants in *aurea* mutant background displayed similar levels of tocopherol as wild type fruits. Several reports demonstrated that phytyl-2P is the most limiting factor in tocopherol biosynthesis, both for *S. lycopersicum* (Almeida *et al*. 2015) and *A. thaliana* (Ajjawi & Shintani 2004). However, this seems not to be the case, since phytol recycling is indeed enhanced by *SlGLK2* overexpression compared to *SlGLK2* wild type ripe fruits by the upregulation of *VTE6* expression (Supplemental Material VII). In this sense, tocopherol increment impairment might be the consequence of the shikimate precursor HGA limitation, reinforced by the fact that there was no effect of *SlGLK2* overexpression on *HPPD2* transcript levels, with both *aurea-Slglk2* and transgenic lines showing decreased relative transcript abundance when compared to *SlGLK2*. These results suggest that SlGLK2 positively regulates the tocopherol content in ripe fruits in two different ways: by increasing chlorophyll content during green stages of fruit development and by enhancing phytol recycling once ripening is triggered. Moreover, SlGLK2 participates in the regulation of chlorophyll, MEP and tocopherol core metabolic genes in a PHY-independent manner, as the effect was observed in *aurea* mutant background.

The combined effects of SlGLK2 and PHY-mediated light perception constitute an intricate regulatory network that controls carbon metabolism in a not yet totally unraveled mechanism. Recently, Bianchetti (2017) described that fruit specific PHY-mediated light perception impairment led to higher levels of *SlGLK2* expression, the downregulation of *SlARF4* and increment in starch content in immature fruits. Moreover, *SlARF4*-silenced tomato plants exhibited increased

expression and activity of AGPase, which explain the increment in the starch content observed in immature fruits from these plants (Sagar *et al*. 2013). Additionally, it has been demonstrated that auxins, which are induced by PHY-mediated light perception, inhibit AMYLASE activity delaying the accumulation of soluble sugars during ripening in climacteric fruits (Purgatto *et al*. 2001). In this context and being demonstrated that *SlGLK2* is downregulated by auxins, we propose that SlGLK2 mediates auxin inhibition of AMYLASE. To sum up, SlGLK2 and PHY-mediated light perception controls the balance between starch synthesis and degradation by regulating both *AGPase* and *AMYLASE* expression and/or enzyme activity (Figure 28).

Our results showed that the presence of *SlGLK2* wild type allele is associated with reduced levels of starch in green stages of fruit development from plants with well-developed chloroplasts, as the case of *SlGLK2*-overexpressing and *SlGLK2* wild type genotypes. This observation can be explained by the SlGLK2 effect over *AMYLASE* expression, which is reinforced by the SlGLK2 binding motifs (Waters *et al*. 2009) found in α- and β-AMYLASE promotor sequence (Supplemental Material V-II). Although contradictory at first glance, higher levels of starch content in *aurea-SlGLK2* compared to *Slglk2* mutant might be explained by the lack of AGPase repression by *SlARF4* due to light perception deficiency. The upregulation of *AMYLASE* by *SlGLK2* might also explain the increase in soluble sugars and °Brix content seen in L2 *SlGLK2*-overexpressing line.

It is worth mentioning that the only reports that have evaluated the effect of SlGLK2 over starch content have shown increased levels of this polymer in *AtGLK/SlGLK*-overexpressing plants, however, this was exclusively addressed at early stages of tomato fruit development (15 days post-anthesis) and in undetermined tomato cultivars. In agreement with our results, these reports have shown higher levels of soluble sugars in the *GLK*-overexpressing ripe fruits (Powell *et al*. 2012; Nguyen *et al*. 2014).

Another important player of carbon metabolism in sink organs are cytokinins, which have shown to act as positive regulators of sink strength in tomato fruits, inducing expression of vacuolar and extracellular invertases, as well as hexose transporters (Roitsch & Ehneß 2000). The results presented here have shown that cytokinin response is upregulated in the presence of *SlGLK2* wild allele, and thus, could further explain the increment in soluble sugars and °Brix content in *SlGLK2*-overexpressing plants. However, it is important to point out that transgenic plants displayed a penalty in aerial biomass without affecting the carbon partitioning between fruits and vegetative aerial organs.

The results obtained here demonstrated that SlGLK2 is a master regulator of chlorophyll and carbon metabolisms, contributing to determine the final VTE and soluble solid content in edible fruits (Figure 28), two important agronomical traits for tomato production.

VI. Conclusions

1. *GLK* genes are a novelty of Embryophyta clade.
2. The duplication that originated *SlGLKs* occurred in Solanaceae lineage prior to the divergence between *Solanum lycopersicum* and *Solanum tuberosum*.
3. The *SlGLK2* transcriptional regulation by light is, at least in part, mediated by PHYs.
4. Auxins downregulate *SlGLK2* expression in fruits.
5. *SlGLK2* wild allele positively affects cytokinin signaling in fruits.
6. SlGLK2 promotes the differentiation of chloroplasts with highly stacked thylakoids in a PHY-independent manner in fruits.
7. SlGLK2 promotes chlorophyll biosynthesis in immature green stages of fruit development, which is proportional to tocopherol content in ripe fruits.
8. SlGLK2-mediated chlorophyll and tocopherol increment are explained, at least in part, by the transcription upregulation of the biosynthetic enzyme encoding genes.
9. SlGLK2 alters carbon metabolism inhibiting starch accumulation at immature stages of fruit development.
10. *SlGLK2* overexpression promotes the accumulation of higher levels of soluble sugar in ripe fruit contributing to higher °Brix.
11. SlGLK2 has a negative effect on productivity traits such as fruit weight and aerial biomass.

VII. References

Ajjawi, I., & Shintani, D. (2004). Engineered plants with elevated vitamin E: a nutraceutical success story. *Trends in biotechnology*, *22*(3), 104-107.

Almeida, J., Quadrana, L., Asís, R., Setta, N., de Godoy, F., Bermúdez, L., Otaiza, S. N., Silva, J. V. C, Fernie, A. R., Carrari, F. & Rossi, M. (2011). Genetic dissection of vitamin E biosynthesis in tomato. *Journal of Experimental Botany*, *62*(11), 3781-3798.

Almeida, J., Asís, R., Molineri, V. N., Sestari, I., Lira, B. S., Carrari, F., Peres, L. E. P. & Rossi, M. (2015). Fruits from ripening impaired, chlorophyll degraded and jasmonate insensitive tomato mutants have altered tocopherol content and composition. *Phytochemistry*, *111*, 72-83.

Almeida, J., Azevedo, M. D. S., Spicher, L., Glauser, G., vom Dorp, K., Guyer, L., Carranza, A. d. V., Asis, R., de Souza, A. P., Buckeridge, M., Demarco, D., Bres, C., Rothan, C., Peres, L. E. P., Hörtensteiner, S., Kessler, F., Dörmann, P., Carrari, F. & Rossi, M. (2016). Down-regulation of tomato PHYTOL KINASE strongly impairs tocopherol biosynthesis and affects prenyllipid metabolism in an organ-specific manner. *Journal of experimental botany*, *67*(3), 919-934.

Bae, G., & Choi, G. (2008). Decoding of light signals by plant phytochromes and their interacting proteins. *Annu. Rev. Plant Biol.*, *59*, 281-311.

Bianchetti, R. E. (2017) *Fruit-localized phytochromes regulate plastid division, starch synthesis and carotenoid metabolism in tomato fruits.* Tese de doutorado. Departamento de Botânica Instituto de Biociências, Universidade de São Paulo, São Paulo, Brasil.

Bianchetti, R. E., Cruz, A. B., Oliveira, B. S., Demarco, D., Purgatto, E., Peres, L. E. P., Rossi, M. & Freschi, L. (2017). Phytochromobilin deficiency impairs sugar metabolism through the regulation of cytokinin and auxin signaling in tomato fruits. *Scientific Reports*, *7*(1), 7822.

Booth, S. L., Golly, I., Sacheck, J. M., Roubenoff, R., Dallal, G. E., Hamada, K., & Blumberg, J. B. (2004). Effect of vitamin E supplementation on vitamin K status in adults with normal coagulation status. *The American journal of clinical nutrition*, *80*(1), 143-148.

Bradford, M. M. (1976). A rapid and sensitive method for the quantitation of microgram quantities of protein utilizing the principle of protein-dye binding. *Analytical biochemistry*, *72*(1-2), 248-254.

Bravo-Garcia, A., Yasumura, Y., & Langdale, J. A. (2009). Specialization of the Golden2-like regulatory pathway during land plant evolution. *New Phytologist*, *183*(1), 133-141.

Carrara, S., Pardossi, A., Soldatini, G. F., Tognoni, F., & Guidi, L. (2001). Photosynthetic activity of ripening tomato fruit. *Photosynthetica*, *39*(1), 75-78.

Carrari, F., & Fernie, A. R. (2006). Metabolic regulation underlying tomato fruit development. *Journal of Experimental Botany*, *57*(9), 1883-1897.

Cherubini, A., Martin, A., Andres-Lacueva, C., Di Iorio, A., Lamponi, M., Mecocci, P., ... & Ferrucci, L. (2005). Vitamin E levels, cognitive impairment and dementia in older persons: the InCHIANTI study. *Neurobiology of aging*, *26*(7), 987-994.

Chow, C. N., Zheng, H. Q., Wu, N. Y., Chien, C. H., Huang, H. D., Lee, Chiang-Hsieh, Y. T., Hou, P. F., Yang, T. Y. & Chang, W. C. (2016). PlantPAN 2.0: an update of plant promoter analysis navigator for reconstructing transcriptional regulatory networks in plants. *Nucleic acids research*, *44*(D1), D1154-D1160.

Cocaliadis, M. F., Fernández-Muñoz, R., Pons, C., Orzaez, D., & Granell, A. (2014). Increasing tomato fruit quality by enhancing fruit chloroplast function. A double-edged sword?. *Journal of experimental botany*, *65*(16), 4589-4598.

Cortleven, A., & Schmülling, T. (2015). Regulation of chloroplast development and function by cytokinin. Journal of experimental botany, 66(16), 4999-5013.

Davuluri, G. R., Van Tuinen, A., Fraser, P. D., Manfredonia, A., Newman, R., Burgess, D., ... & Bramley, P. M. (2005). Fruit-specific RNAi-mediated suppression of DET1 enhances carotenoid and flavonoid content in tomatoes. *Nature biotechnology*, *23*(7).

Di Rienzo, J. A. (2009). Statistical software for the analysis of experiments of functional genomics. RDNDA, Argentina, (http://sites.google.com/site/fgStatistics/).

Di Rienzo J.A., Casanoves F., Balzarini M.G., Gonzalez L., Tablada M., Robledo C.W. InfoStat versión 2016. Grupo InfoStat, FCA, Universidad Nacional de Córdoba, Argentina. URL http://www.infostat.com.ar

Egea, I., Bian, W., Barsan, C., Jauneau, A., Pech, J. C., Latché, A., ... & Chervin, C. (2011). Chloroplast to chromoplast transition in tomato fruit: spectral confocal microscopy analyses of carotenoids and chlorophylls in isolated plastids and time-lapse recording on intact live tissue. Annals of botany, 108(2), 291-297.

Fischer, R. L., & Bennett, A. B. (1991). Role of cell wall hydrolases in fruit ripening. Annual review of plant biology, 42(1), 675-703.

Fitter, D. W., Martin, D. J., Copley, M. J., Scotland, R. W., & Langdale, J. A. (2002). GLK gene pairs regulate chloroplast development in diverse plant species. The Plant Journal, 31(6), 713-727.

Fraser, P. D., Truesdale, M. R., Bird, C. R., Schuch, W., & Bramley, P. M. (1994). Carotenoid biosynthesis during tomato fruit development (evidence for tissue-specific gene expression). *Plant physiology*, *105*(1), 405-413.

Freschi, L., Rodrigues, M. A., Tiné, M. A. S., & Mercier, H. (2010). Correlation between citric acid and nitrate metabolisms during CAM cycle in the atmospheric bromeliad Tillandsia pohliana. *Journal of plant physiology*, *167*(18), 1577-1583.

Garapati, P., Xue, G. P., Munné-Bosch, S., & Balazadeh, S. (2015). Transcription factor ATAF1 in Arabidopsis promotes senescence by direct regulation of key chloroplast maintenance and senescence transcriptional cascades. *Plant physiology*, pp-00567.

Giovannoni, J. (2001). Molecular biology of fruit maturation and ripening. *Annual review of plant biology*, *52*(1), 725-749.

Giovannoni, J. J. (2004). Genetic regulation of fruit development and ripening. The plant cell, 16(suppl 1), S170-S180.

Goff, S. A. (2011). A unifying theory for general multigenic heterosis: energy efficiency, protein metabolism, and implications for molecular breeding. New Phytologist, 189(4), 923-937.

Goodstein, D. M., Shu, S., Howson, R., Neupane, R., Hayes, R. D., Fazo, J., ... & Rokhsar, D. S. (2011). Phytozome: a comparative platform for green plant genomics. Nucleic acids research, 40(D1), D1178-D1186.

Guyer, L., Hofstetter, S. S., Christ, B., Lira, B. S., Rossi, M., & Hörtensteiner, S. (2014). Different mechanisms are responsible for chlorophyll dephytylation during fruit ripening and leaf senescence in tomato. *Plant physiology*, *166*(1), 44-56.

Gyula, P., Schäfer, E., & Nagy, F. (2003). Light perception and signalling in higher plants. Current opinion in plant biology, 6(5), 446-452.

Hagen, G., & Guilfoyle, T. (2002). Auxin-responsive gene expression: genes, promoters and regulatory factors. Plant molecular biology, 49(3-4), 373-385.

Isaacson, T., Ronen, G., Zamir, D., & Hirschberg, J. (2002). Cloning of tangerine from tomato reveals a carotenoid isomerase essential for the production of β-carotene and xanthophylls in plants. *The Plant Cell*, *14*(2), 333-342.

Isogai, M., Uyeda, I., & Lee, B. C. (1998). Detection and assignment of proteins encoded by rice black streaked dwarf fijivirus S7, S8, S9 and S10. *Journal of General Virology*, *79*(6), 1487-1494.

Jarvis, P., & López-Juez, E. (2013). Biogenesis and homeostasis of chloroplasts and other plastids. *Nature Reviews Molecular Cell Biology*, *14*(12), 787-802.

Jefferson, R. A., Kavanagh, T. A., & Bevan, M. W. (1987). GUS fusions: beta-glucuronidase as a sensitive and versatile gene fusion marker in higher plants. *The EMBO journal*, *6*(13), 3901.

Jiang, Q., Christen, S., Shigenaga, M. K., & Ames, B. N. (2001). γ-Tocopherol, the major form of vitamin E in the US diet, deserves more attention. *The American journal of clinical nutrition*, *74*(6), 714-722.

Jiang, Q., Wong, J., Fyrst, H., Saba, J. D., & Ames, B. N. (2004). γ-Tocopherol or combinations of vitamin E forms induce cell death in human prostate cancer cells by interrupting sphingolipid synthesis. *Proceedings of the National Academy of Sciences of the United States of America*, *101*(51), 17825-17830.

Karimi, M., Inzé, D., & Depicker, A. (2002). GATEWAY™ vectors for Agrobacterium-mediated plant transformation. *Trends in plant science*, *7*(5), 193-195.

Kendrick, R. E., Kerckhoffs, L. H. J., Tuinen, A. V., & Koornneef, M. (1997). Photomorphogenic mutants of tomato. *Plant, Cell & Environment*, *20*(6), 746-751.

Kobayashi, K., Baba, S., Obayashi, T., Sato, M., Toyooka, K., Keränen, M., ... & Masuda, T. (2012). Regulation of root greening by light and auxin/cytokinin signaling in Arabidopsis. *The Plant Cell*, *24*(3), 1081-1095.

Kobayashi, K., Ohnishi, A., Sasaki, D., Fujii, S., Iwase, A., Sugimoto, K., ... & Wada, H. (2017). Shoot removal induces chloroplast development in roots via cytokinin signaling. *Plant Physiology*, *173*(4), 2340-2355.

Koornneef, M., Cone, J. W., Dekens, R. G., O'Herne-Robers, E. G., Spruit, C. J. P., & Kendrick, R. E. (1985). Photomorphogenic responses of long hypocotyl mutants of tomato. *Journal of Plant Physiology*, *120*(2), 153-165.

Lamesch, P., Berardini, T. Z., Li, D., Swarbreck, D., Wilks, C., Sasidharan, R., ... & Karthikeyan, A. S. (2011). The Arabidopsis Information Resource (TAIR): improved gene annotation and new tools. *Nucleic acids research*, *40*(D1), D1202-D1210.

Lau, O. S., & Deng, X. W. (2012). The photomorphogenic repressors COP1 and DET1: 20 years later. Trends in plant science, 17(10), 584-593.

Lee, J., He, K., Stolc, V., Lee, H., Figueroa, P., Gao, Y., ... & Deng, X. W. (2007). Analysis of transcription factor HY5 genomic binding sites revealed its hierarchical role in light regulation of development. The Plant Cell, 19(3), 731-749.

Lira, B. S., Rosado, D., Almeida, J., de Souza, A. P., Buckeridge, M. S., Purgatto, E., ... & Rossi, M. (2016). Pheophytinase knockdown impacts carbon metabolism and nutraceutical content under normal growth conditions in tomato. Plant and Cell Physiology, 57(3), 642-653.

Lira, B. S., Gramegna, G., Trench, B. A., Alves, F. R., Silva, E. M., Silva, G. F., ... & Nogueira, F. T. (2017). Manipulation of a senescence-associated gene improves fleshy fruit yield. *Plant Physiology*, *175*(1), 77-91.

Liu, L., Shao, Z., Zhang, M., & Wang, Q. (2015). Regulation of carotenoid metabolism in tomato. *Molecular plant*, *8*(1), 28-39.

Lytovchenko, A., Eickmeier, I., Pons, C., Osorio, S., Szecowka, M., Lehmberg, K., ... & Hedtke, B. (2011). Tomato fruit photosynthesis is seemingly unimportant in primary metabolism and ripening but plays a considerable role in seed development. *Plant Physiology*, *157*(4), 1650-1663.

Mello, C. C., & Conte Jr, D. (2004). Revealing the world of RNA interference. Nature, 431(7006), 338.

Mène-Saffrané, L., Jones, A. D., & DellaPenna, D. (2010). Plastochromanol-8 and tocopherols are essential lipid-soluble antioxidants during seed desiccation and quiescence in Arabidopsis. *Proceedings of the National Academy of Sciences*, *107*(41), 17815-17820.

Miret, J. A., & Munné-Bosch, S. (2015). Redox signaling and stress tolerance in plants: a focus on vitamin E. *Annals of the New York Academy of Sciences*, *1340*(1), 29-38.

Morris, M. C., Schneider, J. A., Li, H., Tangney, C. C., Nag, S., Bennett, D. A., ... & Barnes, L. L. (2015). Brain tocopherols related to Alzheimer's disease neuropathology in humans. *Alzheimer's & Dementia*, *11*(1), 32-39.

Muramoto, T., Kami, C., Kataoka, H., Iwata, N., Linley, P. J., Mukougawa, K., ... & Kohchi, T. (2005). The tomato photomorphogenetic mutant, aurea, is deficient in phytochromobilin synthase for phytochrome chromophore biosynthesis. Plant and cell physiology, 46(4), 661-665.

Nashilevitz, S., Melamed-Bessudo, C., Izkovich, Y., Rogachev, I., Osorio, S., Itkin, M., ... & Wolf, S. (2010). An orange ripening mutant links plastid NAD (P) H dehydrogenase complex activity to central and specialized metabolism during tomato fruit maturation. The Plant Cell, 22(6), 1977-1997.

Nguyen, C. V., Vrebalov, J. T., Gapper, N. E., Zheng, Y., Zhong, S., Fei, Z., & Giovannoni, J. J. (2014). Tomato GOLDEN2-LIKE transcription factors reveal molecular gradients that function during fruit development and ripening. The Plant Cell, 26(2), 585-601.

Notredame, C., Higgins, D. G., & Heringa, J. (2000). T-Coffee: A novel method for fast and accurate multiple sequence alignment. *Journal of molecular biology*, *302*(1), 205-217.

Oh, K., Ivanchenko, M. G., White, T. J., & Lomax, T. L. (2006). The diageotropica gene of tomato encodes a cyclophilin: a novel player in auxin signaling. *Planta*, *224*(1), 133-144.

Pan, Y., Bradley, G., Pyke, K., Ball, G., Lu, C., Fray, R., ... & Boyden, L. (2013). Network inference analysis identifies an APRR2-like gene linked to pigment accumulation in tomato and pepper fruits. *Plant physiology*, *161*(3), 1476-1485.

Parks, B. M., Jones, A. M., Adamse, P., Koornneef, M., Kendrick, R. E., & Quail, P. H. (1987). The aurea mutant of tomato is deficient in spectrophotometrically and immunochemically detectable phytochrome. *Plant molecular* biology, 9(2), 97-107.

Pfaffl, M. W., Horgan, G. W., & Dempfle, L. (2002). Relative expression software tool (REST©) for group-wise comparison and statistical analysis of relative expression results in real-time PCR. Nucleic acids research, 30(9), e36-e36.

Pino, L. E., Lombardi-Crestana, S., Azevedo, M. S., Scotton, D. C., Borgo, L., Quecini, V., ... & Peres, L. E. (2010). The Rg1 allele as a valuable tool for genetic transformation of the tomato'Micro-Tom'model system. Plant *methods*, *6*(1), 23.

Porra, R. J., Thompson, W. A., & Kriedemann, P. E. (1989). Determination of accurate extinction coefficients and simultaneous equations for assaying chlorophylls a and b extracted with four different solvents: verification of the concentration of chlorophyll standards by atomic absorption spectroscopy. *Biochimica et Biophysica Acta (BBA)-Bioenergetics*, *975*(3), 384-394.

Powell, A. L., Nguyen, C. V., Hill, T., Cheng, K. L., Figueroa-Balderas, R., Aktas, H., ... & Lopez-Baltazar, J. (2012). Uniform ripening encodes a Golden 2-like transcription factor regulating tomato fruit chloroplast development. *Science*, *336*(6089), 1711-1715.

Purgatto, E., Lajolo, F. M., do Nascimento, J. R. O., & Cordenunsi, B. R. (2001). Inhibition of β-amylase activity, starch degradation and sucrose formation by indole-3-acetic acid during banana ripening. *Planta*, *212*(5-6), 823-828.

Pyke, K. (2011). Analysis of plastid number, size, and distribution in Arabidopsis plants by light and fluorescence microscopy. *Chloroplast Research in Arabidopsis: Methods and Protocols, Volume I*, 19-32.

Quadrana, L., Almeida, J., Otaiza, S. N., Duffy, T., Da Silva, J. V. C., de Godoy, F., ... & Rossi, M. (2013). Transcriptional regulation of tocopherol biosynthesis in tomato. *Plant molecular biology*, *81*(3), 309.

Rastogi, A., Yadav, D. K., Szymańska, R., Kruk, J., Sedlářová, M., & Pospíšil, P. (2014). Singlet oxygen scavenging activity of tocopherol and plastochromanol in Arabidopsis thaliana: relevance to photooxidative stress. *Plant, cell & environment*, *37*(2), 392-401.

Rauf, M., Arif, M., Dortay, H., Matallana-Ramírez, L. P., Waters, M. T., Nam, H. G., ... & Balazadeh, S. (2013). ORE1 balances leaf senescence against maintenance by antagonizing G2-like-mediated transcription. *EMBO reports*, *14*(4), 382-388.

Rensing, S. A. (2014). Gene duplication as a driver of plant morphogenetic evolution. *Current opinion in plant biology*, *17*, 43-48.

Reynolds, E. S. (1963). The use of lead citrate at high pH as an electron-opaque stain in electron microscopy. *The* Journal of cell biology, 17(1), 208.

Rizvi, S., Raza, S. T., Ahmed, F., Ahmad, A., Abbas, S., & Mahdi, F. (2014). The role of vitamin E in human health and some diseases. Sultan Qaboos University Medical Journal, 14(2), e157.

Roitsch, T., & Ehneß, R. (2000). Regulation of source/sink relations by cytokinins. *Plant Growth Regulation*, *32*(2-3), 359-367.

Ruijter, J. M., Ramakers, C., Hoogaars, W. M. H., Karlen, Y., Bakker, O., Van den Hoff, M. J. B., & Moorman, A. F. M. (2009). Amplification efficiency: linking baseline and bias in the analysis of quantitative PCR data. Nucleic acids research, 37(6), e45-e45.

Sagar, M., Chervin, C., Mila, I., Hao, Y., Roustan, J. P., Benichou, M., ... & Pech, J. C. (2013). SlARF4, an auxin response factor involved in the control of sugar metabolism during tomato fruit development. Plant physiology, 161(3), 1362-1374.

Sakuraba, Y., Jeong, J., Kang, M. Y., Kim, J., Paek, N. C., & Choi, G. (2014). Phytochrome-interacting transcription factors PIF4 and PIF5 induce leaf senescence in Arabidopsis. *Nature communications*, *5*, 4636.

Sattler, S. E., Gilliland, L. U., Magallanes-Lundback, M., Pollard, M., & DellaPenna, D. (2004). Vitamin E is essential for seed longevity and for preventing lipid peroxidation during germination. *The plant cell*, *16*(6), 1419-1432.

Shen, W. J., & Forde, B. G. (1989). Efficient transformation of Agrobacterium spp. by high voltage electroporation. *Nucleic acids research*, *17*(20), 8385.

Sila, D. N., Van Buggenhout, S., Duvetter, T., Fraeye, I., De Roeck, A., Van Loey, A., & Hendrickx, M. (2009). Pectins in processed fruits and vegetables: Part II—Structure–function relationships. *Comprehensive Reviews in Food Science and Food Safety*, *8*(2), 86-104.

Song, Y., Yang, C., Gao, S., Zhang, W., Li, L., & Kuai, B. (2014). Age-triggered and dark-induced leaf senescence require the bHLH transcription factors PIF3, 4, and 5. *Molecular plant*, *7*(12), 1776-1787.

Sousa Abreu, R., Penalva, L. O., Marcotte, E. M., & Vogel, C. (2009). Global signatures of protein and mRNA expression levels. *Molecular BioSystems*, *5*(12), 1512-1526.

Stone, W. L., Krishnan, K., Campbell, S. E., Qui, M., Whaley, S. G., & Yang, H. (2004). Tocopherols and the treatment of colon cancer. *Annals of the New York Academy of Sciences*, *1031*(1), 223-233.

Tang, X., Miao, M., Niu, X., Zhang, D., Cao, X., Jin, X., ... & Sui, Y. (2016). Ubiquitin-conjugated degradation of golden 2-like transcription factor is mediated by CUL4-DDB1-based E3 ligase complex in tomato. *New Phytologist*, *209*(3), 1028-1039.

Tomato Genome Consortium. (2012). The tomato genome sequence provides insights into fleshy fruit evolution. *Nature*, *485*(7400), 635-641.

Thomas, H., & Ougham, H. (2014). The stay-green trait. *Journal of Experimental Botany*, *65*(14), 3889-3900.

Tieman, D., Taylor, M., Schauer, N., Fernie, A. R., Hanson, A. D., & Klee, H. J. (2006). Tomato aromatic amino acid decarboxylases participate in synthesis of the flavor volatiles 2-phenylethanol and 2-phenylacetaldehyde. *Proceedings of the National Academy of Sciences*, *103*(21), 8287-8292.

Tieman, D. M., Loucas, H. M., Kim, J. Y., Clark, D. G., & Klee, H. J. (2007). Tomato phenylacetaldehyde reductases catalyze the last step in the synthesis of the aroma volatile 2-phenylethanol. *Phytochemistry*, *68*(21), 2660-2669.

Triantaphylidès, C., & Havaux, M. (2009). Singlet oxygen in plants: production, detoxification and signaling. *Trends in plant science*, *14*(4), 219-228.

Vidi, P. A., Kanwischer, M., Baginsky, S., Austin, J. R., Csucs, G., Dörmann, P., ... & Bréhélin, C. (2006). Tocopherol cyclase (VTE1) localization and vitamin E accumulation in chloroplast plastoglobule lipoprotein particles. *Journal of Biological Chemistry*, *281*(16), 11225-11234.

Wang, P., Fouracre, J., Kelly, S., Karki, S., Gowik, U., Aubry, S., ... & Hibberd, J. M. (2013). Evolution of GOLDEN2-LIKE gene function in C3 and C4 plants. *Planta*, *237*(2), 481-495.

Waters, M. T., & Langdale, J. A. (2009). The making of a chloroplast. *The EMBO journal*, *28*(19), 2861-2873.

Waters, M. T., Wang, P., Korkaric, M., Capper, R. G., Saunders, N. J., & Langdale, J. A. (2009). GLK transcription factors coordinate expression of the photosynthetic apparatus in Arabidopsis. *The Plant Cell*, *21*(4), 1109-1128.

Watson, M. L. (1958). Staining of tissue sections for electron microscopy with heavy metals. *The Journal of Cell Biology*, *4*(4), 475-478.

Werner, T., Motyka, V., Laucou, V., Smets, R., Van Onckelen, H., & Schmülling, T. (2003). Cytokinin-deficient transgenic Arabidopsis plants show multiple developmental alterations indicating opposite functions of cytokinins in the regulation of shoot and root meristem activity. *The Plant Cell*, *15*(11), 2532-2550.

Yasumura, Y., Moylan, E. C., & Langdale, J. A. (2005). A conserved transcription factor mediates nuclear control of organelle biogenesis in anciently diverged land plants. *The Plant Cell*, *17*(7), 1894-1907.

Zouine, M., Maza, E., Djari, A., Lauvernier, M., Frasse, P., Smouni, A., ... & Bouzayen, M. (2017). TomExpress, a unified tomato RNA-Seq platform for visualization of expression data, clustering and correlation networks. *The Plant Journal*.

VIII. Supplemental Material

Supplemental Material I

Primers sequences

Name	5' – 3' sequence	Primer concentration for qPCR
RT-GLK1 (F/R)	GCTGTAGAGCAACTAGGTGTAGATAAGG / CAACTCGCTGCCTCCACTTC	200 µM
RT-GLK2 (F/R)	ATGTTTGGGGGCATCCACATG / GCAAATCAGAGGCAACTGTGTC	200 µM
OE_GLK2_R	TCAAGTTGGGGGTATTTTGG	-
GLK2_seq (F/R)	CACCATGCTTGCTCTATCTTCATCATTG / CTTGAGGATTTTTGATTTTGCTAG	-
M13 (F/R)	GTAAAACGACGGCCAG / GGAAACAGCTATGAC	-
TIP41 (F/R)	GCTGCGTTTCTGGCTTAGG / ATGGAGTTTTTGAGTCTTCTGC	400 µM
Expressed (F/R)	TGGGTGTGCCTTTCTGAATG / GCTAAGAACGCTGGACCTAATG	400 µM
35S F	GCAGGTCACTGGATTTTGG	-
Act (F/R)	TGGCATCATACCTTTTACAA / TCCGGGCATCTGAACCTCT	-
DXS(1) (F/R)	CAGGACTGGTGTGGTTTCAG / GGGATAGTTCACAGTGTCC	200 µM
GGDR (F/R)	CAGAGACGCTCGCTAAGG / GCTTCAGAGTCTGTCCGATATC	800 µM
VTE1 (F/R)	CGAACTCCTCATAGCGGGTATC / CACGCCAGTAAACCGAGGC	200 µM
VTE2 (F/R)	CAATTCCAGTTCCTGCTGAG / CCTCCAACATGCTCTTGCGTG	400 µM
VTE3(1) (F/R)	CTTGACCAATCTCCTCATC / GCACGCCTTTCCTCCAGG	400 µM
VTE4 (F/R)	CAGATCATCGTGCTGCTCAG / CCTCTCTGCTTGTACAGGAC	200 µM
VTE5 (F/R)	CGTATCAGGACGGGCTCGC / TCACCACCACACATCATTGCTAATG	200 µM
VTE6 (F/R)	AGCACAAGCATCAGTGTCTG / AAGAAAGCAGCCGCAATACC	200 µM
PPH (F/R)	TATGGAGGGAGCAAGTACGC / TGGAGGGCAGAGGAAAAGTAC	200 µM
PPHL1 (F/R)	GATTTGGTGCTTCTGCCTTTC / GCTGTTTCTTCAGTTCCTTC	200 µM
CHLG (F/R)	CCAATTCCTTCAGGTGCGGT / CCCACCAAGGCAAGCTGATA	200 µM
HPPD2 (F/R)	GGTGCTCCAAAATACAATGGGC / TCATTCGACAGCAGCTACTTG	800 µM
aurea (F/R)	ATGGAGTGTTTTTCTTCACTAGG / TCAGACAATCTCAACTCTATCG	-
aurea mid (F/R)	GGCTAATGGACAGATCAGAAG / CTCCTTGTAATCTTCTTGATCCAT	-

Supplemental Material II

Sequences used for phylogenetic analysis

Species	Protein name	Phytozome access number
Arabidopsis thaliana	GLK1	AT2G20570.2
Arabidopsis thaliana	GLK2	AT5G44190.1
Brassica rapa	GLK A	Brara.B02773.1
Brassica rapa	GLK B	Brara.F03760.1
Brassica rapa	GLK C	Brara.I04696.1
Oryza sativa	GLK A	LOC_Os06g24070.1
Oryza sativa	GLK B	LOC_Os01g13740.1
Physcomitrella patens	GLK A	Pp3c7_5800V3.1
Physcomitrella patens	GLK B	Pp3c11_21140V3.1
Panicum virgatum	GLK A	Pavir.Db01285.1
Panicum virgatum	GLK B	Pavir.Ea00014.1
Panicum virgatum	GLK C	Pavir.Eb00063.1
Phaseolus vulgaris	GLK A	Phvul.005G100700.1
Phaseolus vulgaris	GLK B	Phvul.011G124200.1
Sorghum bicolor	GLK A	Sobic.010G096300.1
Sorghum bicolor	GLK B	Sobic.003G002600.1
Solanum lycopersicum	GLK1	Solyc07g053630.2.1
Solanum lycopersicum	GLK2	Solyc10g008160
Selaginella moellendorffii	GLK	402806
Solanum tuberosum	GLK A	PGSC0003DMP400016574
Solanum tuberosum	GLK B	PGSC0003DMP400016575
Solanum tuberosum	GLK C	PGSC0003DMP400037861
Solanum tuberosum	GLK D	PGSC0003DMP400037860
Zea mays	GLK A	GRMZM2G026833
Zea mays	GLK B	GRMZM2G087804

Supplemental Material III

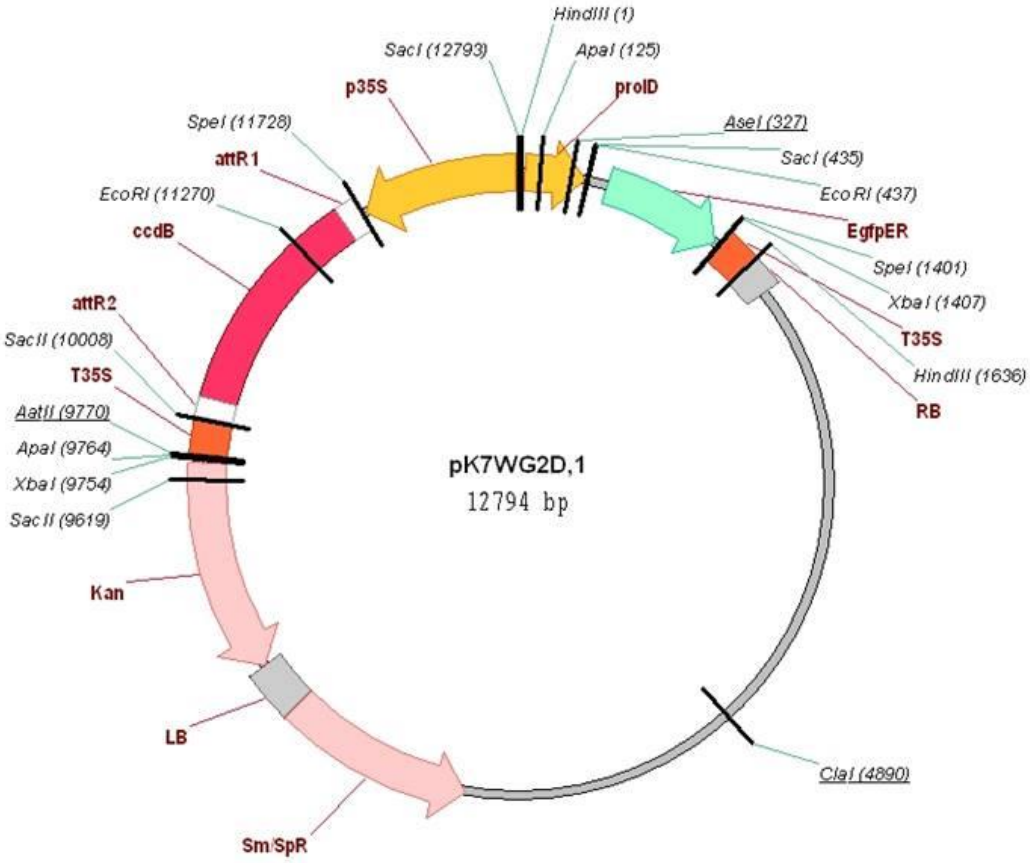

Plasmid used for *Agrobacterium tumefaciens*-mediated transformation.

pK7WG2D,1 plasmid map. RB: right border; T35S: 35S terminator (CaMV); *EgfpER*: coding gene for reporter protein GFP (*green fluorescence protein*), with peptide signal for endoplasmic reticulum; proID: independent promoter for gene *EgfpER*; p35S: constitutive promoter 35S (CaMV); attR1/R2: GATEWAY recombination sites; *ccdB*: coding gene for cytotoxic protein ccdB; *Kan*: gene that confers resistance to kanamycin in plants; LB: left border; *Sm/SpR*: gene that confers resistance to spectinomycin/streptomycin in bacteria.

Supplemental Material IV

qPCR relative transcript values

I. Relative expression data of Figure 9.

A)

	SlGLK2				Slglk2				au-SlGLK2			
	IG3	IG5	MG	BR	IG3	IG5	MG	BR	IG3	IG5	MG	BR
Top	**3.44 ± 0.47**	**4.73 ± 0.33**	**2.62 ± 0.00**	**3.06 ± 0.09**	**2.49 ± 0.23**	**6.07 ± 0.25**	**3.26 ± 0.37**	**2.99 ± 0.34**	**4.08 ± 0.28**	**22.72 ±0.19**	**2.36 ± 0.53**	**3.58 ± 0.19**
Bottom	1.00 ± 0.66	1.00 ± 0.48	1.00 ± 0.00	1.00 ± 0.00	1.00 ± 0.33	1.00 ± 0.26	1.00 ± 0.15	1.00 ± 0.43	1.00 ± 0.28	1.00 ± 0.25	1.00 ± 0.76	1.00 ± 0.00

B)

	IG3	IG5	MG	Br	Br3	Br5
SlGLK2	1.00 ± 0.19	**2.05 ± 0.14**	1.28 ± 0.14	0.78 ± 0.16	**0.22 ± 0.21**	**0.11 ± 0.11**
Slglk2	1.00 ± 0.07	0.69 ± 0.18	**5.81 ± 0.34**	**3.75 ± 0.2**	**0.25 ± 0.02**	**0.03 ± 0.02**
aurea	1.00 ± 0.27	0.84 ± 0.21	**0.70 ± 0.24**	**0.19 ± 0.03**	**0.01 ± 0**	**0.00 ± 0.00**

C)

	IG3	IG5	MG	Br	Br3	Br5
SlGLK2	1.00 ± 0.19	1.00 ± 0.00	1.00 ± 0.00	1.00 ± 0.11	1.00 ± 0.19	1.00 ± 0.11
Slglk2	**0.16 ± 0.14**	**0.05 ± 0.17**	0.73 ± 0.35	0.77 ± 0.21	**0.18 ± 0.01**	**0.04 ± 0.00**
aurea	**2.93 ± 0.24**	**0.05 ± 0.09**	1.59 ± 0.14	0.73 ± 0.20	**0.18 ± 0.15**	**0.09 ± 0.00**

Bold type indicates statistically significant differences against bottom.

II. Relative expression data of Figure 14.

IG5	DXS	GGDR	VTE1	VTE2	VTE3	VTE4	VTE5	VTE6
SlGLK2	1.00 ± 0.12	1.00 ± 0.04	1.00 ± 0.08	1.00 ± 0.07	1.00 ± 0.08	1.00 ± 0.02	1.00 ± 0.03	1.00 ± 0.02
Slglk2	**0.76 ± 0.03**	**0.58 ± 0.01**	0.94 ± 0.01	0.91 ± 0.03	**1.43 ± 0.05**	**0.85 ± 0.01**	**1.35 ± 0.02**	**0.76 ± 0.01**
au-SlGLK2	0.94 ± 0.45	0.89 ± 0.18	0.86 ± 0.08	0.99 ± 0.08	**1.55 ± 0.08**	**0.56 ± 0.01**	**1.23 ± 0.05**	0.89 ± 0.10

Br+5	DXS	GGDR	VTE1	VTE2	VTE3	VTE4	VTE5	VTE6
SlGLK2	1.00 ± 0.17	1.00 ± 0.02	1.00 ± 0.03	1.00 ± 0.04	1.00 ± 0.05	1.00 ± 0.06	1.00 ± 0.02	1.00 ± 0.19
Slglk2	0.69 ± 0.15	1.15 ± 0.07	**1.78 ± 0.03**	1.45 ± 0.21	**1.27 ± 0.05**	**0.46 ± 0.02**	1.06 ± 0.02	0.93 ± 0.10
au-SlGLK2	**0.45 ± 0.14**	**0.15 ± 0.01**	**3.74 ± 0.07**	**0.21 ± 0.02**	**2.45 ± 0.11**	**0.40 ± 0.03**	0.92 ± 0.00	**0.67 ± 0.12**

Bold type indicates statistically significant differences against *SlGLK2*.

III. Relative expression data of Figure 22.

IG5	DXS	GGDR	VTE1	VTE2	VTE3	VTE4	VTE5	VTE6	HPPD2	PPH	PPHL1	CHLG
au-Slglk2	1.00 ± 0.31	1.00 ± 0.07	1.00 ± 0.24	1.00 ± 0.09	1.00 ± 0.10	1.00 ± 0.10	1.00 ± 0.08	1.00 ± 0.02	1.00 ± 0.07	1.00 ± 0.07	1.00 ± 0.08	1.00 ± 0.16
L2	***4.23 ± 0.15***	***1.56 ± 0.05***	***3.3 ± 0.05***	***2.14 ± 0.04***	***1.92 ± 0.06***	*1.61 ± 0.05*	*1.52 ± 0.03*	***3.15 ± 0.02***	1.1 ± 0.16	**1.84 ± 0.05**	**1.49 ± 0.10**	***2.7 ± 0.07***
L7	1.06 ± 0.17	0.82 ± 0.31	**0.6 ± 0.08**	0.66 ± 0.10	0.88 ± 0.11	0.65 ± 0.13	**0.55 ± 0.15**	1.15 ± 0.20	1.29 ± 0.13	0.68 ± 0.09	**0.53 ± 0.22**	1.1 ± 0.10
L8	0.85 ± 0.40	1.25 ± 0.26	**0.62 ± 0.17**	0.66 ± 0.23	0.85 ± 0.23	0.74 ± 0.12	0.9 ± 0.13	1.06 ± 0.20	0.85 ± 0.49	0.77 ± 0.15	0.94 ± 0.25	0.89 ± 0.25
SlGLK2	**2.35 ± 0.44**	**2.83 ± 0.08**	1.05 ± 0.07	1.07 ± 0.21	1.36 ± 0.25	0.84 ± 0.24	0.83 ± 0.13	1.72 ± 0.14	**2.85 ± 0.25**	**1.74 ± 0.29**	1.41 ± 0.08	1.64 ± 0.24

Br+6	DXS	GGDR	VTE1	VTE2	VTE3	VTE4	VTE5	VTE6	HPPD2	PPH	PPHL1	CHLG
au-Slglk2	1.00 ± 0.88	1.00 ± 0.04	1.00 ± 0.17	1.00 ± 0.30	1.00 ± 0.09	1.00 ± 0.02	1.00 ± 0.06	1.00 ± 0.30	1.00 ± 0.29	1.00 ± 0.34	1.00 ± 0.02	1.00 ± 0.22
L2	***4.65 ± 0.43***	0.65 ± 0.02	**2.43 ± 0.11**	1.68 ± 0.46	1.99 ± 0.13	**2.23 ± 0.08**	**2.28 ± 0.09**	***3.53 ± 0.72***	1.56 ± 0.28	1.67 ± 0.80	**2.62 ± 0.07**	***3.16 ± 0.50***
L7	1.50 ± 0.23	0.61 ± 0.03	0.83 ± 0.05	1.12 ± 0.10	0.90 ± 0.04	1.13 ± 0.03	1.40 ± 0.01	1.62 ± 0.41	1.47 ± 0.10	0.85 ± 0.12	1.53 ± 0.03	1.32 ± 0.14
L8	1.02 ± 0.04	**0.34 ± 0.03**	1.06 ± 0.11	0.72 ± 0.15	1.07 ± 0.12	0.96 ± 0.08	1.05 ± 0.03	1.43 ± 0.27	1.46 ± 0.23	0.83 ± 0.38	**1.63 ± 0.03**	1.08 ± 0.29
SlGLK2	0.97 ± 0.22	0.79 ± 0.02	1.54 ± 0.07	1.17 ± 0.16	1.20 ± 0.08	**1.76 ± 0.03**	1.80 ± 0.01	1.32 ± 0.09	1.25 ± 0.16	1.13 ± 0.23	**1.95 ± 0.00**	1.50 ± 0.03

Bold type indicates statistically significant differences against *aurea-Slglk2*. Italic type indicates statistically significant differences between L2 and *SlGLK2*

Supplemental Material V

I. ARF binding sites in *SlGLK2* promoter. SlARF (Solyc11g069190) binding sites in *SlGLK2* (Solyc10g008160) promoter. The canonical (TGTCTC, red arrowhead) and non-canonical (TGTCG[AG], purple arrowhead) ARF binding sites are indicated (Hagen & Guilfoyle 2002). The motifs were identified using PlantPAN2.0 (Chow et al., 2015)

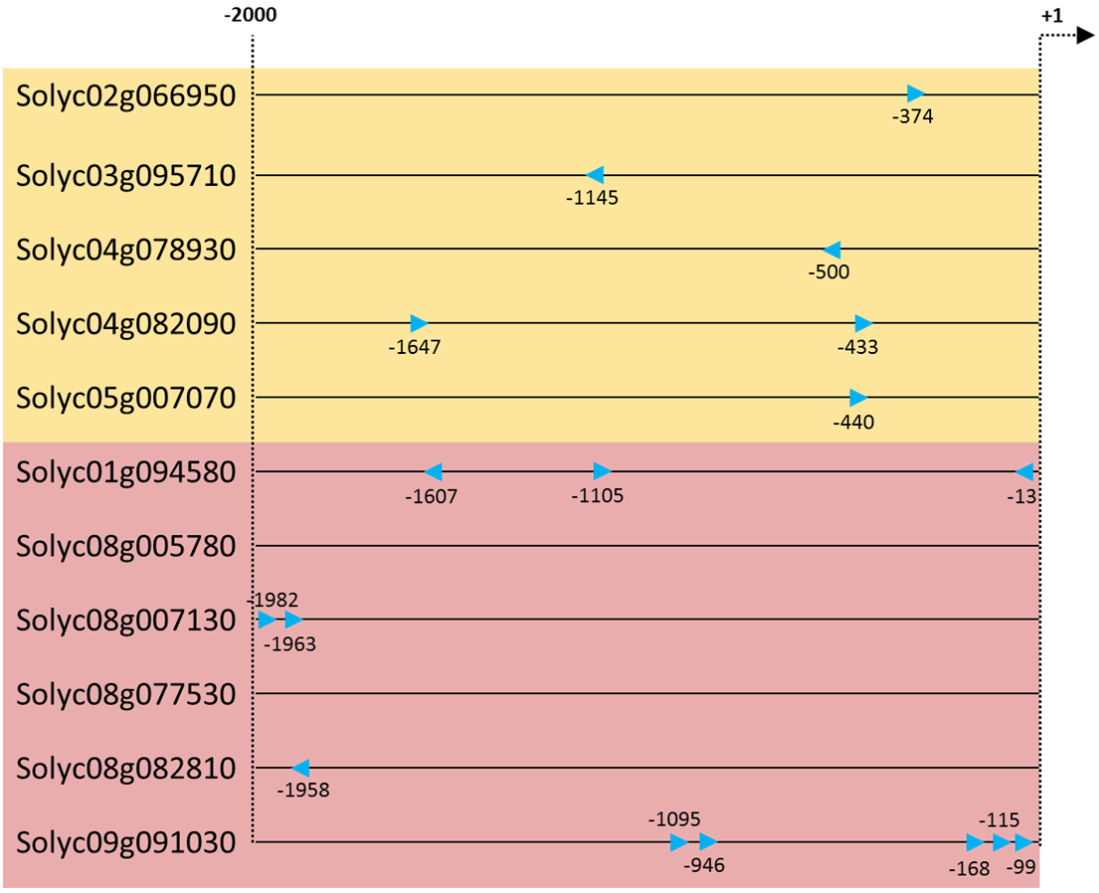

II. SlGLK2 (Solyc10g008160) binding sites in AMYLASE-encoding gene promoters. All genes coding for α-AMYLASE (yellow) or β-AMYLASE (red) were identified from the SolCyc database (http://solcyc.solgenomics.net/). SlGLK2 binding motifs (CCAATC, CACGTG; Waters *et al*. 2009) are indicated by the blue arrowheads.

Supplemental Material VI

Data from leaves of transgenic lines and controls.

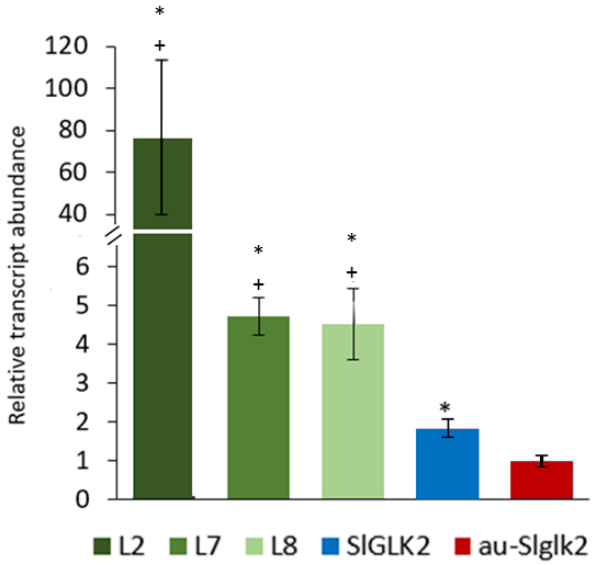

I. *SlGLK2* expression profile in leaves of transgenic plants.
Asterisk (*) indicates statistically significant differences compared to control *aurea-Slglk2* (P<0,05). Plus signal (+) indicates statistically significant difference between transgenic lines and control *SlGLK2* genotype (P<0,05). Relative transcript abundance values are relative to *aurea-Slglk2* mutant samples and represent mean ± SE of at least three biological replicates.

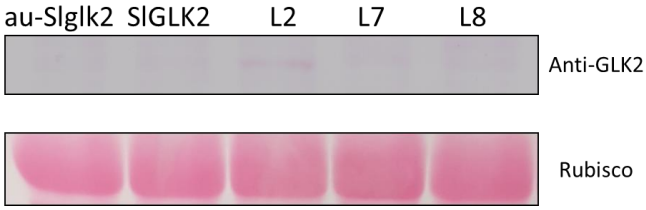

II. *SlGLK2* protein profile in leaves of transgenic lines.
Detection of SlGLK2 protein by Western blot was performed from source leaves of the transgenic lines (L2, L7 and L8) and the control genotypes, *SlGLK2* and *aurea-Slglk2*, using a polyclonal antibody anti-SlGLK2.

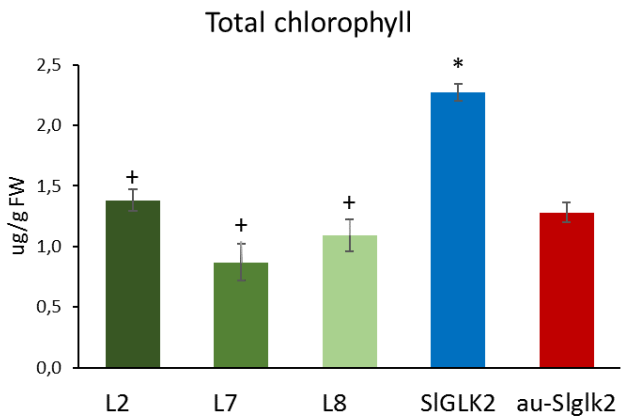

III. Total chlorophyll in leaves from transgenic lines.
Asterisk (*) indicates statistically significant differences compared to control *aurea-Slglk2* (P<0,05). Plus signal (+) indicates statistically significant difference between transgenic lines and control *SlGLK2* genotype (P<0,05). Values represent mean ± SE of at least three biological replicates.

Supplemental Material VII

Expression profile of tocopherol and chlorophyll metabolic enzyme encoding genes in fruits of transgenic lines compared against *SlGLK2*.

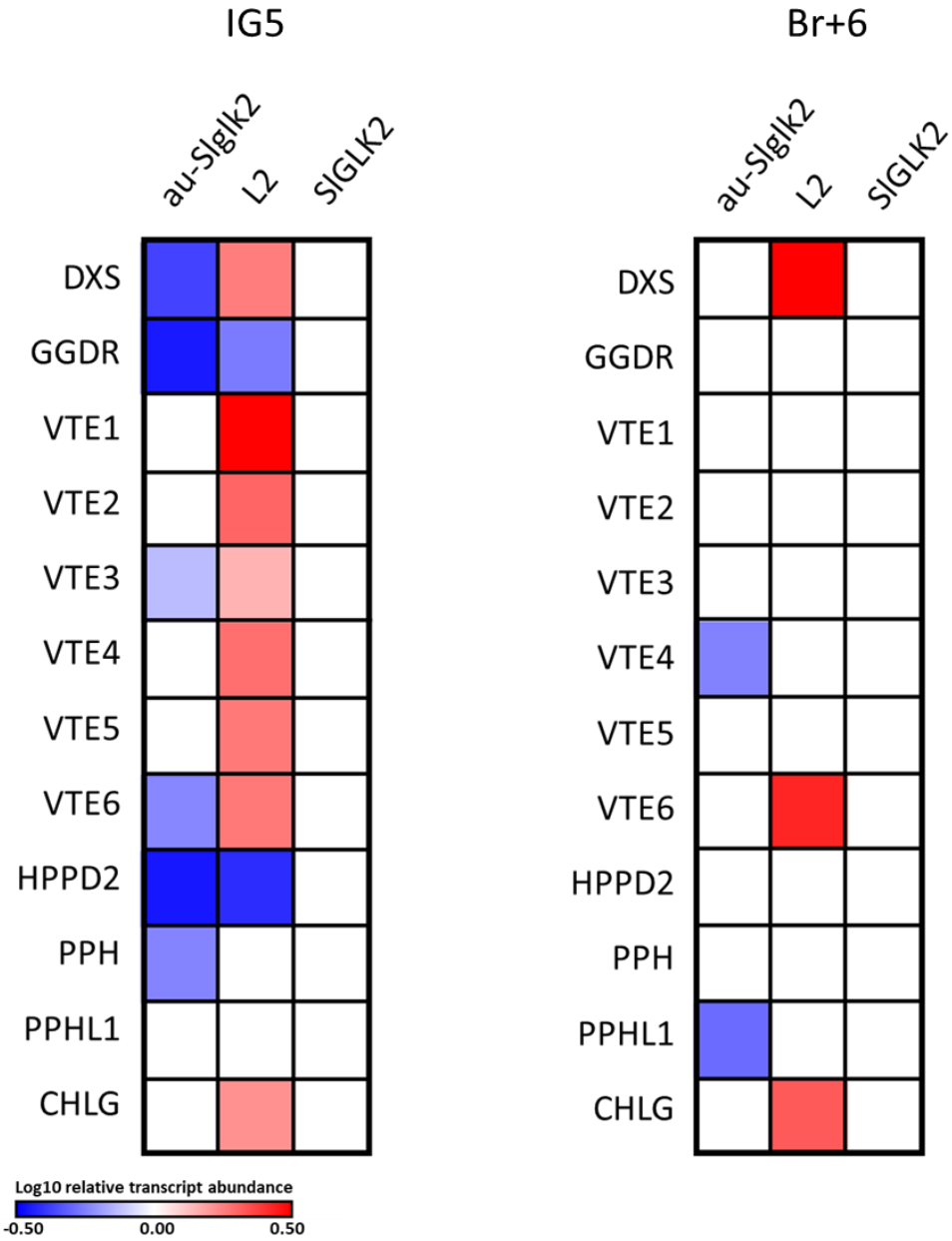

Expression profile obtained by qPCR from fruit at IG5 and Br+6 stages. The heatmap represents statistically significant differences in relative transcript levels detected in L2 and *aurea-Slglk2* compared to *SlGLK2* control ($P<0.05$). Values represent mean of at least three biological replicates. DXS: 1-DEOXY-D-XYLULOSE-5-P SYNTHASE; HPPD2: 4-HYDROXYPHENYLPYRUVATE DIOXYGENASE (2); GGDR: GERANYLGERANYL DIPHOSPHATE REDUCTASE; VTE1: TOCOPHEROL CYCLASE; VTE2: HOMOGENTISATE PHYTYL TRANSFERASE; VTE3: 2,3-DIMETHYL-5-PHYTYLQUINOL METHYL TRANSFERASE; VTE4: TOCOPHEROL Γ -METHYL TRANSFERASE; VTE5: PHYTOL KINASE; VTE6: PHYTYL-PHOSPHATE KINASE; PPH: PHEOPHYTINASE; PPHL1: PHEOPHYTINASE LIKE-1; CHLG: CHLOROPHYLL SYNTHASE.